



FACULDADE DE CIÊNCIAS E TECNOLOGIA

UNIVERSIDADE DE COIMBRA

# **Evaluation of Corneal Nerve Morphology for Detection and Follow-up of Diabetic Peripheral Neuropathy**

Master's Degree in Biomedical Engineering

**IULIAN OTEL**

Coimbra, September 2012





FACULDADE DE CIÊNCIAS E TECNOLOGIA  
UNIVERSIDADE DE COIMBRA

# **Evaluation of Corneal Nerve Morphology for Detection and Follow-up of Diabetic Peripheral Neuropathy**

Thesis submitted for the degree of Master in Biomedical Engineering

Supervisor: Professor Doutor António Miguel Morgado

IULIAN OTEL

Coimbra, September 2012

This work is funded by FEDER, through the Programa Operacional Factores de Competitividade-COMPETE and by National funds through FCT- Fundação para a Ciência e Tecnologia in the frame of project PTDC/SAU-BEB/104183/2008, F-COMP-01-0124-FEDER-010941

Este trabalho é financiado pelo FEDER, através do Programa Operacional Factores de Competitividade-COMPETE e fundos nacionais através da FCT- Fundação para a Ciência e Tecnologia no âmbito do projeto PTDC/SAU-BEB/104183/2008, F-COMP-01-0124-FEDER-010941



Esta cópia da tese é fornecida na condição de que quem a consulta reconhece que os direitos de autor são pertença do autor da tese e que nenhuma citação ou informação obtida a partir dela pode ser publicada sem a referência apropriada.

This copy of the thesis has been supplied on condition that anyone who consults it is understood to recognize that its copyright rests with its author and that no quotation from the thesis and no information derived from it may be published without proper acknowledgement.

*To my parents*

## ACKNOWLEDGEMENTS

It is with a great sense of responsibility, and at the same time, gladness that I come to the end of what has been a challenging and remarkable project. The work presented in this thesis has been carried out during the academic year 2011-2012, representing an important part of the NEUROCORNEA-project.

The project was a joint effort of IBILI - Institute of Biomedical Research on Light and Image, from the Faculty of Medicine, University of Coimbra; the Instrumentation Center, from the Physics Department of the Faculty of Science and Technology, University of Coimbra; and the Departments of Ophthalmology, Endocrinology and Neurology, from Coimbra University Hospitals.

The accomplishment of my thesis could, however, not have been possible without the support and encouragement of several people. It is a great pleasure to show my gratitude to all those who contributed directly or indirectly to my work and made this thesis possible.

Foremost, I would like to thank my supervisor, Professor António Miguel Morgado, for the trustworthy supervision, useful suggestions and unfailing support. It has been a privilege to have the benefit of your important counsel, which clearly made this thesis better.

I would like to show my gratitude to all members involved in this project, professors and medical doctors, who provided me an inspiring working environment and significant support over the course of this project.

Thanks are due to all people that volunteered for this study.

Finally, I would like to express my gratitude to my family, for their valuable support, positive encouragement and for showing me always the right direction. I am truly thankful for their priceless advices and wisdom.

Coimbra, September 2012

IULIAN OTEL

## ABSTRACT

*Diabetes Mellitus*, especially its most prevalent type, type 2 diabetes, is one of the most common and challenging chronic health problems, affecting an increasingly large part of the world population and continuing to increase considerably in numbers and significance. This metabolic disease affects substantially the quality of life, and its complications are main causes of morbidity and mortality.

One of most frequent chronic complications associated with diabetes is diabetic peripheral neuropathy (DPN). This condition encompasses a wide variety of progressive peripheral nerve disorders induced by diabetes over time, affecting substantially proximal and distal peripheral sensory as well as motor nerves.

The diagnosis and classification of neuropathy is usually based on a combination of neuropathic clinical symptoms, clinical signs and electrophysiological studies and findings. Additionally, other rigorous assessment techniques, such as nerve conduction studies and quantitative sensory testing are used in order to provide an extremely accurate diagnosis of peripheral neuropathy, being very useful in characterizing neuropathic expression.

However, there is ample evidence that peripheral nerve abnormalities are directly connected to pathological changes in human corneas, showing also that diabetic neuropathies can be diagnosed and classified through computed analysis of corneal nerve morphology.

*In vivo* corneal confocal microscopy (CCM) is increasingly used to acquire *in vivo* corneal nerve images, enabling real time examination of the living human cornea. This non-invasive technique represents an ideal approach for research and clinical examination, producing high-quality images and visualizing the corneal layers, membranes and cells with high resolution.

We present here a pilot study, aiming mainly to evaluate the ability of detecting and quantifying DPN, using the morphology of corneal nerves imaged by CCM. The study



consisted in a detailed evaluation of a small cohort of 12 healthy controls and 8 diabetic type 2 patients, divided according the presence/absence and severity degree of DPN.

We have obtained promising results, similar to those obtained in prior research studies. The parameters that have shown diabetic neuropathy assessment potential were Nerve Fiber Density (NFD), Nerve Fiber Length (NFL), Nerve Fiber Width (NFW) and Nerve Branch Density (NBD). NFD, NFL and NBD are significantly lower in diabetics compared to controls ( $p < 0.05$ ), establishing inverse correlations with severity degree of DPN. NFW is increased in diabetics compared to controls ( $p < 0.05$ ), varying according to DPN severity. NFD and NFL revealed differences statistically significant ( $p < 0.05$ ) between no DPN cases and DPN patients, and most important, within diabetics (mild DPN and moderate DPN groups) and healthy controls.

We found that CCM can be successfully used as complementing technique for the clinical and electrophysiological diagnosis of DPN, as defined by consensus criteria using nerve conduction studies.

**Keywords:** diabetes, diabetic peripheral neuropathy, corneal confocal microscopy, corneal nerves, morphometric parameters.

## RESUMO

A *Diabetes Mellitus*, principalmente a Diabetes tipo 2, é uma das doenças crónicas mais prevalentes, e mais desafiantes. A diabetes atinge uma grande parte da população mundial, com este número a aumentar consideravelmente nos últimos anos. Esta doença metabólica afeta substancialmente a qualidade da vida, resultando em complicações graves, que são as principais causas da morbidez e mortalidade.

Estão associadas à diabetes várias complicações crónicas. Uma das mais frequentes é a neuropatia diabética periférica (DPN) – a principal causa de incapacidade em diabéticos. Esta condição patológica inclui uma variedade de danos neurológicos periféricos, que são progressivos e que afetam principalmente os nervos sensitivos proximais e distais, bem como os nervos motores.

O diagnóstico e a classificação da neuropatia é geralmente baseada numa combinação de sintomas clínicos e sinais neuropáticos, e em estudos electrofisiológicos. Adicionalmente, são utilizados outros métodos, como os estudos de condução nervosa (NCS) e os testes sensitivos quantitativos (QST). Estes métodos conferem maior exatidão ao diagnóstico efetuado por exame clínico, sendo extremamente úteis na caracterização da expressão neuropática.

Estudos recentes mostraram que as anomalias dos nervos periféricos estão diretamente relacionadas com as alterações no plexo nervoso sub-basal corneano, sugerindo que a neuropatia periférica pode ser diagnosticada e avaliada através da análise morfométrica dos nervos da córnea. Esta abordagem tem recebido uma crescente atenção.

A microscopia confocal da córnea (CCM) é uma técnica frequentemente utilizada para adquirir *in vivo* imagens dos nervos da córnea. Esta técnica é não-invasiva e permite a obtenção de imagens da córnea em tempo real. A microscopia confocal representa um método ideal para investigação e avaliação clínica, produzindo imagens com alta qualidade e permitindo a visualização das camadas e das células da córnea com uma resolução elevada.

Apresentamos Aqui um estudo piloto em que se avalia a deteção e classificação da neuropatia periférica através da análise morfométrica dos nervos da córnea. O estudo consiste numa avaliação pormenorizada dum pequeno grupo de 12 voluntários não-diabéticos e 8 doentes diabéticos tipo 2, classificados consoante a presença e o grau de severidade da neuropatia.

Os resultados que obtivemos são promissores e similares aos reportados em estudos anteriores. Os parâmetros Densidade de Fibras Nervosas (NFD), Comprimento de Fibras Nervosas (NFL), Largura de Fibras Nervosas (NFW) e Densidade de *Branching* de Nervos (NBD) apresentaram o melhor desempenho na avaliação da neuropatia diabética. Os valores de NFD, NFL e NBD são significativamente mais baixos ( $p < 0.05$ ) nos doentes diabéticos quando comparados com os controlos, e exibem correlações inversas com o grau de severidade da neuropatia. Os valores de NFW são significativamente superiores nos doentes diabéticos, variando com o grau de severidade da neuropatia. Os parâmetros NFD e NFL mostram diferenças estatisticamente significativas ( $p < 0.05$ ) entre os casos sem neuropatia e os doentes com neuropatia, mostrando também diferenças significativas ( $p < 0.05$ ) entre os grupos dos diabéticos (classificados consoante a severidade da neuropatia), diferenciando os grupos com grau ligeiro e moderado de neuropatia, do grupo de controlos não-diabéticos.

Concluimos que a CCM pode ser utilizada com êxito para complementar os resultados de avaliação da neuropatia periférica, obtidos através de exames clínicos e electrofisiológicos.

**Palavras-Chave:** diabetes, neuropatia diabética periférica, microscopia confocal da córnea, nervos da córnea, parâmetros morfométricos.

# TABLE OF CONTENTS

Acknowledgements .....	II
Abstract .....	III
Resumo .....	V
Table of contents .....	VII
List of tables .....	X
List of figures .....	XI
List of abbreviations.....	XIV
<b>SECTION I – INTRODUCTION.....</b>	<b>1</b>
<b>CHAPTER 1 – CORNEAL ANATOMY AND PHYSIOLOGY.....</b>	<b>2</b>
1.1 – The normal healthy human cornea.....	2
1.1.1 - Macroscopic corneal anatomy.....	3
1.1.2 - Corneal epithelium.....	4
1.1.3 - Bowman’s layer.....	4
1.1.4 - Corneal stroma.....	5
1.1.5 - Descemet’s membrane.....	5
1.1.6 - Corneal endothelium.....	5
1.1.7 - Limbus.....	5
1.2 - Corneal nerves.....	6
<b>CHAPTER 2 – DIABETES MELLITUS.....</b>	<b>7</b>
2.1 – Definition, characteristics and impact.....	7
2.2 – Diabetes types.....	8
2.2.1 - Type 1.....	8
2.2.2 - Type 2.....	8
2.2.3 - Gestational diabetes.....	9
2.2.4 - Other causes of diabetes.....	9
2.3 – Consequences of diabetes.....	10

<b>CHAPTER 3 – DIABETIC NEUROPATHY.....</b>	<b>11</b>
<b>3.1 – Definition of diabetic neuropathy.....</b>	<b>11</b>
<b>3.2 – Pathogenesis and etiology of diabetic neuropathy.....</b>	<b>12</b>
<b>3.2.1 - Metabolic nerve injuries.....</b>	<b>13</b>
<b>3.2.2 - Vascular/Ischemic nerve injuries.....</b>	<b>14</b>
<b>3.2.3 - Autoimmune nerve injuries.....</b>	<b>16</b>
<b>3.3 – Classification and characteristics of diabetic neuropathy.....</b>	<b>16</b>
<b>3.3.1 - Diabetic distal symmetrical polyneuropathy (DSPN).....</b>	<b>18</b>
<b>3.3.2 - Diabetic autonomic neuropathy (DAN).....</b>	<b>20</b>
<b>3.3.3 - Focal and multifocal neuropathies.....</b>	<b>21</b>
<b>3.4 – Diagnosis of diabetic neuropathy.....</b>	<b>22</b>
<b>3.4.1 - Clinical examination of DPN.....</b>	<b>23</b>
<b>3.4.2 - Scoring of signs and symptoms in DPN.....</b>	<b>25</b>
<b>3.4.3 - Neurophysiologic examination.....</b>	<b>30</b>
<b>3.4.4 - Quantitative sensory testing (QST).....</b>	<b>34</b>
<b>3.4.5 - Other methods of assessment.....</b>	<b>36</b>
<b>CHAPTER 4 – CORNEAL CONFOCAL MICROSCOPY.....</b>	<b>40</b>
<b>4.1 – Introduction.....</b>	<b>40</b>
<b>4.2 – Principles of confocal microscopy.....</b>	<b>41</b>
<b>4.3 – Types of confocal microscopes.....</b>	<b>43</b>
<b>4.3.1 - Tandem Scanning Confocal Microscope (TSCM).....</b>	<b>43</b>
<b>4.3.2 - Slit Scanning Confocal Microscope (SSCM).....</b>	<b>44</b>
<b>4.3.3 - Laser Scanning Confocal Microscope (LSCM).....</b>	<b>45</b>
<b>4.4 – Clinical examination.....</b>	<b>46</b>
<b>4.5 – Clinical applications.....</b>	<b>47</b>
<b>SECTION II – STATE OF ART.....</b>	<b>49</b>
<b>CHAPTER 5 – ASSESSMENT OF CORNEAL NERVE MORPHOLOGY WITH IVCCM.....</b>	<b>50</b>
<b>SECTION III – RESEARCH DESIGN AND METHODOLOGY.....</b>	<b>59</b>
<b>CHAPTER 6 – RESEARCH DESIGN, AIMS AND METHODS.....</b>	<b>60</b>
<b>6.1 – Key steps of study.....</b>	<b>60</b>
<b>6.2 – Team and institutions involved in NeuroCornea project.....</b>	<b>61</b>

6.3 – Classification of DPN case and control individuals.....	61
6.4 – Diabetic patients: exclusion of other causes for neuropathy.....	64
6.4.1 - Alcohol related neuropathy.....	64
6.4.2 - Nutritional neuropathy.....	64
6.4.3 - Neuropathy caused by pernicious anemia/gastritis.....	65
6.4.4 - Uremic neuropathy.....	66
6.4.5 - Hypothyroidism related neuropathy.....	67
6.4.6 - Cancer-related neuropathy.....	67
6.4.7 - Neuropathy caused by porphyria.....	68
6.4.8 - Inflammatory neuropathy.....	68
6.4.9 - Neuropathy induced by medication.....	69
6.5 – Electrophysiological measurements and nerve conduction studies (NCS).....	70
6.6 – CCM image acquisition.....	72
6.7 - Image Analysis: Morphometric parameters.....	74
6.8 – Corneal nerve segmentation algorithm.....	76
6.8.1 - CCM image: artifacts.....	76
6.8.2 - Segmentation algorithm.....	77
6.9 – Statistical methods.....	80
<b>SECTION IV – RESULTS.....</b>	<b>81</b>
<b>CHAPTER 7 – RESULTS ANALYSIS.....</b>	<b>82</b>
7.1 – Nerve fiber density (NFD).....	83
7.2 – Nerve fiber width (NFW).....	84
7.3 – Nerve fiber length (NFL).....	85
7.4 – Tortuosity coefficient (TC).....	86
7.5 – Nerve branching density (NBD).....	87
7.6 – Nerve branching pattern (NBP).....	88
7.7 – Nerve branching angle (NBA).....	89
7.8 – Electrophysiological findings.....	90
7.9 – Correlations tests and distribution charts.....	92
<b>SECTION V – OVERVIEW: RELEVANCE OF THE STUDY.....</b>	<b>97</b>
<b>CHAPTER 8 – DISCUSSION AND CONCLUSIONS.....</b>	<b>98</b>
<b>CHAPTER 9 – FUTURE WORK.....</b>	<b>102</b>
<b>REFERENCES.....</b>	<b>103</b>

## LIST OF TABLES

### SECTION I

#### Chapter 3

<b>Table 1</b> - Classification of physiopathological factors of diabetic neuropathy [11].....	<b>13</b>
<b>Table 2</b> - Most common abnormalities implicated in the pathogenesis of diabetic neuropathy [16].....	<b>15</b>
<b>Table 3</b> – Classification of diabetic neuropathy [17, 19].....	<b>17</b>
<b>Table 4</b> – Guidelines for Diagnosis and Outpatient management of DPN [28].....	<b>24</b>
<b>Table 5</b> – Modified NDS [32].....	<b>26</b>
<b>Table 6</b> – Toronto Clinical Neuropathy Scoring System [41, 42].....	<b>29</b>

### SECTION IV

#### Chapter 7

<b>Table 7</b> – Summary of the four participants groups.....	<b>82</b>
<b>Table 8</b> – Descriptive statistics: evaluation of the segmentation algorithm performance..	<b>82</b>
<b>Table 9</b> – NFD for automatically segmented and manually delineated images.....	<b>83</b>
<b>Table 10</b> – NFW for automatically segmented nerves.....	<b>84</b>
<b>Table 11</b> – NFL for automatically segmented and manually delineated images.....	<b>85</b>
<b>Table 12</b> – TC for automatically segmented and manually delineated images.....	<b>86</b>
<b>Table 13</b> – NBD for automatically segmented and manually delineated images.....	<b>87</b>
<b>Table 14</b> – NBP for automatically segmented and manually delineated images.....	<b>88</b>
<b>Table 15</b> – NBA for automatically segmented and manually delineated images.....	<b>89</b>
<b>Table 16</b> – Electrophysiological measurements.....	<b>90</b>
<b>Table 17</b> – Summary of correlation tests between morphometric parameters.....	<b>92</b>

## LIST OF FIGURES

### SECTION I

#### Chapter 1

- Figure 1** - The structure of the human eye [2].....2  
**Figure 2** - Anatomy of the cornea [1].....4

#### Chapter 4

- Figure 3** - Illustration of the principle of confocal microscopy [74].....41  
**Figure 4** – Schematic illustration of the optical pathway used in TSCM [76].....44  
**Figure 5** - Schematic diagram of the optical pathway used in the SSCM [74].....45  
**Figure 6** - Schematic diagram of the optical pathway in LSCM [78].....46

### SECTION III

#### Chapter 6

- Figure 7 – a)** Pie-chart representing the individuals involved in our study, divided in four groups: control; diabetics without DPN, with mild DPN and with moderate DPN; **b)** Scatter chart representing the mean age values  $\pm$  standard deviations, corresponding to the four groups.....62  
**Figure 8** – MNSI: Physical assessment (University of Michigan, 2000), [106].....62  
**Figure 9** – MNSI Questionnaire (University of Michigan, 2000), [106].....63  
**Figure 10** – Sample of sEMG signals from a diabetic subject, corresponding to: **a)** right peroneal nerve; **b)** sympathetic nerve response; **c)** right and **d)** left sural nerve. [CHUC, Department of Neurology, EMG and EP Lab; measurement performed in May, 2012], [133].....71  
**Figure 11** – IVCCM (384 x 384) pixel images of the healthy living cornea, illustrating **a)** three different corneal layers (starting from the bottom): basal epithelium, Bowman’s layer and stroma; **b)** basal epithelium; **c)** sub-basal nerve plexus with corneal nerves; **d)** anterior stroma; **e)** mid-stroma (with less cells), and **f)** endothelium [135].....73



**Figure 12** – Representative examples of CCM image artifacts and noise, with: **a)** corneal tissue deformity; **b)** illumination artifacts and blood vessel; **c)** blurring effect from saccadic eye movement; **d)** bright structures; **e)** stromal cells; **f)** depth differences and bright structures; **g)** and **h)** illumination artifacts. [Images obtained during several IVCCM image acquisition sessions, 2012], [135].....77

**Figure 13** – Representation of the two initial steps of *Cornea3* segmentation algorithm applied to CCM images: **a)** original image, **b)** local equalization step, and **c)** phase-shift step. [Results obtained in July, 2012], [138].....79

**Figure 14** – Representative sample images and obtained results after the nerve reconstruction step: **a)** original CCM image, **b)** reference image (manually delineated), **c)** segmented image and **d)** reconstructed nerves. [Results obtained in July, 2012], [138].....79

## SECTION IV

### Chapter 7

**Figure 15** – Representative boxplots (with median, interquartile range, outliers, and extreme cases of individual variables) of NFD parameter in **a)** segmented images by the algorithm, and **b)** manually traced nerves. [Results obtained in August, 2012].....83

**Figure 16** – **a)** Representative boxplot (with median, interquartile range, outliers, and extreme cases of individual variables) and **b)** scatterplot of NFW parameter in segmented images by the algorithm. [Results obtained in August, 2012].....84

**Figure 17** – Representative boxplots (with median, interquartile range, outliers, and extreme cases of individual variables) of NFL parameter in **a)** segmented images by the algorithm, and **b)** manually traced nerves. [Results obtained in August, 2012].....85

**Figure 18** – Representative boxplots (with median, interquartile range, outliers, and extreme cases of individual variables) of TC parameter in **a)** segmented images by the algorithm, and **b)** manually traced nerves. [Results obtained in August, 2012].....86

<b>Figure 19</b> – Representative boxplots (with median, interquartile range, outliers, and extreme cases of individual variables) of NBD parameter in <b>a)</b> segmented images by the algorithm, and <b>b)</b> manually traced nerves. [Results obtained in August, 2012].....	<b>87</b>
<b>Figure 20</b> – Representative boxplots (with median, interquartile range, outliers, and extreme cases of individual variables) of NBP parameter in <b>a)</b> segmented images by the algorithm, and <b>b)</b> manually traced nerves. [Results obtained in August, 2012].....	<b>88</b>
<b>Figure 21</b> – Representative boxplots (with median, interquartile range, outliers, and extreme cases of individual variables) of NBA parameter in <b>a)</b> segmented images by the algorithm, and <b>b)</b> manually traced nerves. [Results obtained in August, 2012] (*NBA value was considered valid only for one individual with Mild DPN).....	<b>89</b>
<b>Figure 22</b> – Representative boxplots (with median, interquartile range, outliers, and extreme cases of individual variables) with nerve conduction velocities for <b>a)</b> motor nerve, and <b>b)</b> sensory nerve. [Results obtained in August, 2012].....	<b>90</b>
<b>Figure 23</b> – Representative boxplots (with median, interquartile range, outliers, and extreme cases of individual variables) with nerve conduction amplitudes (expressed in $\mu\text{V}$ ) for <b>a)</b> motor nerve, <b>b)</b> sensory nerve, and <b>c)</b> sympathetic nerve response (latency time [ms]). [Results obtained in August, 2012].....	<b>91</b>
<b>Figure 24</b> – Representative scatterplots showing the distribution of individuals according to NFD and <b>a)</b> NFW; <b>b)</b> NFL; <b>c)</b> NBD; <b>d)</b> motor NCV; <b>e)</b> sensory amplitude; and <b>f)</b> motor amplitude [Results obtained in August, 2012].....	<b>93</b>
<b>Figure 25</b> – Representative scatterplots showing the distribution of individuals according to NFL and <b>a)</b> NBD; <b>b)</b> NFW; <b>c)</b> NBP; and <b>d)</b> sensory amplitude. [Results obtained in August, 2012].....	<b>94</b>
<b>Figure 26</b> – Representative scatterplots showing the distribution of individuals according to NFW and <b>a)</b> NFD; <b>b)</b> NFL; <b>c)</b> NBD; and <b>d)</b> NBP. [Results obtained in August, 2012].....	<b>95</b>
<b>Figure 27</b> – Representative scatterplots showing the distribution of individuals according to; <b>a)</b> TC and NBA; <b>b)</b> NBP and TC; <b>c)</b> NFL and TC; and <b>d)</b> NFL and NBA [Results obtained in August, 2012].....	<b>96</b>

## LIST OF ABBREVIATIONS

- AAN** - American Academy of Neurology
- AANEM** - American Academy of Neuromuscular and Electrodiagnostical Medicine
- AAPM&R** - American Academy of Physical Medicine and Rehabilitation
- AIDP** – Acute Inflammatory Demyelinating Polyradiculoneuropathies
- ANS** – Autonomic Nervous System
- CCD** – Charge-Coupled Device
- CCM** – Corneal Confocal Microscopy
- CIDP** – Chronic Inflammatory Demyelinating Polyradiculoneuropathies
- CLSM** – Confocal Laser Scanning Microscopy
- CMAP** – Compound Muscle Action Potential
- DAN** – Diabetic Autonomic Neuropathy
- DR** – Diabetic Retinopathy
- DPN** – Diabetic Peripheral Neuropathy
- DSPN** – Distal Symmetrical Polyneuropathy
- DSP** – Diabetic Sensorimotor Polyneuropathy
- EFNS** – European Federation of Neurological Societies
- EMG** – Electromyography
- EMG and EP Lab** – Electromyography and Evoked Potentials Laboratory
- HRC** – Highly Reflective Cells
- HRT CRM** – Heidelberg Retinal Tomograph equipped with a Cornea Rostock Module
- IENF** – Intra-epidermal Nerve Fibers
- IGT** – Impaired Glucose Tolerance
- IVCM** – *in vivo* Confocal Microscopy
- IVCCM** – *in vivo* Corneal Confocal Microscopy

**LSCM** – Laser Scanning Confocal Microscope

**LSD** – Least Significant Difference

**MNSI** - Michigan Neuropathy Screening Instrument

**MRI** – Magnetic Resonance Imaging

**NBA** – Nerve Branching Angle

**NBD** – Nerve Branching Density

**NBP** – Nerve Branching Pattern

**NCS** – Nerve Conduction Study

**NCV** – Nerve Conduction Velocity

**NDS** - Neuropathy Disability Score

**NFD** – Nerve Fiber Density

**NFL** – Nerve Fiber Length

**NFW** – Nerve Fiber Width

**NNB** – Number of Nerve Beadings

**NSS** – Neuropathy Symptom Score

**PRK** – Photorefractive Keratectomy

**QSART** – Quantitative Sudomotor Axon Reflex Testing

**QST** – Quantitative Sensory Testing

**RC** – Reflectivity Coefficient

**SBN** – Sub-basal Nerves

**SSCM** – Slit Scanning Confocal Microscope

**SNAP** – Sensory Nerve Action Potential

**TC** – Tortuosity Coefficient

**TCNS** – Toronto Clinical Neuropathy Score

**TSCM** – Tandem Scanning Confocal Microscopy



## **SECTION I**

### **INTRODUCTION**

## CHAPTER 1 – CORNEAL ANATOMY AND PHYSIOLOGY

### 1.1 - The normal healthy human cornea

The cornea is the most significant refractive medium in the eye, representing its optical window that is essential for humans to see. The lens and cornea are the main optical systems that focus entering light rays into an image upon the retina. The cornea has greater optical potency than the lens in focusing light, as the incoming rays are bent more in the transition from air into the cornea than they are when passing into or out of the lens [1, 2].

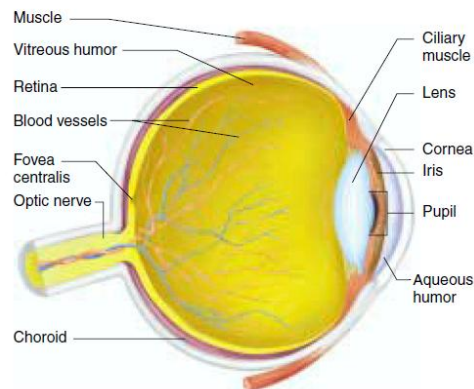


**Figure 1** - The structure of the human eye [2].

The normal diameter of the adult cornea may vary between 10 - 13 mm. The surface of the cornea is curved so that the received light rays from a single point source hit the cornea at distinct angles and are bent different amounts, directing the light rays back to a point after emerging from the lens. When the object is situated in the center of the field of view, the corresponding image is centered on a specific area identified as the *fovea centralis*, the area of the retina that is responsible for the highest visual clarity. The image on the retina is inverted relative to the original light source and it is reversed right to left as well [1, 2].

The cornea's most important tasks are to transmit and focus light onto the retina, contributing up to 75% of the eye's total focusing power. This fundamental structure is

also responsible for maintaining the intraocular pressure and providing a protective interface with the environment. The cornea act effectively as a shield against germs, dust and other detrimental matter, acting additionally as a filter and protecting the retina against UV-B and UV-C radiation [1, 3-5].

### **1.1.1 - Macroscopic corneal anatomy**

The corneal tissue is positioned at the front of the eye. This connective, transparent and avascular structure is also one of the most densely innervated tissues in the human body, being abundantly supplied by sensory and autonomic nerve fibers [1].

Corneal transparency is mostly due to several factors, such as the homogeneous arrangement of the lamellae of collagen fibrils in the corneal stroma and the extremely smooth endothelial and epithelial surface produced by the intraocular pressure. Other factor that seriously influences the transparency is the water content of the corneal stroma. The dual action of the epithelium and endothelium maintains constant the water content at 70% [3-5].

The surface of the cornea consists in a stratified non-keratinized squamous epithelium that regenerates rapidly when injured. Epithelial defects are rapidly closed (within 1 hour) by cell migration and quick cell division [1].

Similarly to lens, sclera and vitreous body, the cornea is a bradytrophic tissue structure. It is nourished with nutritive metabolites, such as amino acids and glucose. These nutrients are delivered through diffusion processes from three sources: the capillaries at its edge, the aqueous humor and the tear film [1].

The corneal tissue consists of five distinct avascular layers: the epithelium, the Bowman's layer, the stroma, the Descemet's membrane and the endothelium. Each of these layers plays a particular role in cornea [1].



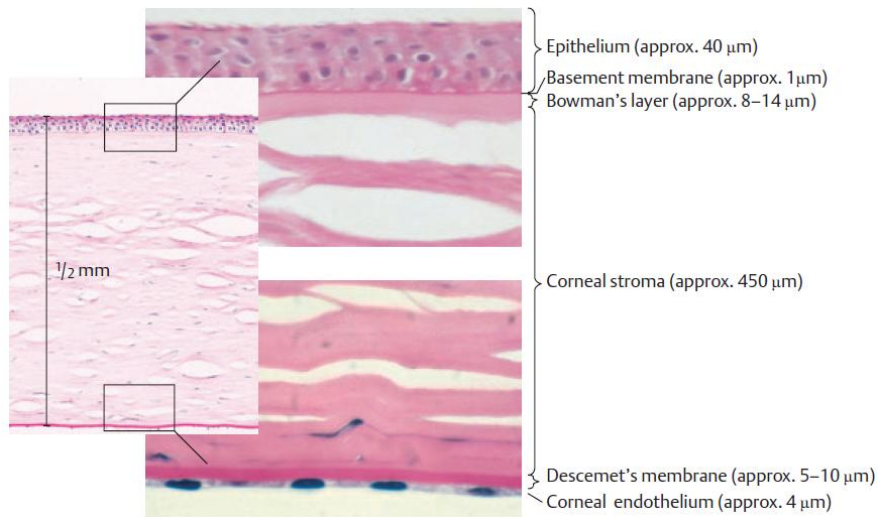


**Figure 2** - Anatomy of the cornea [1].

### **1.1.2 - Corneal epithelium**

The corneal epithelium is constantly maintained by the balance between permanent cell loss by shedding of surface epithelium, and regular cell substitution by proliferation of basal epithelial cells [1]. This layer contains numerous tiny nerve endings, which makes the cornea extremely sensitive to the slightest touching. Adjacent cells are joined circumferentially, acting as a semi-permeable membrane and giving the surface epithelium its blocking barrier function against invasion by pathogens or other foreign material. Epithelial permeability level normally increases with age, exposing the cornea to possible infections [3-5].

### **1.1.3 - Bowman's layer**

Bowman's layer is an acellular and transparent lamella of tissue, consisting of arbitrarily oriented, closely packed collagen fibrils, and being placed right below the epithelium [1]. This layer is very resistant but cannot regenerate following wounds. Consequently, injuries to Bowman's layer usually cause corneal scarring, which could seriously affect the vision. This layer contains several nerves, that branch to form a basal epithelial nerve plexus. These nerves are rapidly and easily identified by confocal microscopy [3-5].

#### **1.1.4 - Corneal stroma**

Beneath Bowman's layer, many collagen fibrils form the corneal stroma. This avascular, transparent and highly bradytrophic tissue, is the largest corneal layer [1]. Its avascularity makes it an immunologically advantaged site for grafting, while the collagen gives the cornea its essential properties: elasticity, strength and form. It has been alleged that corneal light-conducting transparency is the effect of the regular spatial arrangement of collagen fibrils. The stroma also contains large nerves and fibroblasts, which are generally nominated as stromal keratocytes [3-5].

#### **1.1.5 - Descemet's membrane**

Descemet's membrane and the corneal endothelium lie on the posterior surface of the corneal stroma. Descemet's membrane is a relatively strong and resistant membrane. Formed by collagen fibers and endothelial cells, this membrane is a valuable shield against infection and injuries [1, 3-5].

#### **1.1.6 - Corneal endothelium**

The corneal endothelium is composed by a single layer of flattened endothelial cells. This intern cell membrane is essential for the prevention of stromal swelling, maintaining a relative condition of deturgescence [1, 2]. This is due to the barrier and pump functions of these cells, which are the most metabolically active cells in the cornea. Oxygen and necessary nutrients are supplied by the aqueous humour. The corneal endothelial cells do not regenerate, leading to a decreased density directly related with ageing. A declined density can result in a lack of hydration regulation, leading to transparency loss [2-4].

#### **1.1.7 - Limbus**

The limbus is the junction between the cornea and sclera [1]. This structure may be subdivided into two anatomical parts: the corneal limbus and the scleral limbus. The

corneal limbus is clearly distinguished by a line joining both terminations of Bowman's layer and Descemet's membrane. Patel [4] has reported that the corneo-scleral limbus plays a decisive role in the maintenance of corneal epithelial integrity, providing epithelial self-renewing stem cells [2-4].

## **1.2 – Corneal nerves**

The human cornea is a vital and remarkably sensitive structure of the eye [1]. Extremely slight tactile sensation may cause an eye closing reflex [2]. Cornea receives its plentiful sensory supply from the ophthalmic and maxillary division of the trigeminal nerve. Most sensory nerves lose the myelin sheath and perineurium, branching into smaller nerves. These smaller branches will perforate the cornea and form the corneal nerves, which have multiple sensory and efferent functions [5, 7].

Any mechanical, thermal or chemical stimulation of the corneal sensory nerves results principally in sensation of pain. Corneal sensation is necessary for keeping the integrity of the ocular surface. The smallest damage to the cornea, such as erosion, foreign-body penetration, or ultraviolet keratoconjunctivitis, may significantly affect the tissue, exposing sensory nerve endings and causing severe pain with reflexive tearing and unintentional eye closing [5-7].

Muller *et al.* [5], affirmed that nerve fiber bundles in the sub-basal plexus continue first in the 3–9 o'clock hours direction, then turn abruptly by 90° and extend in the 6–12 o'clock hours direction. After a second abrupt bifurcation, nerve fibers follow in the 3–9 o'clock hours direction. Nevertheless, current human studies with *in vivo* confocal microscopy (IVCM) propose a different model of central sub-basal corneal innervation, where most leashes of nerve fibers follow through the corneal apex preferentially in the 6–12 o'clock direction, while other leashes approach the apex in different directions. However, due to technical reasons, IVCM images are limited mainly to the corneal apex and cover a reduced area of the central cornea. As a result, the orientation of sub-basal nerves in peripheral regions of the human cornea continues partly unrevealed [5].

## CHAPTER 2 – DIABETES MELLITUS

### 2.1 – Definition, characteristics and impact

*Diabetes Mellitus* is one of the most common and challenging chronic health problems [8]. This metabolic disease affects a large part of the world population and continues to increase considerably in numbers and significance [9].

Diabetes is characterized by uncontrolled chronically rising levels of blood glucose caused by a deficiency in insulin secretion and/or insulin resistance (depending on its' type), resulting in the incapacity of the insulin hormone in transforming the glucose [10].

The prevalence of diabetes (principally type 2) is increasing due to demographic changes, such as population growth, ageing and especially better care health, improving longevity of patients with diabetes. Economic development and urbanization lead to changing sedentary lifestyles characterized by decreased physical activity and increased obesity, extremely detrimental for human health [9, 10].

Consequently, the prevalence of this metabolic disease has developed to epidemic proportions with a population that is now overweight and obese. According to several clinical reports and data sources [9], approximately 366 million people had diabetes in 2011. The number is expected to increase up to 552 million by 2030, corresponding to a 50.7 % increase in worldwide adult population with diabetes [9, 10].

The pattern of diabetes show significant differences in developed countries, where most population with diabetes are aged over 60 years, when compared with developing countries, where the majority with diabetes are of working age, varying between 40 and 60 years. This discrepancy is expected to remain present in 2030, although less noticeable, as the average age of developing countries' populations is estimated to increase a little more than in the developed countries [9].

## **2.2 – Diabetes types**

There are two major types of diabetes: type 1 and type 2 (described below). A different, but well-known type is the gestational diabetes, a condition that develops only during pregnancy. Several other types of diabetes, previously known as secondary diabetes, are mainly caused by other illnesses or medications [11, 12].

### **2.2.1 – Type 1**

Type 1 diabetes, also known as insulin-dependent diabetes or juvenile-onset diabetes, includes those cases attributable to an autoimmune disorder, associated to a massive destruction of the insulin-producing beta cells in the pancreas. Patients with type 1 diabetes show total insulin insufficiency and generally require insulin early in the disease [9].

It can occur at all ages, but normally presents at young age, encompassing the most part of cases which are primarily due to pancreatic islet beta-cell destruction or reveal ketoacidosis [9, 11]. Its occurrence reveals obvious geographical differences and is mainly common in Caucasians in Finland, Denmark, Norway, Sweden and Sardinia [13].

### **2.2.2 – Type 2**

Type 2 diabetes represents the common major form of diabetes, accounting for approximately 95% of diagnosed cases of diabetes worldwide. It results principally from relative (rarely absolute) insulin deficiency and defects in insulin secretion, usually connected to insulin resistance [12]. Consequently, there is insufficient insulin to completely compensate for the insulin resistance. Most people with this form of diabetes are sedentary and obese, and the obesity leads to a certain degree of insulin resistance. This type is also called non-insulin-dependent diabetes or adult-onset diabetes [12, 13].

Type 2 diabetes occurrence varies significantly between countries and ethnic groups, varying between 5–8% in Europe. The top 10 countries, in numbers of patients with diabetes, are at the moment India, China, the United States, Indonesia, Japan, Pakistan, Russia, Brazil, Italy, and Bangladesh [9, 11].

Type 2 diabetes mellitus prevails mostly among Hispanics, Native Americans, African Americans, and Asians/Pacific Islanders than in non-Hispanic whites. Undeniably, this disease is becoming practically pandemic in several groups of Native Americans and Hispanic people. Type 2 diabetes usually has a later age of onset, but a frightening increase in the occurrence of this form among adolescents and children has been reported by numerous clinical sources [11-13].

### **2.2.3 – Gestational diabetes**

Gestational diabetes represents a carbohydrate intolerance, followed by hyperglycemia of different severity degrees with onset only during pregnancy. In many cases glucose intolerance may be previously unrecognized and precede pregnancy. The definition remains valid and irrespective of whether or not insulin is used for treatment or if the disease continues after pregnancy [13].

### **2.2.4 – Other causes of diabetes**

Other specific forms are at the moment less common causes of *Diabetes Mellitus*, but are those in which the underlying factor can be identified in a relatively precise way. These types of diabetes generally depend on the primary process involved, such as destruction of pancreatic beta cells or development of peripheral insulin resistance [13].

These types of diabetes have many similarities with type 1 or type 2 diabetes. Most prevalent forms are associated with pancreas complications, such as hemochromatosis, pancreatitis, cystic fibrosis and pancreatic cancer. These types are often caused by hormonal syndromes, which severely interfere with insulin secretion, such as

pheochromocytoma, or induce peripheral insulin resistance, such as acromegaly, Cushing syndrome and pheochromocytoma. Diabetes is increasingly caused by drugs, for example phenytoin, glucocorticoids or estrogens [12, 13].

### **2.3 – Consequences of diabetes**

Diabetes represents an enormous problem. Its high prevalence is largely attributed to type 2 diabetes, resulting in considerably increasing health care costs. This disease usually leads to other pathologies; its effects comprise long-term damage, dysfunction and failure of distinct organs. People with diabetes have a substantially higher probability to progressively develop cardiovascular, peripheral vascular and cerebrovascular diseases [8, 11].

Diabetes affects substantially the quality of life, and its complications are main causes of morbidity and mortality. The complications encompass both micro-vascular (neuropathy, nephropathy, and retinopathy) and macro-vascular (atherosclerotic) disease. It is the major initiating cause for foot ulceration, Charcot's neuroarthropathy and lower extremity amputation [11-12].

## **CHAPTER 3 – DIABETIC NEUROPATHY**

### **3.1 – Definition of diabetic neuropathy**

Diabetic neuropathy is among the commonest long-term complications of diabetes, representing the main cause of chronic disability in diabetic patients. This condition encompasses a large spectrum of nerve disorders induced by diabetes over time, leading to the development of nerve damage throughout the human body [10, 11].

Peripheral nerve involvement is extremely frequent in diabetes mellitus and it has been revealed that neuropathy is estimated to be present in approximately 8% of newly diagnosed diabetic patients [14].

According to members of international consensus meeting on diagnosis and management of diabetic neuropathy, this complication can be defined as the obvious presence of symptoms and signs of peripheral nerve dysfunction, either clinically evident or subclinical, that occurs in the setting of diabetes after the exclusion of other causes. This disorder comprises the manifestations in the somatic and/or autonomic parts of peripheral nervous system [15].

It is developed by more than 50% of the patients with long-standing disease within 25 years of diagnosis [14]. The prevalence of diabetic neuropathies is dramatically increasing with the enormous burden of type 2 diabetes, but the true occurrence remains unrevealed, with variable reports in diabetic patients depending mostly on the criteria and methods used to identify neuropathy [15, 16].

Some patients with nerve damage have no symptoms, whilst most part have extremely painful symptoms, such as burning pain, squeezing, constricting, freezing, allodynia or non-painful neuropathic deficits, such as asleep, tingling, numbness—loss of feeling—in the hands, arms, feet, and legs [11, 14].



Nerve complications can easily occur in different organ systems, including the digestive tract and cardiovascular system. In long term, unrevealed and untreated neuropathy is the main cause of foot infections that not heal, foot ulcers followed in many cases by inevitable amputation. Diabetic neuropathy is associated to 50-75% of non-traumatic amputations [14, 17].

### **3.2 – Pathogenesis and etiology of diabetic neuropathy**

According to Vinik *et al.* [14], diabetic neuropathy is among the least recognized and understood complications of diabetes despite its considerable negative impact on survival and quality of life.

Despite latest knowledge about pathophysiological mechanisms for numerous of the long term complications of diabetes, the exact pathogenesis of diabetic neuropathy continues unrevealed. Different multi-factorial mechanisms have been proposed to explain pathogenesis of diabetic neuropathy, but none has achieved general acceptance and approval [14, 16].

Risk factors for its development comprise diabetes duration, degree of hyperglycemia, hyperlipidemia, hypertension, and height. Retinopathy and nephropathy are highly associated with peripheral neuropathy, occurring in approximately 55% and 32% of type 1 and type 2 diabetic patients, respectively [11, 15].

Hypotheses regarding the multiple etiologies of diabetic neuropathy include a wide range of metabolic injuries to nerve fibers and vascular/ischemic sources. Autoimmune factors are also thought to play an essential role in the development of this nerve disorder. Main pathophysiological factors and mechanisms are summarized in Table 1 [11, 16].

In addition, neuro-hormonal growth factor lack, nutritional deficiencies and hereditary factors can lead to this disease. Often the condition is idiopathic, as no cause can be detected [11, 16].

**Table 1** - Classification of physiopathological factors of diabetic neuropathy [11].

<b>Metabolic</b>	Polyol pathway (aldose reductase) Glycosylation of essential proteins (glycation end products) Free radicals and oxidative stress Neuronal growth factors and insulin deficiency
<b>Vascular/Ischemic</b>	Basement membrane reduplication in vasa nervorum Reduced endoneurial blood flow Reduced endoneurial oxygen tension
<b>Autoimmune</b>	Auto-antibodies against adrenal medulla, sympathetic ganglia and vagal nerve Autonomic ganglia infiltrated by immune cells Calcium-dependent apoptosis of neuronal cells

### **3.2.1- Metabolic nerve injuries**

#### **Hyperglycemia**

Among the metabolic factors, hyperglycemia is doubtless the most frequent initiating factor. In hyperglycemia, excess of glucose is transformed to sorbitol via the enzyme aldose reductase (through the polyol pathway) leading to accumulation of sorbitol and reduction of myo-inositol in nerve tissue. This usually results in large nerve damages, which can happen at very early stages of diabetes. It has been suggested that duration and severity of exposure to hyperglycemia has a great impact on the severity degree of diabetic neuropathy [15, 16].

#### **Polyol pathway**

Hyperglycemic activation of polyol pathway may lead to significant changes in the NAD/NADH ratio, leading to direct neuronal injury and/or decreased nerve blood flow.

Increased glucose flux through the polyol pathways induces frequently peripheral nerve damages and modifications to the crystalline lens in the eye. In experimental studies, these metabolic alterations stimulate osmotic swelling and variation in sodium-potassium ATPase activity in diabetic nerves. A decrease in sodium-potassium ATPase activity can be associated to slowing of nerve conduction velocity [15, 16].

### **Oxidative stress**

Diabetes induces a substantial increase in the concentration of intracellular of glucose content, leading to a more intensive interaction between glucose and reactive oxygen species, which results in increased extracellular osmotic stress [14, 15].

Oxidative stress generally affects mitochondrial permeability, which activates the programmed cell death caspase pathways, inducing apoptosis of neurons and Schwann cells. Several neuronal growth factors and insulin itself promote survival and outgrowth of neurons. Nevertheless, due to apoptosis, the nerve regeneration is frequently impaired and signaling from the growth factors fails, causing irreversible permanent nerve damages and leading to peripheral neuropathy [15, 16].

### **3.2.2 - Vascular/Ischemic nerve injuries**

In the past years, diabetic peripheral neuropathy has been often associated with microvascular complications. Microangiopathy with endothelial dysfunction of the *vasa nervorum* is considered the main vascular factor causing conditions of ischemia and hypoxia in nerves of diabetic patients [11, 15].

Recent pathological studies of sural nerves of diabetic patients reveal several alterations, counting thickening of the endoneurial capillary basement membrane, capillary closure, endothelial cell hypertrophy and hyperplasia, and pericyte degeneration [11, 16].

Impaired vasodilatation of the vasa nervorum may lead to early and significant microangiopathic alterations, consequently causing narrowing of the capillary lumen, resulting in decreased capillary blood flow, hypoxia. This promotes a fast progression of neuropathy, accompanied by a gradual degeneration of myelinated and unmyelinated nerve fibers [11, 16].

As previously described, main factors are classified into two major subgroups: abnormalities involved in metabolic etiology and abnormalities that suggest a vascular etiology. Table 2 summarizes the hypothesis implicated in the pathogenesis of diabetic neuropathy [16].

**Table 2** - Most common abnormalities implicated in the pathogenesis of diabetic neuropathy (according to the two major proposed sub-groups) [16].

<b>Vascular etiology</b>	<b>Metabolic etiology</b>
Hyperglycemia	Hyperglycemia/hypoinsulinemia
Increased endoneural vascular resistance	Dyslipidaemia
Decreased nerve blood flow	Increased aldose reductase activity
Endothelial dysfunction	Decreased nerve Na/K ATP-ase
Advanced glycation of vessel wall	Decreased rate of synthesis and transport of intra-axonal proteins
Basement membrane thickening	Increased glycogen accumulation
Endothelial cell swelling and pericyte degeneration	Increased monoenzymatic peripheral nerve protein glycosylation
Closed and collapsed capillaries	Decreased incorporation into myelin of glycolipids and aminoacids
Occlusive platelet thrombi	Abnormal inositol lipids metabolism
Epineural vessel atherosclerosis	Decreased nerve L-carnitine level
Increased oxygen free radicals activity	Increased protein kinase C activity

### **3.2.3 – Autoimmune nerve injuries**

Diabetic neuropathy pathogenesis involves triggers that may activate different autoimmune mechanisms in susceptible individuals. Numerous studies suggest that autoimmune activation in both type 1 and type 2 diabetes results from the reaction of circulating antibodies with nervous autonomic tissue [15, 16].

Despite latest provided information, it is not clearly understood whether autoimmunity plays a major role in the pathogenesis; more probable, it accelerates peripheral neuropathy promoted by metabolic or vascular injuries. Autoimmune mechanisms may accompany hyperglycemia in order to progressively damage sensory and/or autonomic neurons [15, 16].

### **3.3 - Classification and characteristics of diabetic neuropathy**

Diabetic neuropathy is a descriptive term that includes a wide variety of abnormalities affecting substantially proximal and distal peripheral sensory as well as motor nerves and the autonomic nervous system. Simplest anatomical classification includes single (mononeuropathy), several (mononeuropathy multiplex) or general multiple nerve damages (polyneuropathy) [17, 18].

More detailed classification comprises numerous clinical and subclinical syndromes, which are known to be heterogeneous by their distinct anatomical distributions, symptoms, pattern of neurological involvement, clinical courses, risk covariates, pathological alterations, and certainly differing primary causes and underlying mechanisms [17]. Each syndrome can be characterized by diffuse or focal damages to peripheral somatic or autonomic nerve fibers, even though some indistinguishable cases may occur idiopathic or develop with other disorders in patients without diabetes mellitus. These are summarized in Table 3 [17-19].

**Table 3** - Classification of diabetic neuropathy [17, 19].

Type of diabetic neuropathy	Sub-types
Rapidly reversible	Hyperglycemic neuropathy
Distal symmetrical polyneuropathies (DSPN), (can occur with/without DAN)	Distal sensori-motor (chronic) polyneuropathy: <ul style="list-style-type: none"> <li>• Small fiber</li> <li>• Large fiber</li> <li>• Mixed</li> </ul> Acute (painful) sensory polyneuropathy variants
Diabetic autonomic neuropathy (DAN):	Abnormal pupillary function Sudomotor dysfunction Genitourinary Gastrointestinal Cardiovascular Hypoglycemia unawareness
Focal and multifocal neuropathies	Mononeuropathy Mononeuropathy multiplex Plexopathy Cranial neuropathy Thoracolumbar radiculoneuropathy Focal limb neuropathy Lumbosacral radiculoplexus neuropathy
Superimposed chronic inflammatory demyelinating neuropathy	N/A

### **3.3.1 – Diabetic distal symmetrical polyneuropathy (DSPN)**

DSPN is by far the most frequent of all diabetic neuropathies, affecting sensory more than motor nerves. This condition is mainly axonal with a mixed large - and small diameter nerve fiber involvement [16, 17]. Confirmation is normally achieved by nerve conduction studies (NCS). Axonal loss results in decreased amplitudes of the compound muscle action potential (CMAP) and sensory nerve action potential (SNAP). Demyelination cases are typically characterized by reduced nerve conduction velocity (NCV) and dispersion [16-20].

The predominantly large-fiber type symmetric polyneuropathies are principally characterized by loss of ankle reflexes, reduced position and vibratory senses, cold thermal perception and sensory ataxia. Large-fiber neuropathies may affect both sensory and motor nerves. These tend to be the neuropathies of signs rather than symptoms. Contrasting the small fibers, these are myelinated and fast conducting fibers. They appear to be affected first mostly due to their length and the predisposition in diabetes for nerves to “die back” (*phenomena* characterized by large extent of axon retraction)[16, 17].

DSPN represents a paradox: at one extreme there are patients with extremely painful neuropathic symptoms who on examination may have only a smallest deficit, whereas at the other extreme are patients with insensate feet who are asymptomatic and may initially reveal with foot ulcers. This neuropathy is an independent risk factor for mortality and morbidity as a result of foot ulceration and amputation [17, 18].

DSPN may be divided into the following two major types: acute sensory (atypical) neuropathy and chronic sensorimotor (typical) neuropathy [18].

Chronic sensorimotor neuropathy is thought to be the commonest variety of diabetic polyneuropathy, as reported from cohort and population-based epidemiological studies. Usually develops on a background of long-lasting chronic hyperglycemia, associated metabolic disorders and cardiovascular risk factors. Metabolic derangements that are also involved in the development include polyol shunting, accumulation of advanced glycation end products, oxidative stress, lipid abnormalities and micro-vessel alterations [18, 20].

Chronic neuropathy is regularly of severe onset and may affect up to 10% of patients with diabetes at the moment of diagnosis. Whereas up to 50% of patients with chronic neuropathy may be asymptomatic, 10–20% may experience worrying symptoms sufficient to justify specific treatment. This type is frequently accompanied by autonomic dysfunction. Its late damage, which encompasses foot ulceration, followed often by amputation, should in many cases be possible to prevent [18, 20].

The prevalence of chronic neuropathy increases with both age and duration of diabetes, and its diagnosis is more frequent in those whose glycemic control has been suboptimal in preceding years. An abnormality of nerve conduction, which is in many cases occurs without signs or symptoms of polyneuropathy, appears to be the first objective and quantitative indication necessary to confirm the diagnosis of this increasingly frequent form of polyneuropathy [18, 20].

Acute sensory neuropathy is a type characterized by acute or subacute onset associated with insidious sensory symptoms, typically with a small number of clinical signs. It differs from typical polyneuropathy in several significant features, such as onset, clinical course, manifestations, associations, and sometimes putative mechanisms [18, 20].

This atypical form can develop at any time during the life of a patient with diabetes mellitus. Onset of symptoms may be acute, subacute, or chronic, but the course is habitually monophasic or variable over time. It is usually caused by glycemic instability, such as ketoacidosis or even after the administration of insulin. Its symptoms improve gradually with the establishment of regular glycemic control and conventional symptomatic therapies [18, 20].



### **3. 3. 2 - Diabetic autonomic neuropathy (DAN)**

DAN is a subtype of the peripheral polyneuropathies that accompany diabetes, being one of the least recognized and understood complications of diabetes regardless of its considerable negative impact on survival and quality of life. Little is known about the epidemiology of this form in the different types of diabetes and much continues to be learned about its natural clinical course [21].

The reported prevalence of DAN is variable, depending on the type and number of tests performed and the presence or absence of signs and symptoms of autonomic neuropathy. The variance results from the different studies that have been carried out in the community, clinic, or tertiary referral center. Other causes that can be considered for the marked variability in reported prevalence rates comprise the lack of a standard definition of DAN, different diagnostic methods, variable study selection criteria, and referral bias. Additionally, the establishment of a more precise estimative is influenced by the existence of other confusing factors, like the wide diversity of clinical syndromes and confounding variables such as age, sex, duration of diabetes, glycemic control, diabetes type, and height [22].

Dysfunction of the autonomic nervous system it has been reported in about 20 to 40% of diabetics and it is not simply an “all or none” phenomenon. Diabetic autonomic neuropathy usually manifests first in longer nerves and occurs as a system-wide disorder involving the entire autonomic nervous system (ANS) [21, 22].

This condition affects significantly the vasomotor, visceromotor and sensory fibers that innervate every organ. Several organs are dually innervated, receiving an ample fibre supply from the parasympathetic and sympathetic divisions of the ANS. As a result, DAN is manifested by dysfunction of one or more organ systems, such cardiovascular, gastrointestinal, genitourinary, sudomotor or ocular [22].

Clinical manifestations of autonomic dysfunction and other micro-vascular complications frequently occur concurrently but in undistinguishable patterns. Clinical symptoms of

autonomic neuropathy usually occur long time after the onset of diabetes. Whereas symptoms revealing the autonomic dysfunction may be frequent they may often be due to other disorders rather than to true autonomic neuropathy. Subclinical autonomic dysfunction can, however, manifest within a year of diagnosis in type 2 diabetes patients and within two years in type 1 diabetes patients [22].

### **3.3.3 – Focal and multifocal neuropathies**

This group should not be considered a separated type, as they frequently co-exist with DSPN. Their etiologies are possible to differ, as these disorders have predominantly a vascular component or a compressive etiology, contrasting with the prominent metabolic component in DSPN. Factors that cause the development of the compression neuropathies are related to either the peripheral nerve itself or the structures adjacent to the point of compression [19, 23].

This group of rare neuropathies includes the following types: mononeuropathies (carpal tunnel syndrome, ulnar neuropathy, radial neuropathy, common peroneal neuropathy, and lateral femoral cutaneous neuropathy), cranial neuropathies (ocular neuropathies, facial neuropathies), diabetic amyotrophy and diabetic truncal neuropathy [23].

Carpal tunnel syndrome is the commonest entrapment neuropathy detected in diabetic subjects. It occurs as a result of median nerve compression under the transverse carpal ligament. Idiopathic carpal tunnel syndrome can be encountered in patients with rheumatoid arthritis, hypothyroidism, and obesity. In about 30% of diabetic patients, it can be diagnosed electrophysiologically, but represents a clinically significant problem in approximately 6% of diabetic subjects [23, 24].

Ulnar neuropathy is another frequent entrapment neuropathy (2.1%), occurring principally as a result of ulnar nerve compression in the cubital tunnel. It may also develop as a consequence of deformity at the elbow joint secondary to fracture or as a consequence of prolonged pressure during surgery. This disorder is often associated with alcoholism.

Typical symptoms are painful paresthesiae in the fourth and fifth digits related with hypothenar and interosseous muscle wasting [23, 25].

Radial neuropathy occurs rarely (0.6%), as a result of radial nerve compression in the spiral groove. This type reveals characteristic motor deficits of wrist drop with extremely rare sensory symptoms of paresthesiae in the dermatomes supplied by the superficial radial nerve. Main causes of idiopathic radial neuropathy are humeral fracture, blunt trauma over the posterolateral aspect of the arm, and external compression [23, 26].

In the case of cranial ocular neuropathies, cranial nerves III, IV, and VI are mainly affected. Among diabetic patients, the relative injury frequency is greater for oculomotor and abducent nerves (3.3%), while for the trochlear nerve is smaller (2.1%). The causal pathology and pathogenesis of this type remains incompletely understood, due to the difficulties in obtaining tissue in such patients. Nevertheless, several studies postulate that focal demyelination occurs as consequence of ischemia [23, 27].

The typical presentation of oculomotor nerve palsy consists in an acute onset of diplopia, followed by papillary sparing related with ipsilateral headache. Pupillary sparing is often used for differentiating diabetic from other structural ophthalmoplegias (such as aneurysm, tumor, or mass). Approximately 14 – 18% of diabetic subjects reveal pupillary dysfunction [23, 27].

### **3.4 – Diagnosis of diabetic neuropathy**

In the past years, detection of DPN has been difficult, for the reason that this disorder affects a broad variety of nerve fibers. For diagnosis is necessary to identify and assess various features of neuropathy [28].

In general, experienced physicians can diagnose and systematically assess neuropathic signs and symptoms of peripheral neuropathy, involving sensory, motor and reflex measures of upper and lower extremities, cranial nerves and autonomic function [19].

The diagnosis of diabetic neuropathy implies also the exclusion of non-diabetic causes, such as metabolic, hereditary, nutritional deficiency, immunological, and toxic causes [19, 28], all explained in Section III, Chapter 6.

Although trained neurologists can diagnose neuropathy with a clinical examination, an enormous discrepancy in diagnostic criteria exists in the literature. The American Academy of Neurology in conjunction with the American Association of Electrodiagnostical Medicine and the American Academy of Physical Medicine and Rehabilitation established general rules and definitions in order to standardize and facilitate clinical research and epidemiologic studies [14, 29].

Accordingly, to obtain a precise diagnose and classification of neuropathy, usually it is required a combination of neuropathic clinical symptoms, clinical signs and electrophysiological studies and findings. Quantitative sensory testing (QST) and autonomic function testing are used in order to provide an extremely accurate diagnosis of peripheral neuropathy, being very useful in characterizing neuropathic expression [28, 29].

Additionally, other rigorous assessment techniques such as NCS, sural nerve biopsy, skin biopsy for evaluation of intra-epidermal nerve fibers, can be performed using appropriate testing conditions, suitable criteria and reference values to address well-defined clinical or research questions [28, 30]

#### **3.4.1 - Clinical examination of DPN**

Currently, screening for neuropathy is normally performed during a patient's routine clinical examinations. Recommendations and suggestions for screening, follow-up and management of this problematic nerve disorder are included in the International Guidelines for Diagnosis and Outpatient Management of DPN and are presented in Table 4 [28, 31]. It is important to mention that these guidelines were rigorously followed during all clinical examinations of our study.

**Table 4** - Guidelines for Diagnosis and Outpatient Management of DPN [28].

<b>Annual Review Assessment</b>	
<b>Patient history</b>	Age, diabetes, physical factors, lifestyle, social circumstances, symptoms, other possible etiological factors
<b>Examination of both feet</b>	Skin status, sweating, infections, ulceration, calluses/blistering, deformity, muscle wasting, arches, palpitation for temperature, pulses, joint mobility
<b>Vascular examination</b>	Check foot pulses
<b>Other</b>	Thyroid function to exclude other etiologies for neuropathy, presence or absence of characteristics of the “at-risk foot”

In most cases, a simple clinical examination is a fine predictor of future foot ulceration, detecting typically a symmetrical sensory loss. The feet are normally examined for ulcers, calluses and deformities [32-34].

The clinical examination includes several tests of peripheral sensation, tendon reflexes, and muscle strength. Neuropathic symptoms with distal sensory loss, absent tendon reflexes, and abnormal nerve conduction studies are highly suggestive of diabetic neuropathy [14, 31].

Diabetic patients have frequently difficulties in describing the symptoms of neuropathy, as they are different than the usual pain that they have before experienced. There is an obvious variation in the description of symptoms between persons with similar pathological injuries. When evaluating symptoms in clinical practice, doctors must not “interpret” or “translate” patient reports; instead, they should record accurately the patient’s description word for word [31-34].

### **3.4.2 - Scoring of signs and symptoms in DPN**

In the last decades, several scoring systems have been proposed to quantify clinically neurological deficits and consequently, identify the presence of neuropathy and also classify its severity degree. Each scoring system has its specific scheme, based on particular scoring scale [28, 32].

#### **Neuropathy Disability Score**

This approach for assessing the clinical signs was originally pioneered by Dyck *et al.* [35] in the Mayo Clinic, who described the Neuropathy Disability Score (NDS). They designed an efficient scheme to detect and grade diabetic peripheral neuropathy.

In the NDS, impairment of sensation to pain, vibration and joint position, muscle strength in the face, torso and extremities, tendon reflexes of the upper and lower extremities are separately scored, and all scores are summed to give a compound score of neurological deficits [35]. Based on a scale of 0-4 (0 = no deficit, 1 = mild deficit, 2 = moderate deficit, 3 = severe deficit, and 4 = complete absence of function or the most severe deficit), this grading system may be used in epidemiological studies and clinical trials, as well as in clinical practice [32, 35].

Although it provides an accurate, comprehensive and reproducible measure of the severity of diabetic neuropathy, this scoring system requires a well-trained neurologist who can correctly assess muscle strength and grade the severity of sensory deficits, limiting the role of this valuable research tool in daily clinical practice [35, 36].

#### **Modified Neuropathy Disability Score**

A modified NDS has been used in many important studies and has been reported as predictor for future foot ulceration. This method, first described by Young *et al.* [38], can

be definitely performed by a non-specialist, providing a sum of the sensory and reflex deficits [37, 38].

The sensory score derives from a complete evaluation, including pain (pin prick), touch (cotton wool), cold (tuning fork immersed in icy water), and vibration (128 Hz tuning fork). Each modality is scored from 0 to 5, according to the anatomical level at which sensation is affected. The average of both feet is calculated and the total of all four deficits represent the sensory score [32, 38].

The reflex score is obtained from the knee and ankle reflexes on a scale from 0 to 2 (0 = normal, 1 = elicited with reinforcement and 2 = absent). A final score from 1 to 5 represents a mild degree, 6–16 moderate, and 17–28 severe grading for neuropathies. Additionally, a more simplified scheme of the modified NDS that varies from zero (normal) to 10 (maximum deficit score) also indicates precisely a total loss of sensation to all sensory modalities and absent reflexes, as shown in Table 5 [32, 38].

**Table 5** – Modified NDS [32].

<b>Neuropathy Disability Score (NDS)</b>			
		<b>Right</b>	<b>Left</b>
<b>Vibration Perception Threshold</b> 128-Hz tuning fork; apex of big toe: normal = can distinguish vibrating/ not vibrating	Normal = 0 Abnormal = 1		
<b>Temperature Perception on Dorsum of the Foot</b> Use tuning fork with beaker of ice/warm water			
<b>Pin-Prick</b> Apply pin proximal to big toe nail just enough to deform the skin; trial pair = sharp, blunt; normal = can distinguish sharp/not sharp			
<b>Achilles Reflex</b>	Present = 0 Present with reinforcement = 1 Absent = 2		
	NDS Total out of 10		

### **Reflex testing**

Traditionally, in neurology are tested all reflexes, while in the assessment of peripheral neuropathy is more frequent to test only the ankle reflexes. These are the most sensitive reflexes to early nerve injury, being usually reduced or absent. However, this method is a very poor predictor for ulceration [28, 31].

The examiner usually dorsiflexes the foot and softly strikes the Achilles tendon with a reflex hammer, repeating the procedure with reinforcement in case of reflex absence. Typically, the scores for the reflex testing are: 0 for absent, 1 for present but decreased, 2 for normal, 3 for increased and 4 for increased with clonus [28, 33].

### **Superficial pain testing (Pinprick)**

Pain sensation can be efficiently tested with a sterilized safety pin. The site of testing is chosen according to a specific algorithm (or neuropathy score) [28]. Most commonly are tested the dorsum and the plantar aspect of the great toe of each foot, applying the stimulus (pinprick) once per feet and asking the patient to identify and describe the sensation, scoring precisely the obtained results. However, this screening method is highly subjective and thus, insufficiently reproducible. For this reason, must be used in combination with other measures [28, 33-34].

### **Vibration Testing**

Vibration threshold perception is another measure used for an accurate evaluation of nerve function. Usually, vibration sensation is measured with a 128-Hz tuning fork, or less frequently with 64- and 256-Hz tuning fork. This method relies especially on examiners experience, revealing a variable correlation with quantitative tests. Physicians must take into account factors like age and body surface area when identifying eventual nerve abnormalities [28, 39].



Although this measure can be highly subjective in grading the neuropathy severity, the absence of vibration perception at the great toe is considerably correlated with development of foot ulcers [28, 33].

### **Temperature Perception**

This simple and inexpensive method requires minimal training and can be performed by nonmedical staff. Heat and/or cool sensation are generally measured with a tuning fork immersed in warm and/or icy water, respectively. This measure relies also on examiners experience and can be highly subjective, requiring additional procedures [28, 31].

### **Neuropathy Symptom Score (NSS)**

This score for defining and assessing symptoms was also developed by Dyck and his colleagues [40]. NSS includes proximal and distal symptoms of muscle weakness, sensory disturbances such as pain, numbness, unsteadiness in walking, and less frequently symptoms of autonomic neuropathy, such as impotence, orthostatic hypotension, nocturnal diarrhea [21, 32].

Many patients report deep aching pain, a burning sensation, “knife-like”, sharp electrical “shock-like” pain, freezing, or a more continuous squeezing and hurting feeling (pressure myalgia). These symptoms are known as positive sensory symptoms because of evident “hyperactivity” of nerves and perceived as a presence of something that is usually absent [21, 32].

Negative sensory symptoms encompass “asleep”, “tingling”, “prickling”, “numbness,” “wooden, rubber, or dead feet” feeling and frequently used descriptors are “a wrapped feeling,” “retained sock feeling,” “cotton wool under soles,” and so on. Hyperalgesia and allodynia are also familiar neuropathic sensory symptoms and are defined as hypersensitivity to a normally mild painful stimulus and painful sensation induced by a normally non-painful stimulus, respectively [21, 32, 40].

In the greater part of diabetic patients both positive and negative sensory symptoms form a complex, acting simultaneously. Usually, these symptoms are identified by systematic questioning, as spontaneous reporting seems to point the positive symptoms [21, 32-34].

In most cases, composed neuropathic symptoms (painful and non-painful) are more accurate than single symptoms in diagnosing peripheral neuropathy. A total of 17 symptoms are graded in the NSS (0 = absent and 1 = present) [40].

### **Toronto Clinical Neuropathy Scoring System**

This clinical scoring system comprises a number of simple screening tests that provide an accurate diagnosis of neuropathy in outpatient clinics. The Toronto group has validated this simplified scoring system (Table 6) against neurophysiological and pathological deficits obtained on sural nerve biopsy, concluding that it can be certainly used to document and monitor diabetic peripheral neuropathy [41, 42].

**Table 6** - Toronto Clinical Neuropathy Scoring System [41, 42].

<b>Symptom scores</b>	<b>Reflex scores</b>	<b>Sensory test scores</b>
Foot Pain Numbness Tingling Weakness Ataxia Upper-limb symptoms	Knee reflexes Ankle reflexes	Pinprick Temperature Light touch Vibration Position
Symptom scores: present, 1; absent, 0. Reflex scores: absent, 2; reduced, 1; normal, 0. Sensory test score: abnormal, 1; normal, 0. Total score ranges between 0 and 19.		

Diabetic patients are precisely questioned as to the presence or absence and specific characteristics of neuropathic symptoms in the feet and upper-limbs, and the presence or absence of unsteadiness when walking, as shown in Table 6 [41, 42].

This recent score highlights more the sensory symptoms and deficits as opposed to motor deficits. Sensory testing is usually performed on the first toe and graded as normal or abnormal while knee and ankle reflexes are graded as normal, reduced, or absent [41, 42].

### **Michigan Neuropathy Screening Instrument (MNSI)**

Several questionnaires can be helpful in screening patients for DPN. The MNSI is a combination of a symptom score (15-item questionnaire) and a physical examination score. The combination of these two scores results in valid and highly predictive value [43, 44], justifying the choice for our study.

The MNSI questionnaire can be used only as complementary method for the physical examination. Any methodology used for the identification, evaluation and documentation of neuropathic signs and deficits, must undoubtedly involve physical exam of the lower limbs, which remains the main aspect in the clinical diagnosis of DPN [44, 45]

In our study, this brief questionnaire was used additionally as a simple screening tool for a more accurate diagnosis of diabetic peripheral neuropathy. All patients were asked to answer this questionnaire, allowing a more precise evaluation of the severity degree of diabetic neuropathy according to the MNSI, which has been developed specifically for distal diabetic polyneuropathy [44].

### **3.4.3 - Neurophysiologic examination**

Nerve conduction studies (NCS) and quantitative sensory testing (QST) are methods used in both routine clinical practice and in clinical trials for examining the peripheral nerve function.

Neurophysiologic assessment (used in our study to differentiate precisely patients according to their severity), mostly NCS and electromyography, are often used in suspected disorders of the peripheral nervous system. These unique techniques, with surface electrodes for nerve stimulation and evoked potential recording, can competently determine the impulse activity of the largest and fastest conducting sensory and motor myelinated nerve fibers [45].

### **Nerve conduction studies (NCS)**

NCS are electrophysiological studies, frequently used in clinical practice to assess and follow-up suspected DPN and other neuromuscular disorders. NCS are the most informative method of the neurophysiologic examination, and their inclusion certainly adds a higher level of specificity to the diagnosis [29]. For this reason, all controls and patients included in our study underwent electrophysiological assessment.

In many cases, these studies are not required for the diagnosis of DPN. Most medical doctors reserve the use of this method to cases with symptomatic, confusing, unusual or severe neuropathy [29].

NCS can be requested in atypical cases of neuropathy in diabetic patients, which might suggest other forms of neuropathy. NCS can be also performed in rapidly progressing limb weakness, asymmetric/multifocal signs (suspected vasculitis), or a family history of neuropathy/feet deformities (suspected Charcot-Marie Tooth neuropathy) [14, 29].

NCS are extremely valuable, as they are non-invasive, objective, and standardized, providing a highly sensitive measure of the functional status of sensory and motor nerves. Both afferent and efferent nerves can be tested; therefore, motor and sensory neuropathies can be accurately diagnosed [45-47].

This method can determine precisely the distribution of abnormality (focal, multifocal, or diffuse) and whether the pathophysiology is mostly segmental demyelination or axonal degeneration [46, 47].

NCS results in reliable, reproducible, and form initial objective outcome measures in trials evaluating pharmaceutical treatment of DPN. Nevertheless, they must be performed in triplicate samples and by trained individuals [46-48].

This useful method consists from an action potential elicited by stimulating the nerve and conducted along a motor or sensory axon. In the normal healthy nerve, the electrical pulse propagates with a NCV of approximately 50–70 m/s. In our study, NCV propagated with 50-55 m/s in healthy controls, whilst varied between 34 and 46 m/s in diabetic patients, according to their DPN status. The NCV value can be measured with great accuracy and objectively used to verify the presence, degree of severity, and level of peripheral nerve dysfunction [14, 48].

The results of NCS usually show amplitudes, distal latency of compound muscle action and sensory potentials, conduction velocity of fastest conducting fibers and minimal F-wave latencies. Hence, these studies are appropriate for longitudinal and population evaluations [28, 45].

The most important measured parameter remains the maximum nerve conduction velocity (NCV) for the segment of nerve between the stimulating and recording electrodes. The amplitude and configuration of the resulting signals are also essential, showing the combined motor action potential (CMAP) evoked from motor fibers and the sensory nerve action potential (SNAP) evoked from sensory fibers [45, 46].

The major factors that are considered to influence NCV are the integrity and degree of myelination of the largest fibers, the mean axonal cross-sectional diameter, the representative inter-nodal distance and the distribution of nodal ion channels [32, 49].

Large diameter axons loss is the principal structural deficit responsible, leading inevitably to a significant reduction of the sensory nerve action potential and compound motor

action potential. Demyelination produces a profound deficit in NCV and increases dispersion. However, it has been suggested to have only a minor influence in slowing of NCV in DPN [48, 49].

In some cases, NCS do not correlate well with symptoms and signs. Several electrodiagnostical abnormalities reproduce metabolic changes that are not associated with symptoms or some symptoms and signs are not clearly connected with electrophysiological variations [28, 45]. Moreover, A $\delta$ - and C-fiber activities cannot be tested with this technique, neither with electromyography. Decreased NCVs or loss of CMAP or SNAP amplitudes, typical signs of peripheral nerve disease either focally or generally, occur mainly as a result of large fiber dysfunction [45].

Moreover, maximal NCV reflects many times incomplete features of neural activity of a small group of large diameter and heavily myelinated axons. This diagnostic method is also insensitive to early functional changes such as a decrease of Na<sup>+</sup>/K<sup>+</sup> ATPase activity. Despite these obvious limitations, numerous consensus panels have highly recommended the addition of entire nerve electrophysiological testing (NCV, F-waves, sensory, and/or motor amplitudes) in multicentre clinical examinations of human DPN [32, 45].

### **Electromyography (EMG)**

EMG is the assessment of muscle activity, frequently used for testing the muscle and motor nerve fiber activities. Atypical EMG characteristics, such as acute or chronic denervation, can be attributed to a substantial loss of large motor nerve fibers, also focally or generally [45].

When a patient with neuropathic pain reveals acute or chronic abnormalities, these can be used to support the clinical impression of injury to a specific peripheral nerve or to peripheral nerves in general as in a DPN, or even diabetic or alcoholic neuropathy. Nevertheless, DPN or focal nerve lesions with only small-fiber contribution can show normal NCVs and EMG values, despite considerable nerve damage and neuropathic pain [45-48].

#### **3.4.4 - Quantitative sensory testing (QST)**

QST is used with increasing frequency, particularly in clinical therapeutic trials, being one of the sensory measurement techniques necessary for neurological evaluation. This method can determine accurately absolute sensory thresholds for pain, touch, vibration, and hot and cold temperature sensations [28, 45].

QST aids in diagnoses by investigating and assessing the peripheral nerve function in specific fibers, such as large myelinated A $\beta$  (vibration detection), small thinly myelinated A $\delta$  (cold, cold-pain) and small unmyelinated C (heat, heat-pain) afferent nerve fibers. This extremely useful method is well accepted due its simplicity, non-invasiveness and non-aversiveness. It allows a precise differentiation between peripheral neuropathy and mononeuropathy [28, 45].

QST systems usually measure the threshold of diverse stimuli related to different neuroanatomic pathways. Elevated sensory thresholds are associated with sensory loss, while lowered thresholds reveal allodynia and hyperalgesia [45].

In a generalized peripheral neuropathy usually all QST thresholds show high values, suggesting that all fiber types are affected. When occurs dissociation, with normal vibration thresholds while other thresholds are abnormal, the presence of a small-fiber neuropathy is alleged. In asymptomatic patients, atypical thresholds are evidence of subclinical nerve damage [45].

There are typically two types of devices that are commercially available: those that produce specified vibration or thermal stimuli, and those that send electrical impulses at certain frequencies. These devices can vary from handheld simple tools to more expensive and sophisticated computerized equipment with complex testing algorithms, standardization of stimulation and recording measures, and comparisons to age- and gender-matched control values [28, 45].

Generally, the testing procedure encompasses two main methods for the threshold detection: the method of limits and the method of levels, both requiring cooperation from the patient. The method of limits implies a generation of increasingly and consecutively decreasingly strong stimuli, being the patient that indicates the first onset of sensation. With the second method, are tested specific levels with the patient reporting if the stimulus is identified [50].

In the method of limits, as already described, the subject is exposed to stimulus with changing intensity. The practical performance of this measurement is frequently influenced by a reaction time artifact which is almost irrelevant for fast conducted sensations, while for relatively slower conducted thermal sensations affects substantially the value of threshold. Reaction time artifact is more significant for warming than cooling, given that the primary afferent nerves are slower conducting. Its undesired effects can be simply reduced by using a slow rate of temperature variation [51].

In the method of levels a specific stimulus of preset intensity and duration is rapidly delivered to the subject, who subsequently describes the sensation. Although free from reaction time artifact, this estimating test lasts inevitably longer than the method of limits, by using series of constant stimuli [51].

The full duration of the method of levels is definitely determined by the device used to stimulate and obtain the subject's response. In many cases, this method is considered to be more suitable than the method of limits, especially in the assessment of thermal perception thresholds in complex regional pain syndromes [51].

In summary, the method of limits proposes a short and quick test, with higher absolute thresholds and highly sensitive results, many times affected by artifacts. Whereas for the method of levels, this represents a longer test, providing accurate results, but with reduced sensitivity for disease detection or greater test–retest reproducibility [50, 51].

In both described methods the sensory stimulus is an objective physical event, while its response usually is a subjective description from a patient or control subject. If the reported value is abnormal, this represents an obvious but complex sign of nerve



dysfunction, being located anywhere along the sensory pathway between the receptor apparatus, the primary sensory cortex, and the association cortex [50, 51].

Additionally, psychological factors play a significant role in sensory function perception. Consequently, QST differs from NCS in which the stimulus generates a precise evoked response that is generally more objective and independent of cooperation from the patient [50, 51].

### **3.4.5 - Other methods of assessment**

#### **Sural nerve biopsy**

Nerve biopsy usually is a useful method in the diagnosis of inflammatory nerve complications such as vasculitis, sarcoidosis or infiltrative disorders such as tumor or amyloidosis [14, 52].

Sural nerve biopsy, has been used in the past years in the study of peripheral neuropathy, mostly when the etiology is undisclosed or in patients with diabetes with atypical neuropathies [52].

However, this method is not normally accepted for the detection of DPN, because is an invasive procedure with well-identified consequences, which include persistent postoperative pain at the site of biopsy, sensory complications and deficits in the nerve distribution and allodynia, particularly in diabetic patient [53].

According to a report published by the American Academy of Neurology (AAN), the American Academy of Neuromuscular and Electrodiagnosical Medicine (AANEM), and the American Academy of Physical Medicine and Rehabilitation (AAPM&R), sural nerve biopsy is less suggested for the detection and the evaluation of peripheral neuropathy [14, 29].

This method can demonstrate the loss of myelinated and/or unmyelinated nerve fibers and segmental demyelination. It also reveals endoneurial microangiopathy characterized

by basement membrane thickening, pericyte degeneration, endothelial cell hyperplasia and luminal narrowing. However, these pathological modifications can be certainly shown with both clinical and neurophysiological examinations of peripheral neuropathy [14, 54].

Hence, there are no indications or recommendations regarding the use of sural nerve biopsy in the evaluation of DPN. This method has been more valuable for the detection of mononeuropathy multiplex or suspected vasculitic neuropathy [53, 54].

Furthermore, the need to repeat contra-lateral nerve biopsy and many other questions on the utility and reliability of this invasive method used to assess axo-glial dysfunction and axonal atrophy has led to serious doubts regarding its use as an end point in any future trials of human DPN [32].

#### **Skin biopsy and quantification of intra-epidermal nerve fibers (IENF)**

Another less invasive and more sensitive method than sural nerve biopsy, which is well-accepted in several clinical trials, is a 3-mm skin biopsy. Skin biopsy has been frequently used in the past years for investigating DPN, and has revealed to be a useful diagnostic tool in small fiber neuropathy. This technique allows a direct study of small nerve fibers, requiring several neuronal markers, such as neuron-specific enolase and somatostatin, or cytoplasmic axonal markers, used to immunostain skin nerves [29, 55].

Skin biopsy enables a detailed visualization and a reliable identification of early alterations in the most distal nerves, confirming many times the earliest damage. This method includes the use of formalin-fixed frozen sections for an accurate quantification of (IENF) density, as number/length of epidermis in patients with impaired glucose tolerance (IGT) and sensory neuropathy [55, 56].

The quantification of IENF density is a sensitive evaluation for different body sites, age, and gender. Reduced IENF density has been detected in both type 1 and type 2 diabetes, as well as in IGT. In several studies were used skin biopsies at multiple sites, revealing a

diminution in IENF density from proximal to more distal sites. This fact suggests that small nerve fibers reduction occurs in a length-dependent way [57, 58].

Assessment of IENF density appears to be a reproducible and diagnostically sensitive method. This valuable technique can clearly show any loss of small-diameter nerve fibers in patients with complaints of burning pain in their feet, in cases when nerve conduction studies and clinical examination reveal normal results [57, 58].

In 2005, was published a guideline by the European Federation of Neurological Societies (EFNS). It describes the use of skin biopsy in DPN and includes recommendations on several methods for tissue processing and quantification of IENF, containing normative data and correlations with other clinical, electrophysiological, and morphologic tests. Moreover, the EFNS concluded that morphologic nerve fiber changes, such as axonal swellings, may reveal the progression of peripheral neuropathy, but additional studies are required to determine their diagnostic accuracy [59].

Recent studies have associated IENF density with other measures of DPN, showing a significant correlation between decreased nerve fiber lengths in the dermis and slowing of sural NCV. Additionally, IENF density in the distal leg has been revealed to correlate with heat and cold perception threshold, heat pain, touch and pressure sensation, and total neurological disability score (NDS). Hence, skin biopsy and IENF quantification could be used in many cases as a complementary method to confirm the obtained results [60-62].

### **Quantitative sudomotor axon reflex testing (QSART)**

In the past years, sophisticated methods, such as axon reflex, magnetic resonance imaging and corneal confocal microscopy were moderately used in clinical trials, and very often used in research environment [32].

The quantitative axon reflex technique is chosen in cases when is necessary to evaluate the postganglionic axon function of the sudomotor system. The axon reflex can be

obtained by stimulating the pain nerve fibers or through iontophoresis of acetylcholine, which controls and stimulates the release of nitric oxide through the axon reflex [63, 64].

This technique has demonstrated to be extremely sensitive in the detection and evaluation of DSPN, showing to be efficient in identifying early nerve injuries of neuropathy. Several recent studies have exposed that the neurovascular response mediated by the nerve axon reflex is lower in diabetic neuropathic patients. This less common method appears to correlate with different nerve function measurements, showing reasonable sensitivity and specificity in identifying and classifying patients with DPN [64, 65].

### **Magnetic Resonance Imaging (MRI)**

MRI has been used in some cases to demonstrate that subjects with DPN have a reduced cross-sectional spinal cord area than healthy controls in the cervical and thoracic regions. Nevertheless, progression or regression of this abnormality has not been assessed in possible studies. As a result, the possible use of this expensive and sophisticated method as an end point in clinical trials of human DPN remains to be confirmed by future works [32, 66].

### **Autonomic system testing**

Quantitative testing of ANS is a complex process and has represented during many years the main measurements of motor nerve function and sensory nerve function failure. Unfortunately, the indifference in the development of this type of measures was partly due to the incorrect but commonly shared opinion that autonomic neuropathy was merely a small and moderately obscure contributor to the peripheral neuropathies affecting patients with diabetes [25, 67].

In patients with diabetes, autonomic dysfunction can occur in two possible ways: as autonomic neuropathy accompanied by a structural injury of the peripheral nerve fiber and/or functional deficit without any identified structural lesion [67, 68].

## CHAPTER 4 – CORNEAL CONFOCAL MICROSCOPY

### 4.1 - Introduction

In the last thirty years various clinical techniques for assessing the living human cornea at the global and cellular level have progressed considerably, being frequently used to diagnose disease, disordered function or disability. These methods include specular microscopy, computerized corneal topography, high frequency ultrasound and *in vivo* corneal confocal microscopy (IVCCM) [4].

IVCCM imaging of the cornea has shown an exponential development over the last two decades. This technique emerged from the laboratory and it has progressively been used more in the clinical setting to evaluate inherited corneal diseases, corneal infections, contact lens wear and the effects of corneal surgery. This exponential progress has led to considerable improvement and enrichment of our knowledge of the human cornea in both its physiologically normal and pathological states. In the past years, numerous research studies have investigated the corneal nerves using IVCCM [69-71].

Modern IVCCM represents a non-invasive technique for obtaining high-resolution optical images from all corneal layers and membranes. This method is increasingly used for examining the living human cornea in normal healthy or pathological conditions, being an extremely useful clinical and research tool. The main characteristic of CCM is its ability to produce in-focus images of thick specimens, a process known as optical sectioning. High-quality images are obtained point-by-point (in some cases, line-by-line) and then reconstructed [69, 70].

IVCCM is also a fast technique, allowing “a prospective and reiterative assessment of the human cornea at high magnification” (Quoted from [70]). This sophisticated method can be unquestionably used to analyze the cellular constituents of the cornea, enabling the detection of slightest changes in characteristics of corneal nerves in DPN [71, 72].

In brief, most recent research studies on corneal disorders and dysfunctions, induced by diabetes, used preferentially IVCCM. The main reason for using this technique is the fact that it allows sequential observations of the corneal sub-basal nerve plexus, giving information comparable or even superior to that obtained with histopathological examination. Furthermore, it provides detailed morphological characteristics of corneal nerves permitting quantification of corneal nerve morphology in normal and diabetic subjects [70-72].

#### 4.2 - Principles of confocal microscopy

The principle of confocal microscopy was originally invented Marvin Minsky in 1955, and patented in 1961. His first prototype, known as the “double focussing stage scanning microscope”, allowed examination of tissue specimens [4, 73].

CCM technique is based on an essential principle in its design, enabling optical sectioning of a quite thick, light scattering object, such as the human cornea. Its basic principle consists in the use of the same objective for two different roles in the process of acquiring a corneal image. For a better understanding of this concept, the principle of this technique is schematically illustrated in Figure 3 [4, 74].

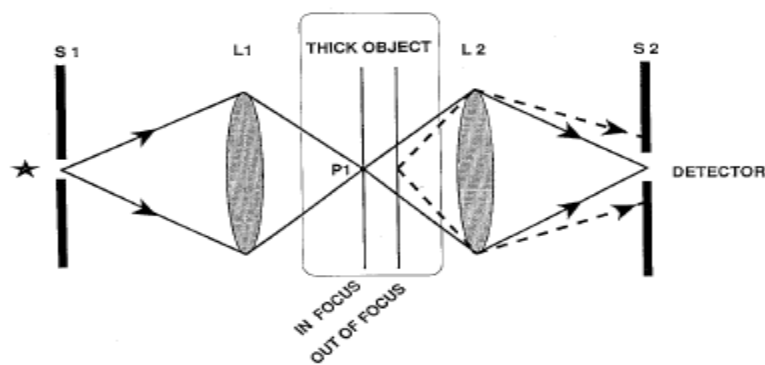


**Figure 3** - Illustration of the principle of confocal microscopy [74].

The schematic representation of Figure 3 shows two separate objectives on each side of the thick specimen. The objective on the left side of the thick object is used for the illumination, while the other on the right side plays the role for collecting the scattered light and forming the image. In this scheme, a point source of light originated in the aperture S1 passes through the lens L1, which focuses this light onto a tiny spot in object, at the lens focal plane. The lens L2 is located in such a way that its focus is situated in the same focal plane as L1. Consequently, L2 yields an image of the small spot at the aperture S2 and all the light that passes through L2 is detected at S2 [74].

Unlike the schematic model, contemporary confocal microscopy systems use only one objective, which, similarly to the described scheme, illuminates a given point of the examined specimen, collecting afterwards the scattered light from the illuminated point. Light is passed through a tiny aperture and focused by an objective lens onto a small area of the specimen. The light is then scattered from the specimen, passing through the objective lens. This light is focused onto a second aperture which is set in a particular way that out of focus light is eliminated. The reflected light is detected by a photo-detector, like a photodiode, an avalanche photodiode or cameras based on a charge-coupled device (CCD camera) [4, 75].

The ability of this system to discriminate the light coming from out of the focal plane generates images of higher lateral and axial resolution compared to conventional microscopy. The main limitation of this system is its small field of view. Nevertheless, it is possible to obtain a larger field of view by scanning the examined specimen. This can be done either by moving the specimen while the microscope remains still, or by moving the confocal system over a fixed specimen [4, 75].

Generally, IVCCM systems move over a stationary sample. The speed at which a single image of the field is obtained determines the microscope's temporal resolution. High temporal resolution is extremely important and is undoubtedly preferred, given that poor resolution is frequently associated with amplified motion artifacts. These artifacts are originated by the involuntary movements of living human subjects during their examination. These unintentional and undesired movements are inevitably caused by pulse, respiration, and eye movement [4, 74-75].

Another important feature that can seriously influence the acquired images is the spatial resolution. It is defined as the smallest distance between two separated points that can be identified and is usually quantified through the Rayleigh Criterion. Higher resolution, which corresponds to lower value of Rayleigh Criterion, is an important requirement for the examination of small corneal structures [74, 75].

In CCM, two types of resolution are usually evaluated: axial and transverse resolution. Axial resolution, also known as depth, is the resolution in direction parallel to the light beam (smallest distance between two separate points along the light beam axis). High value of axial resolution in confocal microscopy can improve the image quality by about 40%, when compared to other conventional techniques. Transverse resolution, also called lateral resolution, is the smallest distance between two different points in direction perpendicular to the light beam axis. Transverse resolution depends on the  $xx$  and  $yy$  coordinates in the plane of a thick object, while axial resolution depends on the  $zz$  coordinate, orthogonal to the plane of the object [74, 75].

### **4.3 - Types of confocal microscopes**

During the last three decades, the original CCM has passed through numerous modifications and developments, resulting in different types of microscopy techniques and microscopes. The most important types are: Tandem Scanning Confocal Microscope (TSCM), Slit Scanning Confocal Microscope (SSCM) and Laser Scanning Confocal Microscope (LSCM). All three types are briefly described in the following paragraphs.

#### **4.3.1 - Tandem Scanning Confocal Microscope (TSCM)**

The TSCM comprises a rotating Nipkow disk with a high number of pinholes (for example, 64.000) distributed in Archimedian spirals. Each pinhole has a corresponding conjugate pinhole diametrically opposite to it on the disk (Figure 4). The Nipkow disk spins extremely fast, depending on the microscope model (for example, 900 rotations per minute), with



the illuminating light passing through numerous pinholes at the same time, and with the reflected light passing through the conjugate pinholes. This fast disk rotation allows a complete scanning of the entire specimen, in a time interval compatible with video signal requirements [76].

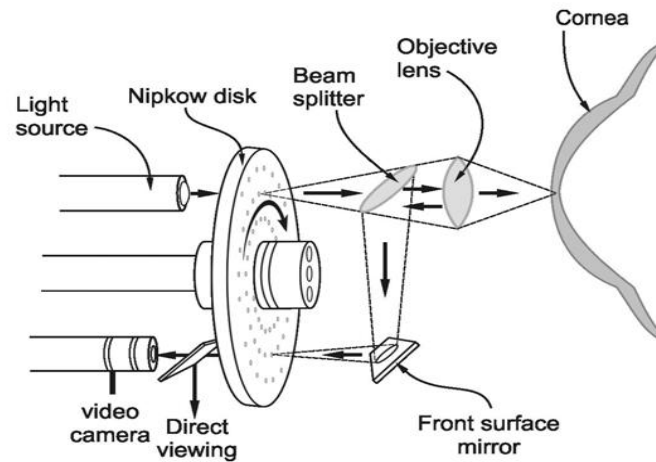


**Figure 4** – Schematic illustration of the optical pathway used in TSCM [76].

TSCM is limited by the ratio of the holes to the disk area, which is very small (approximately 1-2%). Consequently, only a small part of the illumination light reaches the specimen, reducing also the fraction of scattered light. Decreased fraction of both illumination and scattered light results in a poor image quality and/or longer acquisition times for a given signal-to-noise ratio. Although less recommended for weakly reflecting specimens (such as human cornea), this scanning system was already used in several research works for studying and evaluating the human corneal morphology, mainly due to the real-time operation at high image acquisition rates [77].

#### **4. 3. 2 - Slit Scanning Confocal Microscope (SSCM)**

The SSCM system is based on two adjustable and optically conjugate slits used for illumination and detection of reflected light. A fast moving two-sided mirror scans the complete image of a slit onto the microscope objective and de-scans the reflected light from the specimen. This principle is schematically represented in Figure 5 [74, 75].

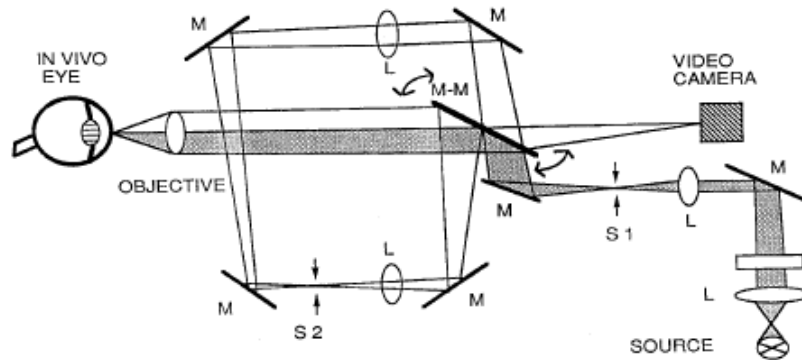


**Figure 5** - Schematic diagram of the optical pathway used in the SSCM [74].

The scanning slit illumination can have several advantages when compared to spot illumination. Firstly, a great part of these devices have adjustable slits, permitting the variation in the thickness of the optical section and the fraction of light that reaches the specimen and the detector. Secondly, light throughput is considerably greater than that of the TSCM. Thirdly, numerous points are scanned in parallel, leading to a shorter scanning time [74, 75].

These advantages enable the system to rapidly acquire high-quality images of transparent specimens. However, its main limitation is that this device can be considered truly confocal only in the axis perpendicular to the slit height. This results in low transverse and axial resolution [74, 75].

#### **4. 3. 3 - Laser Scanning Confocal Microscope (LSCM)**

LSCM represents the latest technique of confocal microscopy. This system was used in most recent investigations, including our study on DPN. This sophisticated and expensive technique has become an extremely precious tool for a wide variety of research studies in the biological and medical fields for the imaging of thin optical sections in living and fixed specimens, varying in thickness up to 100 micrometers [78].

This device uses coherent light emitted by a laser source and the beam is scanned over the back focal plane of the microscope by a set of galvanometer scanning mirrors. This microscopy system uses pinhole apertures. The emitted light passes through two different pinholes before reaching the photomultiplier detector. The first pinhole is positioned in a conjugate plane with the scanning point on the specimen. The second pinhole is located in front of the detector. The second pinhole plays the role of a “filter”, blocking the passage of out of focus light. The dichroic mirror has two main functions, reflecting the emitted laser beam onto the specimen, and allowing the passage of the reflected light onto the second pinhole aperture, as shown below in Figure 6 [74, 78].

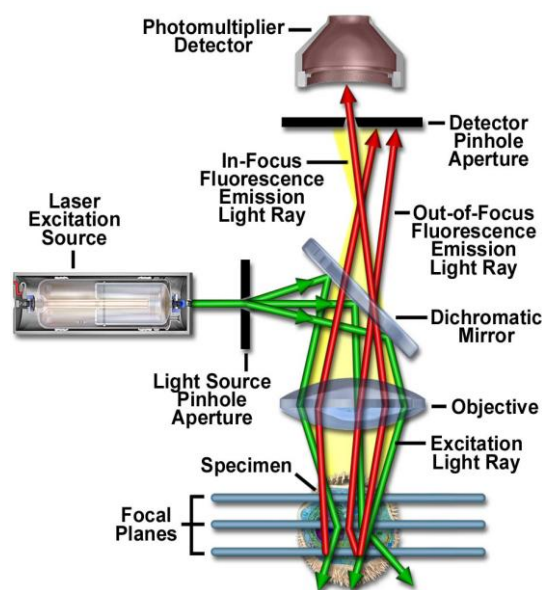


**Figure 6** - Schematic diagram of the optical pathway in LSCM [78].

#### 4.4 - Clinical examination

Currently, IVCCM devices involve contact with the cornea under local anesthesia. All available confocal microscopes used to examine the central region of the cornea require a coupling medium (gel) between eye and front surface of the lens, with the working distance dependent on the objective lens used [4].

The front surface of the lens is moved forward gradually with a joystick until reaches the corneal apex, visualizing and allowing the identification of each of the five corneal basic layers. Thus, image acquisition starts when the objective lens is correctly aligned with the central cornea and properly positioned on the corneal surface, with eventual fine adjustments in the X-Y plane in order to improve the position. The obtained images are rapidly projected onto a highly sensitive camera, connected to sophisticated quantitative image analysis systems, and finally displayed on the monitor [4].

#### **4.5 - Clinical applications**

As described previously, IVCCM allows ophthalmologists and researchers to detect and visualize living tissues at high resolutions. It can provide quantitative and qualitative morphological information, being often used for identifying and quantifying the pathological states of the corneal nerves and/or endothelial cell shape and density observations [74, 79].

In the past years it was increasingly used in the detection and management of different pathological and infectious conditions. This technique has shown good results in the detection of corneal dystrophies and ecstasies, detection of infective keratitis, pre and post refractive surgery evaluation, monitoring of contact lens induced corneal modifications and also identification of corneal micro-deposits. In the last decade it was frequently used in the assessment of peripheral nerve damage and dysfunction in a wide range of different studies on DPN (described in details in Section II) [8, 69-79].

In the case of corneal dystrophies, the clinical diagnosis, assessment and differentiation were based mainly on slit-lamp bio-microscopy. However, this technique has limitations in providing morphological description at cellular level. The use of CCM technique allows researchers to visualize the slightest changes non-invasively and to clearly distinguish between different types of dystrophy in Bowman's layer and the stroma, avoiding the use of invasive procedures such as biopsy with histopathological examination [79-81].

CCM has proven to have a significant clinical relevance in the diagnosis of infective keratitis, being extremely useful in several studies that revealed different causes of this painful condition, which results in inflamed eye and impaired vision [79].

In the case of refractive surgery, IVCCM has confirmed to be an invaluable tool, allowing the ophthalmologists to follow the corneal evolution after surgical intervention. This technique has been used for the quantitative and qualitative assessment of temporal modifications in keratocyte density, subepithelial deposits, stromal changes, and also nerve regeneration following photorefractive keratectomy (PRK) [79, 82-83].

CCM was frequently used in numerous research studies on corneal changes caused by contact-lens wear. This technique has shown to be very helpful in the detection of different types of stromal modifications, quantification of keratocytes loss and identification of inflammatory mediators release in the patients that use contact lenses.

It has been also revealed that long-term contact lens wear may decrease the corneal sensitivity without necessarily affecting the distribution and morphology of corneal nerves, verifying the same with endothelial cells in diabetic contact lens wearers [79, 84-86].

As for the corneal microdot deposits, CCM has been intensively used to detect this condition usually caused by several pathological factors, such as Fabry's disease, Wilson's disease, hyperlipidemia, refractive surgery and also long-term contact lens wear [87-90].

Other clinical and research applications, regarding specially the study of corneal nerve morphology in diabetic patients, are described in the following section.

## **SECTION II**

### **STATE OF ART**

#### **ASSESSMENT OF CORNEAL NERVE MORPHOLOGY WITH IVCCM**

## CHAPTER 5 – ASSESSMENT OF CORNEAL NERVE MORPHOLOGY WITH IVCCM

In the last decade, several research groups have used IVCCM to study corneal nerve morphology and distribution in healthy and diabetic subjects. In this chapter are described the main aspects of different methods and objectives of most relevant and recent works in this area. All the papers here mentioned represent a field preparation for our own research work, given that in all these studies were defined, assessed and quantified corneal nerve morphologic alterations and dysfunctions by CCM.

In a study on corneal structure and sensitivity, Rosenberg et al. [91], have used this non-invasive diagnostic technique to show significantly reduced sub-basal nerve fiber bundles in insulin-dependent diabetic patients with DPN, compared to non-diabetic subjects. Reduced bundles and lower nerve ramification are associated with reduced corneal sensitivity in patients with severe degree of DPN. This study has also revealed considerably thinner epithelium in diabetic subjects with severe DPN compared to healthy subjects.

In an improvement of the previous study, Malik et al. [92], have found considerably lower nerve fiber density, length as well as nerve branch density in diabetic patients (type 2) compared with controls. Other relevant aspect is that all mentioned measures are inversely correlated with the increasing severity of DPN.

Later, Kallinikos et al. [93], have performed a different study in order to define possible alterations in the tortuosity (TC) of corneal nerve fibers in relation to age, duration of diabetes (type 2), glycemic control, and neuropathic severity. They concluded that IVCCM is an appropriate technique that enables a rapid and non-invasive *in vivo* evaluation of corneal nerve tortuosity. They found that an increased tortuosity is a morphologic abnormality associated to the degree of severity of somatic neuropathy, reflecting changes in the nerve degeneration and regeneration in diabetic patients.

Confocal Laser Scanning Microscopy (CLSM) was used in a research study performed on the epithelial nerve structure in the human cornea (Stachs et al. [94],). The main objective was to visualize the spatial arrangement of the epithelium, nerves and keratocytes.

The obtained corneal images reconstructed three-dimensionally have revealed that thin nerves run in the subepithelial plexus aligned parallel to Bowman's layer, being partially interconnected. CCM allowed an accurate quantification of the diameter of main corneal nerve fibers [94].

Parwez et al. [70] used IVCCM to detect and assess changes in the corneal architecture in diabetic patients (type 2) that suffer from DPN. They have confirmed that nerve fiber density (NFD) and length (NFL) in diabetic subjects are significantly affected, showing also that these morphometric parameters are inversely correlated with increasing degree of severity (mild, moderate or severe) of DPN compared with healthy controls.

A useful study based on IVCCM and microstructural analysis, performed by Grupcheva et al. [95], has identified changes in corneal nerve density and morphology, with a precise quantification of number and diameter of the nerve beadings. Furthermore, it was established a correlation between the identified changes and subjects age.

In a posterior study, Mocan et al. [96], have studied the morphologic alterations in both corneal stromal and sub-basal nerves in diabetic patients (type 2). They revealed that sub-basal nerve length and total nerve branching are significantly lower in diabetic patients compared to controls. It was shown also that stromal nerve thickness as well as sub-basal nerve plexus thickness and tortuosity are significantly higher in diabetics.

In 2007, Quattrini et al. [97], have performed a valuable study on small fiber damage in human diabetic neuropathy. They have quantified small nerve fiber pathological changes in diabetic patients using the IVCCM technique, complementing the obtained results with the IENF assessment. In their study, all diabetic patients selected for neuropathy classification underwent neurological examination, neurophysiological evaluation, quantitative sensory testing (QST), skin biopsy for IENF quantification and CCM in order to identify and quantify corneal nerve fibers. It was found that IENF density, corneal nerve fiber density (NFD), branch density (NBD) and length (NBL) were progressively reduced in diabetic patients, according to their severity degree of neuropathy. This research group concluded that IVCCM technique can accurately identify and quantify small nerve



damages, detecting early stages of corneal nerve damage and recommended this technique for the diagnose and assessment of human DPN.

Later, was performed an interesting study on the diagnosis of neuropathy in patients with Fabry disease (Tavakoli et al. [98],). This research group has also used CCM to quantify small-fiber pathology, complementing with non-contact corneal aesthesiometry (NCCA) to quantify loss of corneal sensation, together with other established tests of neuropathy, such as detailed quantification of neuropathic symptoms, neurological deficits, neurophysiology and quantitative sensory testing (QST). Its results have clearly shown that all patients with Fabry disease had significant neuropathic symptoms. According to CCM quantification, corneal nerve fiber (NFD) and branch densities (NBD) were significantly reduced in both female and male patients when compared with control subjects. Moreover, the severity degree of neuropathic symptoms, as well as the neurological component of the Mainz Severity Score Index correlated significantly with the obtained results with QST and CCM. The authors indicated that both CCM and NCCA techniques provide accurate information, to detect and quantify early nerve fiber damage and dysfunction, respectively, in patients with Fabry disease.

In the article published by Lalive et al. [99], the corneal stromal nerve alterations imaged by laser scanning *in vivo* confocal microscopy (LSCM), in a patient with peripheral autoimmune neuropathy, were well described. This group has clearly shown that the application of this technology is appropriate for following the nerve damage progression, as well for assessing the responses to treatment. The authors have suggested that LSCM may be a valuable tool in the early detection of DPN.

Other recent study, performed by Visser et al. [100], has described an analogous population of thin and tortuous corneal nerves with a beaded form in healthy subjects, confirming and complementing the data described by Lalive et al. [99] They stated that an accurate distinction between the nerves in cases with and without peripheral neuropathy could be made through the difference in nerve diameter.

A latest study on automatic analysis of DPN, published in 2011 by Dabbah et al. [8], has also shown the importance and utility of CCM for the analysis of corneal nerve

morphology. The authors of this research work have published various articles in the past years. In this interesting article, they mentioned that existing methods are in many cases insufficient, with poor sensitivity and requiring expert assessment. Most of recent diagnose and follow-up techniques focus only on large fibers (neurophysiology) or are invasive (skin/nerve biopsy).

Inspired by other recent studies (Malik et al., [92]; Kallinikos et al., [93]; Parwez et al., [70]), and confirming with their own results, Dabbah et al. [8] have described several advantages of CCM technique, pointing out that this non-invasive and reiterative method might be an ideal surrogate for early diagnosis and an early biomarker for human DPN. CCM could identify the patients at risk, requiring if necessary a quick and more intense intervention including improved glycemic, blood pressure and lipid control. In addition, the authors mentioned that a sensitive surrogate endpoint would considerably reduce the difficulties of the development of disease-modifying therapeutics by improving the ability to test therapeutic efficacy.

The system for automated analysis of CCM images presented in their paper uses the dual-model property in a multi-scale framework, in order to generate feature vectors from localized data at each pixel [8]. As in other prior similar studies, corneal nerve fibers in CCM images are shown as bright linear structures that follow a principal direction. However, these fibers appear to have their own independent local orientation, different dimensions of length and diameter. According to the authors, longer nerve fibers with larger diameter are considered to be the primary trunks, while smaller nerve fibers emerging from these main trunks are called secondary nerve fibers (or nerve branches) [8].

Dabbah et al. [8], also revealed promising results in distinguishing control and patient groups using features such as nerve fiber length (NFL), nerve fiber density (NFD), nerve branch density (NBD) and tortuosity (TC) of nerve fibers. Once more, the authors have confirmed that abnormal subjects usually have less nerve fibers and more tortuous structures than healthy normal subjects. They concluded that the multi-scale dual-model method can be successfully used to detect corneal nerve fibers in CCM images. Furthermore, in their evaluation the proposed method outperformed other previous

methods and obtained the lowest error, achieving this performance with reduced training. The authors suggested that the simplicity of the developed method might be a potentially important matter in the practical implementation in the clinical field.

The authors mentioned that the clinical utility of the dual-model method was also evaluated by comparing the automatic detection and classification against expert manual delineation of the images. The obtained results have shown encouraging clinical performance for the stratification of neuropathic severity. According to them, the automated analysis produces equivalent results to manual analysis, while being a faster and potentially more reliable and practical choice due to its stability and immunity to inter/intra-observer variability. The authors have used for the comparison and assessment of the correspondence between manual and automatic detection of results, the NDS score, which is, in their opinion, adequate for establishing the clinical severity of neuropathy, but not enough for a more detailed assessment of clinical utility because it does not detect small fiber damage. For this reason, CCM was clearly recommended by the authors, as it can evaluate small fiber damage, a performance that can only be achieved by either nerve or skin biopsy, both of which are invasive and require an intensive labor assessment [8].

A most recent study on detection of diabetic sensorimotor polyneuropathy (DSP), published in 2012 by Ahmed et al. [101], aimed to identify the concurrent and predictive validity of CCM parameters in the cross-sectional identification of DSP and in the prediction of future DSP in longitudinal analysis, intending to determine in CCM images the finest parameter that best identifies this pathological condition in type 1 diabetes and also to describe its performance features. The authors intended to include type 1 diabetic subjects with a wide range of nerve injury, varying between absent and detectable nerve damage to severe DSP. This was possible by using the Toronto Clinical Neuropathy Score (TCNS, previously described with more detail), an validated grading system score to evaluate history and physical exam components that allowed to stratify the number of subjects according to their severity degree (absent, mild, moderate, and severe) of diabetic polyneuropathy at the time of study [101].

Similarly to some previous studies, all patients underwent examination in both eyes of corneal nerve fibers in the Bowman layer of the cornea. The mean of the two obtained images from contralateral eyes was calculated to determine the mean values of CCM parameters, such as NFL, NFD, NBD, and TC, all measured with analytical software. DSP was diagnosed using well-known clinical and electrophysiological criteria (published by the American Academy of Neurology, the American Association of Electrodiagnostic Medicine, and the American Academy of Physical Medicine and Rehabilitation, Neurology in 2005). The authors were based on this consensus, defining electrophysiological abnormality according to the presence as a minimum of one abnormal nerve conduction parameter in both dominant-side sural and peroneal nerve distributions. They found that DSP was present in 37% subjects, showing that CCM parameters were significantly lower in these subjects, with the exception of tortuosity. They concluded that among identified CCM parameters, NFL best differentiated DSP cases from control/healthy subjects [101].

Labbé *et al.* [102], have presented a study focused on the sub-basal nerve morphology, aiming to evaluate the relationship between the *in vivo* confocal microscopic (IVCM) morphology of sub-basal corneal nerves and corneal sensitivity in patients treated for glaucoma. In this study, the authors performed unilateral IVCM (i. e., only one eye of each subject was included) in all patients, assessing the corneal nerve fibers in the Bowman layer of the cornea. The authors analyzed the following nerve parameters: density (NFD), width (NFW), number of nerve beadings (NNB), branching density (NBD), tortuosity (TC) and reflectivity (RC). The obtained results have revealed a significantly decreased corneal sensitivity in glaucoma and dry eye patients compared to normal control subjects [102].

The density and number of sub basal corneal nerves were also significantly reduced in glaucoma and dry eye patients compared to healthy controls. However, there were no significant differences in terms of sub basal nerve width, number of beadings, tortuosity, reflectivity and number of branching between the glaucoma, the dry eye and the control groups [102].

Other recent study, also published in 2012, by Edwards *et al.* [103], was focused on the diagnosis and monitoring of DPN and shown promising results. The authors, as in many previous studies, used IVCCM to measure morphologic parameters of sub-basal corneal

nerves. The patients with diabetes that were involved were with predominantly mild or no neuropathy. All individuals (patients and healthy controls) underwent evaluation of diabetic neuropathy symptom score (NSS), neuropathy disability score (NDS), testing with 10g monofilament, quantitative sensory testing (QST) (warm, cold, vibration detection) and nerve conduction studies (NCS).

Edwards *et al.* [103], analyzed the following corneal morphologic parameters: NFL, NBD and TC, determining differences between subjects with and without DPN and healthy controls and using correlations between the measured parameters and traditional tests of DPN. They found that the NFL was significantly reduced in diabetic individuals with mild DPN compared to both controls and diabetic individuals without DPN. NBD was significantly decreased in individuals with mild DPN compared to controls. NFL and NBD revealed weak correlations to most measures of neuropathy, with the strongest correlations to NCS parameters. Regarding the corneal nerve fiber tortuosity (TC), the authors did not quantify significant differences, showing only a frail correlation to the vibration detection threshold. The authors have recommended CCM for the assessment of corneal nerve morphology, clearly calling attention to the fact that is a non-invasive and fast technique capable of showing noticeable differences between persons with and without DPN [103].

*In vivo* corneal confocal microscopy (IVCCM) was employed in a study (published by Nitoda *et al.*, [104]) with a different approach. The authors intended to assess the variety of corneal nerve fiber alterations between diabetic patients (type 2), categorized into three different groups according to retinopathy status, and non-diabetic patients. In this work, CCM images of the sub-basal nerve plexus of the diabetic and healthy participants were collected. The chosen parameters for analysis were: corneal nerve fiber density (NFD), nerve branch density (NBD), nerve fiber length (NFL), and nerve fiber tortuosity (TC). Diabetic patients were stratified into three groups according to the classification of diabetic retinopathy severity degree, based on indirect fundoscopy, fundus photography, and fluorescein angiography findings. Additionally, a separate classification into four distinct groups according to the severity of DPN was also used, based on the results of clinical and electro-diagnostic examinations [104].

The results obtained confirmed prior results, showing that average values of NFD, NBD, and NFL are lower, differing significantly according to DR status and DPN severity, whereas TC was found to be higher in diabetic patients than healthy control subjects. The authors have found a positive correlation between corneal and peripheral nerve damage in diabetics. Moreover, nerve fiber damage of the sub-basal nerve plexus of diabetic corneas was found to progress jointly with DR and DPN. Once more, CCM method was clearly recommended as a promising adjuvant technique for the early diagnosis and assessment of human DPN [104].

Other relevant study on retinopathy complications was performed by Popper *et al.* [105], at the IBILI Center of Ophthalmology, in partnership with Departments of Instrumentation, IBILI and Physics Department of University of Coimbra. The research group involved members that are currently involved in NeuroCornea Project, A. M. Morgado and M. J. Quadrado. The study employed confocal imaging to evaluate *in vivo* changes in density and morphology of subbasal nerves (SBN) and highly reflective cells (HRC) in corneas of diabetic patients with mild and moderate diabetic retinopathy. The authors affirmed that basal cell density in diabetics was significantly decreased, fact that may explain the neurotrophic state and poor epithelial healing, characteristic for diabetics. Furthermore, the authors observed that the number of very HRC beneath the basal epithelial cells' layer was significantly higher in diabetics than healthy controls. They concluded that the decrease in the number of SBN and of basal epithelial cells in the corneas of diabetic patients characterizes the retinopathy condition and these changes might be related to each other.

Resuming the information described in all studies mentioned in this chapter, many research groups obtained good results. Most of them focused principally on three essential parameters: nerve fiber density (NFD), nerve fiber length (NFL) and nerve branching density (NBD). These studies revealed that all three parameters are significantly lower in diabetic patients compared with controls. Furthermore, some studies have shown also that these morphometric parameters are inversely correlated with increasing degree of severity (mild, moderate or severe) of DPN compared with healthy controls.

Other groups evaluated in their studies parameters like nerve fiber width (NFW) and tortuosity (TC), proving that these parameters were significantly higher in diabetics patients compared with healthy controls.

At last, some research groups complemented the existing data with information on additional parameters, such as nerve branching density (NBD), nerve branching pattern and branching degree, as well as number of nerve beadings (successive changes in nerve fiber caliber, calculated as the number of well-defined hyper-reflective points per unit of length), showing that it is possible to identify major changes between control and diabetic patients, and within diabetic groups, according to the severity degree of DPN.

However, a substantial part of these results are partially inconclusive, requiring for additional study and improvement to identify and quantify with more accuracy the differences between the corneal nerve morphology of diabetics (with and without DPN) and control groups.

Our study aims principally to complement and at the same time to confirm with our own findings the existing data on the following parameters: NFD, NFL, NFW, TC, NBD, NBP and NBA. All parameters were assessed in individuals divided in control groups, and diabetic groups, according to the severity degree of DPN.

The selection of these parameters is entirely justified by the published results of all described studies. The exact methodology of our study is described in the following section, explaining in detail different steps of our study, including patients' selection and classification, image acquisition and selection, electrophysiological measurements, as well as the algorithm and automatic image processing description.

## **SECTION III**

### **RESEARCH DESIGN AND METHODOLOGY**



## **CHAPTER 6 – RESEARCH DESIGN, AIMS AND METHODS**

### **6.1 – Key steps of study**

In numerous studies described in previous chapters, it was clearly accentuated that an accurate and earlier diagnosis, as well as follow-up of DPN has a supreme importance for establishing proper prevention methods or treatment. However, the earlier diagnosis continues to be a true challenge.

The main goal of NeuroCornea project is the development of an automatic segmentation method for extracting corneal nerve morphologic characteristics for the early diagnosis and follow-up of DPN. The automated algorithm should be able to identify and perform a detailed analysis of several morphometric parameters from corneal sub-basal nerve plexus. This project is also focused on the development of an optical confocal module, designed to be included in standard slit-lamp equipment for corneal imaging.

The main objectives of my work are to identify and assess the concurrent and predictive validity of CCM morphologic parameters in the case-control identification and classification of DPN. The evaluation of the morphology of the corneal nerves is a well-structured process that involved different steps in order to achieve its purpose. The key steps are precisely described as follows:

- To obtain CCM images from randomly selected diabetic type 2 patients and healthy controls, in order to evaluate the distribution and morphology of corneal nerves (random selection was performed to reduce bias);
- To define and quantify alterations in the morphologic characteristics of sub-basal corneal nerve fibers in diabetic patients affected by DPN, according to the severity degree categorization;
- To assist the development and improvement of an automatic algorithm for the identification, extraction and quantification of several morphometric parameters of corneal nerves, evaluating it against manual segmentation of the corneal nerves by an experienced examiner;

- To compare and correlate the obtained results with traditional neurological and electrophysiological tests used for the screening and assessment of DPN;
- To identify the most relevant morphometric parameters and to evaluate their suitability for the early detection and follow-up of DPN with CCM.

## **6.2 – Team and institutions involved in NeuroCornea project**

Our project is a joint effort by IBILI - Institute of Biomedical Research on Light and Image, from the Faculty of Medicine, University of Coimbra; the Instrumentation Center, from the Physics Department of the Faculty of Science and Technology, University of Coimbra; and the Departments of Ophthalmology, Endocrinology and Neurology, from Coimbra University Hospitals.

The team consists of researchers with expertise on optical and electronic instrumentation, medical image processing and experienced medical doctors (ophthalmologists, endocrinologists and a neurophysiologist). Currently, more students are involved in the project, with their thesis based on works that cover different aspects of the project.

## **6.3 – Classification of DPN case and control individuals**

In our study were included 12 randomly selected diabetic patients (type 2, insulin-treated, with mean age of  $58 \pm 10$  years), followed at the Department of Endocrinology of the Coimbra University Hospitals, and 8 age-matched non-diabetic control individuals (with mean age of  $54 \pm 7$  years).

Initially, we intended to classify all selected diabetic patients in 4 groups, according to the degree of severity of neuropathy (absent, mild, moderate and severe) by physical examination, consisting in a complete evaluation of reflex and sensory deficits, according to Michigan Neuropathy Screening Instrument (MNSI) [106].

The obtained classification (shown in Figure 7) was slightly different of the expected one, with diabetics divided in the following 3 main groups: absent (4 patients,  $53 \pm 11$  years), mild (5 patients,  $58 \pm 9$  years) and moderate DPN (3 patients,  $60 \pm 9$  years), without any patient with severe degree.

**Evaluation of Corneal Nerve Morphology for Detection and Follow-up of Diabetic Peripheral Neuropathy**

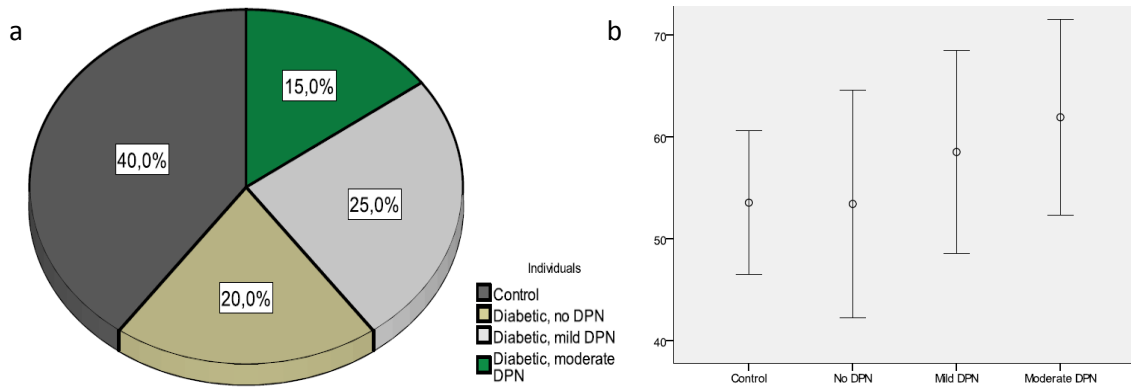


**Figure 7 – a)** Pie-chart representing the individuals involved in the study, divided in four groups: control; diabetics without DPN, with mild DPN and with moderate DPN; **b)** Scatter chart representing the mean age values  $\pm$  standard deviations, corresponding to the four groups.

Physical assessment was conducted according to guidelines of the Declaration of Helsinki and submitted to approval by the Medical Ethics Committee of the Faculty of Medicine, Coimbra University. All clinical examinations were performed according to the International Guidelines for Diagnosis and Management of DPN (presented in Table 4, Chapter 3.4.1), and according to MNSI (Figure 8), comprising feet appearance evaluation, ulceration, ankle reflex testing and sensory deficit evaluation (superficial pain evaluation, light touch perception, and vibrating sensation) graded according to the severity level that is associated to impaired sensation.

**MICHIGAN NEUROPATHY SCREENING INSTRUMENT**

**B. Physical Assessment** (To be completed by health professional)

1. Appearance of Feet

<p style="text-align: center;"><b>Right</b></p> <p>a. Normal <input type="checkbox"/> a Yes <input type="checkbox"/> i No <input type="checkbox"/></p> <p>b. If no, check all that apply:</p> <p>Deformities <input type="checkbox"/></p> <p>Dry skin, callus <input type="checkbox"/></p> <p>Infection <input type="checkbox"/></p> <p>Fissure <input type="checkbox"/></p> <p>Other <input type="checkbox"/></p> <p>specify: _____</p>	<p style="text-align: center;"><b>Left</b></p> <p>Normal <input type="checkbox"/> a Yes <input type="checkbox"/> i No <input type="checkbox"/></p> <p>If no, check all that apply:</p> <p>Deformities <input type="checkbox"/></p> <p>Dry skin, callus <input type="checkbox"/></p> <p>Infection <input type="checkbox"/></p> <p>Fissure <input type="checkbox"/></p> <p>Other <input type="checkbox"/></p> <p>specify: _____</p>
--	---

<p style="text-align: center;"><b>Right</b></p> <p>2. Ulceration <input type="checkbox"/> a Absent <input type="checkbox"/> i Present</p> <p>3. Ankle Reflexes <input type="checkbox"/> a Present <input type="checkbox"/> a s Present/Reinforcement <input type="checkbox"/> i Absent</p> <p>4. Vibration perception at great toe <input type="checkbox"/> a Present <input type="checkbox"/> a s Decreased <input type="checkbox"/> i Absent</p> <p>5. Monofilament <input type="checkbox"/> a Normal <input type="checkbox"/> a s Reduced <input type="checkbox"/> i Absent</p>	<p style="text-align: center;"><b>Left</b></p> <p>2. Ulceration <input type="checkbox"/> a Absent <input type="checkbox"/> i Present</p> <p>3. Ankle Reflexes <input type="checkbox"/> a Present <input type="checkbox"/> a s Present/Reinforcement <input type="checkbox"/> i Absent</p> <p>4. Vibration perception at great toe <input type="checkbox"/> a Present <input type="checkbox"/> a s Decreased <input type="checkbox"/> i Absent</p> <p>5. Monofilament <input type="checkbox"/> a Normal <input type="checkbox"/> a s Reduced <input type="checkbox"/> i Absent</p>
--	---

Signature: \_\_\_\_\_ Total Score \_\_\_\_\_ /10 Points

**Figure 8 – MNSI: Physical assessment (University of Michigan, 2000), [106]**

**Evaluation of Corneal Nerve Morphology for Detection and Follow-up of Diabetic Peripheral Neuropathy**

For a more complete evaluation, we used additionally a brief 15-item questionnaire (Figure 9) as a complementary screening tool for a more precise diagnosis of DPN. All patients were kindly asked to answer this questionnaire, allowing a more accurate evaluation of the severity degree of diabetic neuropathy according to the MNSI, which has been developed particularly for distal diabetic polyneuropathy [106].

Each physical examination and questionnaire evaluation was performed by experienced medical doctors at the Department of Endocrinology of the Coimbra University Hospital, in a random testing order, without previous information of other test results to reduce bias.

Furthermore, we verified the entire clinical history of each diabetic patient to ensure that peripheral neuropathy is a consequence only of diabetes, excluding other rare possible causes that are described in next section.

**Patient Version**

**MICHIGAN NEUROPATHY SCREENING INSTRUMENT**

**A. History** (To be completed by the person with diabetes)

Please take a few minutes to answer the following questions about the feeling in your legs and feet. Check yes or no based on how you usually feel. Thank you.

- |   |                              |                             |
|---|------------------------------|-----------------------------|
| 1. Are you legs and/or feet numb?   | <input type="checkbox"/> Yes | <input type="checkbox"/> No |
| 2. Do you ever have any burning pain in your legs and/or feet?                                  | <input type="checkbox"/> Yes | <input type="checkbox"/> No |
| 3. Are your feet too sensitive to touch?  | <input type="checkbox"/> Yes | <input type="checkbox"/> No |
| 4. Do you get muscle cramps in your legs and/or feet?   | <input type="checkbox"/> Yes | <input type="checkbox"/> No |
| 5. Do you ever have any prickling feelings in your legs or feet?                                | <input type="checkbox"/> Yes | <input type="checkbox"/> No |
| 6. Does it hurt when the bed covers touch your skin?  | <input type="checkbox"/> Yes | <input type="checkbox"/> No |
| 7. When you get into the tub or shower, are you able to tell the hot water from the cold water? | <input type="checkbox"/> Yes | <input type="checkbox"/> No |
| 8. Have you ever had an open sore on your foot?   | <input type="checkbox"/> Yes | <input type="checkbox"/> No |
| 9. Has your doctor ever told you that you have diabetic neuropathy?                             | <input type="checkbox"/> Yes | <input type="checkbox"/> No |
| 10. Do you feel weak all over most of the time?   | <input type="checkbox"/> Yes | <input type="checkbox"/> No |
| 11. Are your symptoms worse at night?   | <input type="checkbox"/> Yes | <input type="checkbox"/> No |
| 12. Do your legs hurt when you walk?  | <input type="checkbox"/> Yes | <input type="checkbox"/> No |
| 13. Are you able to sense your feet when you walk?  | <input type="checkbox"/> Yes | <input type="checkbox"/> No |
| 14. Is the skin on your feet so dry that it cracks open?  | <input type="checkbox"/> Yes | <input type="checkbox"/> No |
| 15. Have you ever had an amputation?  | <input type="checkbox"/> Yes | <input type="checkbox"/> No |

Total: \_\_\_\_\_

**Figure 9 – MNSI Questionnaire (University of Michigan, 2000), [106]**

#### **6.4 – Diabetic patients: exclusion of other causes for neuropathy**

As mentioned before, in patients, to ensure that peripheral neuropathy is a resulting condition only of diabetes, we have checked the complete clinical history of each patient, in order to exclude other potential causes.

We have thoroughly verified the existence of several different abnormalities implicated in the pathogenesis of this nerve disorder, such as alcohol related neuropathy, frequently associated to nutritional neuropathy (vitamins B<sub>1</sub>, B<sub>3</sub>, B<sub>6</sub> and especially B<sub>12</sub> deficiency), uremic neuropathy (uremic toxins), hypothyroidism (uncommon cause, can lead to carpal tunnel syndrome), cancer-related neuropathy, inflammatory, as well as neuropathy caused by pernicious anemia (associated to gastritis), porphyria, and neuropathy caused by specific medications. For a better understanding, all these conditions are described in the following sub-sections.

##### **6.4.1 – Alcohol related neuropathy**

Alcoholic neuropathy is a complex condition and most likely due to several factors that are associated to nutrition disorders and alcoholism. The toxicity of alcohol can result in direct poisoning of the nerve fibers, or in indirect consequences, such as poor nutritional status and vitamin deficiencies. The indirect consequences are in many cases difficult to determine, given the existing limitations in assessing efficiently nutritional deficiencies versus alcohol toxicity [107].

##### **6.4.2 – Nutritional neuropathy**

Neuropathies related to nutritional and vitamin deficiencies are frequently associated to extended parenteral nutrition, nutrition disorders (poor quality or/and insufficient quantity), alcohol abuse, physiological states (such as pregnancy), and certain medications (such as isoniazid or penicillamine that are pyridoxine antagonists), which may also result in a deficiency condition [107].

Evidence supporting a worse nutritional condition related to alcohol toxicity is the discovery that alcohol reduces vitamin B<sub>1</sub> (thiamine) absorption in the intestine and

decreases hepatic thiamine storage. Consequently, a diminished phosphorylation of thiamine leads to a decrease of the active form of thiamine [107, 108].

There are many conditions associated with a diminished ability to an impaired absorption. These conditions comprise autoimmune diseases, pancreatic diseases, pernicious or unexplained anemia, ileal resection, Crohn's disease, HIV infection, gastritis, gastric or small intestine surgical interventions, malabsorption syndromes, multiple sclerosis, and the use of histamine receptor antagonists or proton pump inhibitors [109, 110].

Vitamin B<sub>6</sub> (pyridoxine) deficiency in most cases occurs in the circumstances of general malnutrition, related with cases of alcoholism, or with medications such as isoniazid hydralazine, which are pyridoxine antagonists. Some studies have revealed cases of neuropathy related to pyridoxine [107, 108].

Vitamin B<sub>12</sub> (cobalamin) is an important dietary nutrient; therefore its deficiency can cause a number of serious undesired conditions including peripheral neuropathy. Vitamin B<sub>12</sub> insufficiency can cause megaloblastic anemia (although not always present in those with prominent neurological manifestations), nerve fiber damage and degeneration of the spinal cord. It is frequent for anemia to develop first, but this is not always the case [107-109].

#### **6.4.3 – Neuropathy caused by pernicious anemia/gastritis**

Neuropathies can be associated in some cases to pernicious anemia (PA), the most frequent cause of vitamin B<sub>12</sub> deficiency. PA represents a relevant condition only when associated with chronic atrophic gastritis, which is recognized mainly by the loss of gastric mucosal folds and thinning of the gastric mucosa. There are two major types of chronic gastritis (based on whether the lesion affects the *antrum*, region that contains gastrin secreting G-cells): type A (autoimmune) and type B (non-autoimmune) [111-113].

PA may be related with several other autoimmune endocrinopathies, such as Hashimoto's thyroiditis, Addison's disease, gonadal failure, hypoparathyroidism, Graves' disease, vitiligo, myasthenia gravis, the Eaton-Lambert syndrome, etc. [111-113].

PA typical symptoms consist of fatigue, weakness, faintness, vertigo, tinnitus, palpitations, angina, and reduced exercise capacity with pallor, slight icterus, tachycardia, and systolic flow murmur on exam [111-113].

PA associated with chronic gastritis lead to B<sub>12</sub> deficiency, which usually results in gastrointestinal complications, such atrophic glossitis, megaloblastosis, diarrhea, malabsorption and gastric adenocarcinoma [111-113].

Most frequent neurologic complications include peripheral neuropathy, often diagnosed by numbness and paresthesias, specific lesions of the dorsal and lateral columns (with typical symptoms, such as limb weakness, spasticity, and extensor plantar reflexes), typical lesions of the spinal cord (mainly sub-acute axonal and myelin degeneration) and cerebrum (with changes varying from mild personality defects, moderated memory loss to obvious psychosis (also called megaloblastic madness) [111-113].

#### **6.4.4 – Uremic neuropathy**

Other type of neuropathy that we aimed to exclude is the uremic neuropathy, a less common type caused by uremic toxins. The severity degree of this neuropathy is strongly correlated with the severity of the renal insufficiency. Uremic neuropathy, in some cases associated to mononeuropathy, is considered a dying-back neuropathy (distal axonopathy) or central-peripheral axonopathy mostly with consequences of secondary demyelination [114, 115].

The pathophysiologic mechanism of uremic neuropathy continues unclear. Fraser *et al.*, [116] suggested that neurotoxic compounds diminish energy supplies in the axon by inhibiting nerve fiber enzymes that are essential for the maintenance of energy production. Even though all neuronal perikarya would be affected likewise by the toxic assault, the long axons would be the most affected, degenerating earlier since the longer the axon, the larger the metabolic load that the perikaryon would tolerate. In toxic neuropathy, dying back of axons is more accentuated in the distal aspect of the neuron and may be caused by a metabolic failure of the perikaryon [114-116].

Regarding the pathophysiology of uremic neuropathy, it has been postulated in some publications that peripheral nerve damage could be also related to an interference with the nerve axon membrane normal function and inhibition of  $\text{Na}^+/\text{K}^+$ -activated ATPase by toxic factors in uremic serum [116].

Bolton et al. [117] theorized that membrane dysfunction was occurring at the perineurium, which plays important role as diffusion barrier between interstitial fluid and nerve, or within the endoneurium, which acted as a barrier between blood and nerve. Consequently, uremic toxins may enter the endoneural space at either site and generate direct nerve damage, with water and electrolyte shifts causing increase or decrease of the space.

#### **6.4.5 – Hypothyroidism related neuropathy**

Hypothyroidism is a clinical condition mainly characterized by deficient levels of thyroid hormones (particularly  $\text{TT}_3$  and  $\text{TT}_4$ ) with raised TSH. Peripheral neuropathy may be associated with hypothyroidism, which typically develops dangerously over a long period of time principally due to irregular drug administration and ineffective replacement of thyroid hormone [118].

Several medical sources affirm that neurological symptoms are infrequent in thyroid disease patients with hypothyroidism. However, in the past years, numerous thyroid patients have complained of neurological type symptoms. Many of these patients endure with great effort these symptoms despite the fact that they are suitably treated to correct their thyroid hormone disproportion [119, 120].

#### **6.4.6 – Cancer-related neuropathy**

One of the most frequent neurologic consequences of cancer is peripheral neuropathy, which can be caused directly by nerve injuries resulting from surgery; damage to nerves from compression or infiltration by tumor tissue; injuries resulting from nerve infections (such as shingles); neurotoxicity of cancer treatment (radiation treatment - depending on



the radiation dose tuning, or chemotherapy – depending on total dose received over time); metabolic derangements; and paraneoplastic disorders [121, 122].

In the case of paraneoplastic disorders, any part of the central or peripheral nervous systems can be injured. Paraneoplastic neuropathies can lead in many cases cause to severe and permanent neurologic morbidity [121, 122].

#### **6.4.7 – Neuropathy caused by porphyria**

Porphyria represents a group of rare metabolic disorders, which are principally characterized by enzymatic deficiencies or failing in the biosynthesis of an element called heme, a metalloporphyrin that is the main result of porphyrin metabolism. There are several distinct forms of porphyria, classified according to the tissues that remain preferentially affected or where the metabolic disorder occurs (acute hepatic porphyrias, acute intermittent porphyria (AIP), hereditary coproporphyria, variegate porphyria, or erythropoietic porphyrias) [123-125].

Porphyric neuropathy usually appears in association with other characteristics of different types of porphyria. In case of acute hepatic porphyria, neuropathy occurs with abdominal pain, distorted mental status changes and autonomic dysfunction. Weakness is a common feature for the patients with acute intermittent or hereditary porphyrias, with particular vulnerability of motor nerve fibers, principally the radial and peroneal nerves. Subclinical neuropathy (characterized by reduced motor and sensory conduction velocities) has also been reported in a small number of patients with latent AIP, which have not revealed any neurologic deficit at the time of examination [124-126].

#### **6.4.8 – Inflammatory neuropathy**

Inflammatory neuropathies are in most cases disorders of peripheral nerves and occasionally of the central nervous system. This type can affect individuals at any age, being related to a single or many of a large group of pathologies, such as polyarteritis, sarcoidosis, Sjögren's syndrome, leper, amiloidosis, Lyme disorder or HIV [127, 128].

Inflammatory neuropathies do not occur frequently. However, it is very important to diagnose because they are treatable. Most known are Guillain-Barre's syndrome, acute (AIDP) and/or chronic inflammatory demyelinating polyradiculoneuropathies (CIDP), multifocal motor neuropathy, Lewis-Sumner syndrome, Fisher syndrome and Bickerstaff brainstem encephalitis (last two types usually occur acutely and have clinical overlap with AIDP) [127].

The course of these neuropathies can be monophasic, relapsing, or progressive. Nerve conduction studies (NCS) have revealed features of demyelination, particularly motor nerve conduction block and temporal dispersion [127, 128].

#### **6.4.9 – Neuropathy induced by medication**

Drug-induced neuropathy is caused primarily by patient's usual medications. Although these neuropathies affect just 2 to 4% of individuals who take specific prescription medications, there are many concerns regarding the resulting symptoms. Drug therapy for pain treatment appears to be very frustrating for many patients [129].

There are numerous powerful drugs that have great potential to generate severe side effects. These drugs have shown to induce neuropathy, being classified in seven wide categories: chemotherapy drugs, antifungal drugs, antibiotics, drugs involved in the treatment of infectious disease, cardiovascular and cholesterol drugs, hypnotics, and psychotherapeutic drugs used especially to treat addictions [129-132].

Numerous iatrogenic neuropathies are due to specific medications, exceptionally prescribed, such as disulfiram, perhexiline, almitrine (usually used in small doses with minimal toxicity), phenytoin, ara-C, or metronidazole (habitually used for short period) [129, 130].

There are several drugs that produce enduring neuropathies, because the primary disease is extremely severe, mostly malignancies and HIV infection. In these particular cases evolving research has been aimed to identify secondary agents or delivery methods to reduce or prevent toxicity [129, 130].

Toxic effects are simpler to recognize when acute or sub-acute onset of symptoms occurs shortly after the first drug exposure or a change of medication dosage. On the contrary, it is much more difficult to identify the symptoms for diagnosing a gradually progressive neuropathy after several months or even years after starting a chronic medication with constant doses [129-131].

### **6.5 – Electrophysiological measurements and nerve conduction studies (NCS)**

All subjects involved in our study were assessed with surface electromyography (EMG), a non-invasive technique that consists in applying cutaneous electrodes to the skin surface for studying muscle and nerve characteristics. EMG is basically a graphical recording method (Figure 10) of muscle nerve action potentials, being frequently used for testing the muscle and motor nerve fiber activities (as described previously in Chapter 3), allowing a more precise evaluation of the severity degree of diabetic neuropathy [133].

EMG is a modern clinical method of investigation that in many cases complements effectively the medical examination. In our case, electrophysiological examinations were performed for evaluating the severity (distinguishing precisely between mild and moderate degree) and monitoring significant injuries and progressions of DPN. In summary, EMG aimed to add a superior level of specificity to the diagnosis [133].

Surface EMG represents a common method of measurement, especially due to its non-invasiveness and simplicity, since it can be accomplished by personnel other than medical doctors, with smallest risk to the subject. Nevertheless, to ensure the maximum safety of all subjects involved in our study, all measurements were performed by an experienced neurophysiologist of the Department of Neurology of Coimbra University Hospitals, and were conducted according to guidelines of the Declaration of Helsinki and submitted to approval by the Medical Ethics Committee of the Faculty of Medicine, Coimbra University.

**Evaluation of Corneal Nerve Morphology for Detection and Follow-up of Diabetic Peripheral Neuropathy**

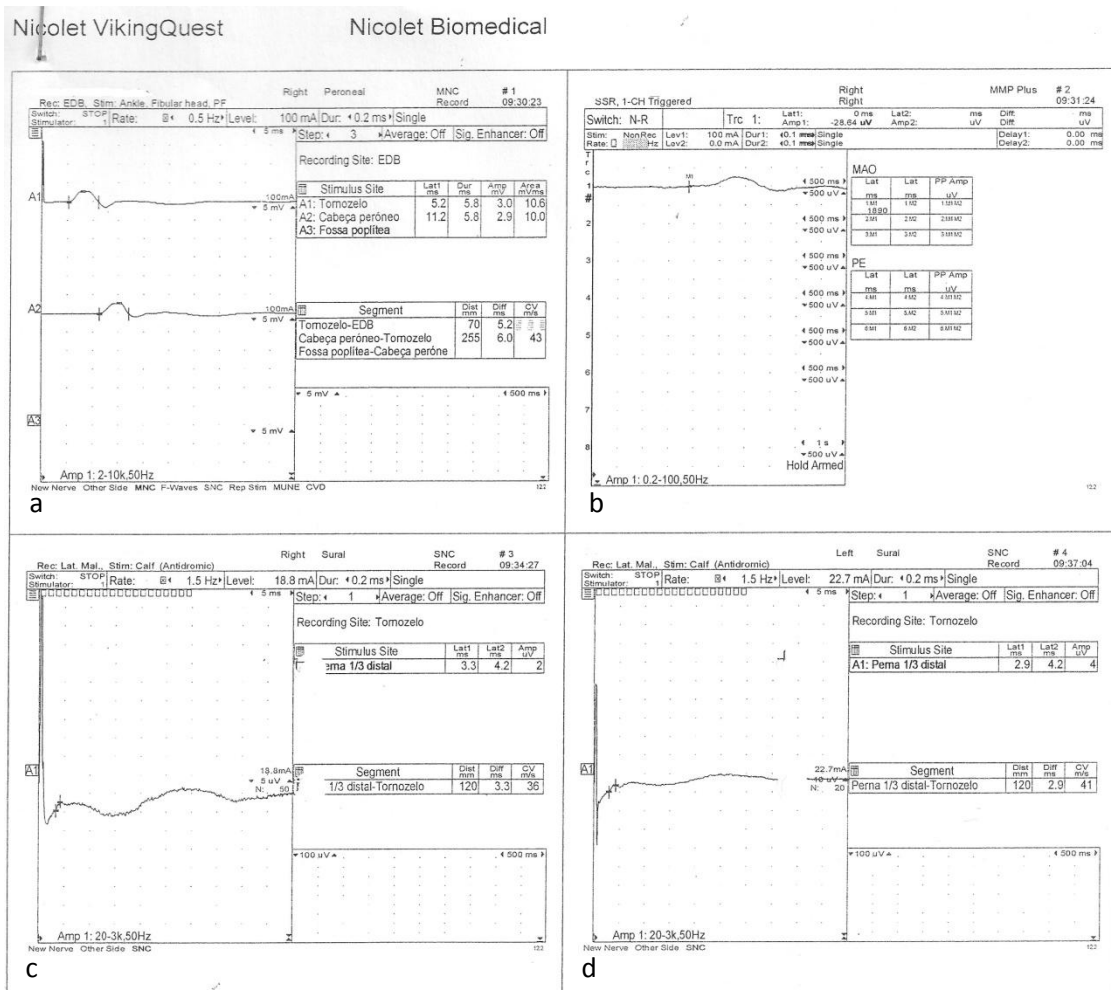


**Figure 10** – Sample of surface EMG signals from a diabetic subject, corresponding to: **a)** right peroneal nerve; **b)** sympathetic nerve response; **c)** right and **d)** left sural nerve. [CHUC, Department of Neurology, EMG and EP Lab; measurement performed in May, 2012], [133]

Electrophysiological measurements were performed using a Nicolet Biomedical EA4 (Nicolet Biomedical, Inc, USA) recording device. The measured signal, called electromyogram, was obtained by applying conductive electrodes to the skin surface. The neurophysiologist placed carefully small electrodes on specific leg surface sites, including the ankle, fibular head and popliteal fossa, and used a stimulator, that applies low amplitude current pulses (that do not cause any hazard to the body), for delivering a controlled electrical current to subjects' skin, forcing the assessed nerves to respond with electric pulses, resulting in EMG signals. These electrical signals, produced by the nerves, were instantly collected by the computer, and the measurement information (Figure 10) was interpreted by the same examiner [133].

EMG measurements comprised nerve conduction evaluation, assessing motor (peroneal) and sensory (sural) NCV and amplitudes, as well as cutaneous sympathetic response measurement.

Surface EMG signal is based on amplitude and time and frequency domain properties, which depend on a number of factors [134], such as:

- Timing and intensity of muscle contraction/nerve impulse (in our case)
- Distance between electrode and the tested nerve
- Properties of the overlying tissue (such as thickness of overlying skin, muscle and adipose tissue)
- Electrode and amplifier properties
- Quality of contact between the applied electrode and the skin surface [134]

## **6.6 - CCM image acquisition**

All CCM images were obtained at the Department of Ophthalmology of the Coimbra University Hospitals. These images were collected using a Heidelberg Retinal Tomograph equipped with a Cornea Rostock Module (HRT-CRM: Heidelberg Engineering, Heidelberg, Germany). The device that we used to scan and examine the corneal area is a Laser-Scanning Confocal Microscope (LSCM), which illuminates the corneal structures using a visible 670-nm red wavelength diode laser [135].

Confocal scans were recorded over a depth varying between 30-50  $\mu\text{m}$ . The 384 x 384 pixels images correspond to a 400  $\mu\text{m}$  x 400  $\mu\text{m}$  area and were saved as JPEG images. Several sample images are shown in Figure 11.

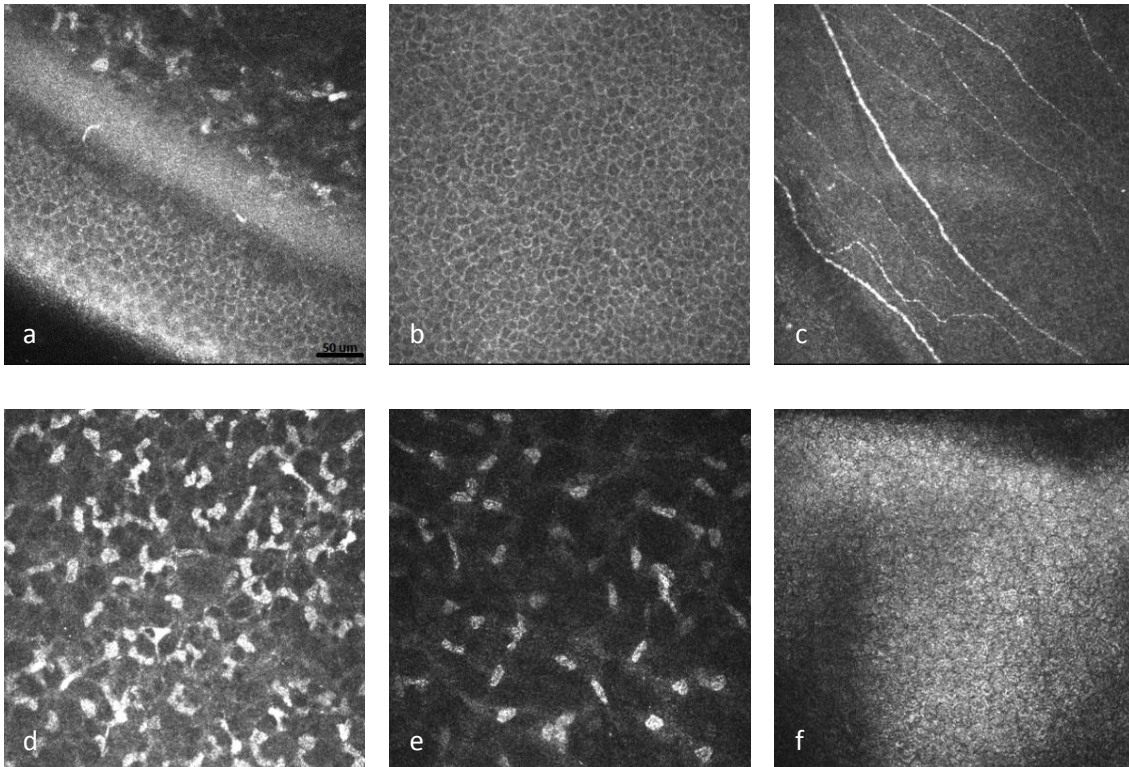


**Figure 11** – IVCCM (384 x 384) pixel images of the healthy living cornea, illustrating **a)** three different corneal layers (starting from the bottom): basal epithelium, Bowman’s layer and stroma; **b)** basal epithelium; **c)** sub-basal nerve plexus with corneal nerves; **d)** anterior stroma; **e)** mid-stroma (with less cells), and **f)** endothelium. [Images obtained at the Coimbra University Hospitals, Department of Ophthalmology; February 2012], [135]

As previously mentioned in the first chapter, the normal human cornea consists of five avascular layers: corneal epithelium, Bowman’s layer, stroma, Descemet’s membrane and corneal endothelium. With the exception of Descemet’s membrane, all corneal layers can be easily shown by IVCCM. The resolution and magnification capacity of the confocal microscope used in our study allowed us to obtain images of different corneal layer cells, with good quality.

All CCM measurements were supervised by an experienced ophthalmologist and were conducted according to guidelines of the Declaration of Helsinki and submitted to approval by the Medical Ethics Committee of the Faculty of Medicine, Coimbra University. In short, the measuring procedure consisted in applying topical anesthetic and a viscous tear gel to the subjects’ eyes to facilitate and ensure a sterile optical contact between the corneal epithelium and disposable cap on the objective lens of the confocal microscope. The gel

also helped to match the refractive index between the objective lens and the cornea decreasing, therefore, losses by reflection that would be present at an air-tear film interface. Patients and volunteers were gently asked to fix their sight on a target placed behind the CCM device and the examiner used a side-view digital video camera to make certain that the apex or the central area of the cornea was entirely scanned. The CCM lens was manually focused on the sub-basal nerve plexus of the cornea by the ophthalmologist, which carefully captured the high-contrast images that best illustrated the corneal nerves [135].

All individuals included in our research study underwent a bilateral examination of the corneal nerve fibers. We used the section mode to capture images from the cornea, acquiring only those that illustrate clearly the corneal nerves. The section mode refers to the option of capturing manually single images (without automatic image capture during axial scanning). This method requires particular focus on nerve fibers, followed by a qualitative choice as to which fibers to show in the obtained image [135].

### **6.7 – Standard Operating Procedure (Image Analysis: Morphometric parameters)**

For the automatic processing and image analysis was initially used a larger set of 200 images (20 sub-sets of 10 bilateral images, corresponding to one sub-set per individual), containing 5 best IVCCM images for each eye (i.e., 10 images per individual that contain only nervous structures, allowing a clear differentiation between the main corneal nerve trunks and secondary nerves, or ramifications) of sub-basal nerve plexus for each subject.

The final selection procedure consisted in choosing one image from the set of these 5 best quality images per eye during visual inspection by the examiner on post examination analysis. The selection of this image was based on the combination of five qualitative criterions (including three parameters): highest density of nerve fibers (NFD), maximum length of nerve fibers (NFL), and highest density of branching (NBD); best image features (well-focused and high contrast image) and maximum sensitivity of automatic nerve detection.

The identification of most relevant morphologic characteristics, as well as the evaluation of their suitability for the early detection and follow-up of DPN with CCM, included the following corneal parameters, observed within a frame: nerve fiber density (NFD), width (NFW) and length (NFL), nerve tortuosity (TC), as well as nerve branching density (NBD), branching pattern (NBP) and angle (NBA). This procedure was performed, as previously mentioned, in all images for each subject included in our study, with a calculated mean value for each of the identified parameter (described in details below).

**Nerve Fiber Density (NFD)**, the total number of count nerves per square millimeter of corneal tissue (number of fibers/mm<sup>2</sup>);

**Nerve Fiber Width (NFW)**, the computed average axe value for each of corneal nerves and/or segments, expressed in μm/mm<sup>2</sup> (2 main axes, the minor axe corresponds to width, the major axe-length);

**Nerve Fiber Length (NFL)**, the total length of all nerve fibers and branches of corneal tissue expressed in mm/mm<sup>2</sup>;

**Tortuosity Coefficient (TC)**, parameter that quantifies if a structure is curved or winding, according to the definition proposed by Kallinikos et al.[93]), giving information on the frequency and magnitude of nerve curvature changes:

$$TC = \sqrt{\sum_{i=1}^{N-1} ((f'(x_i, y_i))^2 + (f''(x_i, y_i))^2)}$$

Where  $N$  represents the number of pixels of the nerve skeleton, while  $f'(x_i, y_i)$  and  $f''(x_i, y_i)$  are the first and second derivatives at the point  $(x_i, y_i)$ , respectively.

**Nerve Branch Density (NBD)**, the number of branches emanating from main nerve trunks per square millimeter of corneal tissue (number of nerve branches/mm<sup>2</sup>);

**Nerve Branching Pattern (NBP)**, expressed as the percentage of branches per total number of nerve fibers;

**Nerve Branching Angle (NBA)**, mean value of the angle formed by the branches with respect to the main nerve trunk (where they start from). General orientations of a branch



can be horizontal (if the angle measured between  $0^\circ$  and  $30^\circ$ ), oblique (between  $31^\circ$  and  $60^\circ$ ) or vertical (between  $61^\circ$  and  $90^\circ$ ).

The results obtained from segmented images with the algorithm developed by our team, were compared with the values of manually traced nerves by an experienced examiner using a commercial program, on the same images. The percentage of nerve length correctly and falsely detected was also calculated.

## **6.8 – Corneal nerve segmentation algorithm**

The method used for the automatic extraction and analysis of sub-basal corneal nerve morphometric parameters is a segmentation algorithm implemented in MatLab, which was applied to a set of 200 images (as mentioned before, corresponding to 10 bilateral corneal images per subject involved in the study).

This automated method was already described in previous publications [136]. It starts by normalizing the image contrast and reducing the noise, using contrast equalization, a phase symmetry-based method and histogram procedure. Subsequently, a quick search is done to find candidate regions that are expanded to recognize corneal nerve fibers. False positives are discarded, whilst all remaining results are joined for an improved identification of complete nerve structure and distribution.

### **6.8.1 - CCM image: artifacts**

Generally, CCM images captured and recorded with good quality show well-defined nerve fibers. These fibers usually appear as connected structures. Nevertheless, many images obtained in our study were affected by noise and the presence of small curvilinear structures (such as tissue deformities and artifacts), typically manifested as unclear and disoriented small fragments. These undesired structures complicated the extraction of nerve fibers. Only after noise reduction the nerve fiber segmentation and extraction becomes an easier task, providing better information for the post-processing stages.

## Types of artifacts

During the CCM image acquisition process, a low number of images were also affected by several types of artifacts, such as saccadic eye movement (which usually resulted in motion or blurring effects of the nerve fibers), nerves located at different depths (causing deeper nerve fibers to appear very faint), focusing in or out of the sub-basal plexus plane (manifested as nerve fiber fluctuations - appear and disappear, affecting also the visual diameter and the brightness of the nerve fiber), illumination artifacts (affects image brightness and contrast) or the presence of small undesired bright structures (usually basal epithelial cells or keratocytes and nerve deformities). Several representative examples of noise and/or artifacts are represented in Figure 12 [135].

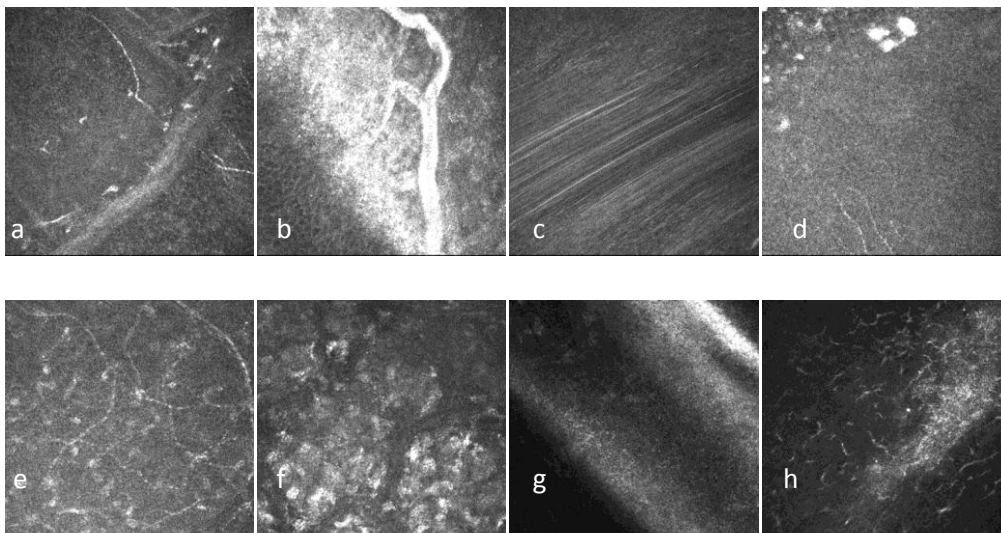


**Figure 12** – Representative examples of CCM image artifacts and noise, with: **a)** corneal tissue deformity; **b)** illumination artifacts and blood vessel; **c)** blurring effect from saccadic eye movement; **d)** bright structures; **e)** stromal cells; **f)** depth differences and bright structures; **g)** and **h)** illumination artifacts. [Images obtained during several IVCCM image acquisition sessions, 2012], [135]

### 6.8.2 – Segmentation algorithm

The segmentation algorithm used in our study is implemented in a Matlab™ code named *Cornea3* and encompasses three main steps: 1) local equalization, for improving image details; 2) phase symmetry, using wavelet transform filter, to recognize the nerves structures; and 3) nerve reconstruction, using morphologic operations [136].

### **Local equalization**

Images obtained through CCM reveal corneal nerves identified as bright well-defined and mostly connected linear structures over a dark background. This background is typically characterized by an intensity variation. For this reason, it is essential to correct this non-uniformity. Histogram equalization is usually required for enhancing the image contrast [137].

*Cornea3* involves a contrast-limited adaptive histogram equalization method, which uses information from numerous histograms corresponding to several small image areas. The contrast is restricted to a limit value, in order to avoid increase in image noise, particularly in homogeneous regions. The current method was applied using an  $8 \times 8$  pixel square mask [136].

### **Phase symmetry**

Symmetry is an essential mechanism to identify the structure and shape of objects. Knowing the symmetry we can specify the invariance of objects under geometric transformations. There are different image features, such as lines, ridges, valleys and blobs that have distinct phase responses. To acquire local phase frequency information, the algorithm included a methodology based on wavelet transform filters, namely log-Gabor filters [136].

This methodology involves two filters: a first filter for calculating the amplitude and a second one for the signal phase, for a specific scale and frequency, at a certain spatial location. Both filters can be preset with arbitrary bandwidth. The phase-shift procedure included six orientations for symmetry searching and produced enhanced images with highlighted tubular structures that clearly show the nerves location [136].

An example of the output images after the first two steps (local equalization and phase symmetry) of the algorithm is presented in Figure 13 [138].

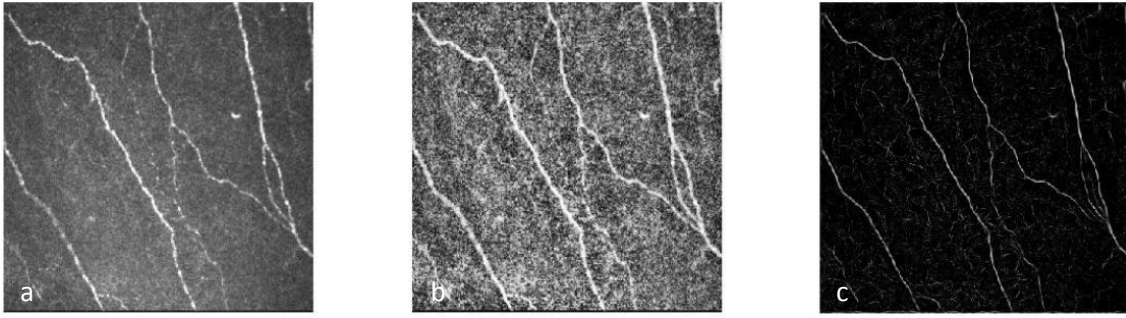


**Figure 13** – Representation of the two initial steps of *Cornea3* segmentation algorithm applied to CCM images: **a)** original image, **b)** local equalization step, and **c)** phase-shift step. [Results obtained in July, 2012], [138]

### Nerve Reconstruction

This final step consists in a complete reconstruction of the corneal nerves, based on tubular structures recognized by the phase symmetry step. It starts with a selection of correct seed points, being complemented with a rejection step. The algorithm analyzes the segmented image, excluding inappropriate structures with incompatible features (i.e., features that do not correspond to corneal nerves) [136].

The selection procedure is performed by computing the skeleton of the image, establishing whether a nerve branch is accepted or discarded. The computed skeleton allows the identification of isolated or disconnected segments. Usually, isolated structures are excluded, since they correspond to non-nerve region or noise. In many cases, stromal keratocytes (cells situated at layers posterior to the sub-basal nerve plexus) are the isolated structures to be rejected [136]. Example results of the nerve reconstruction step are shown in Figure 14 [138].

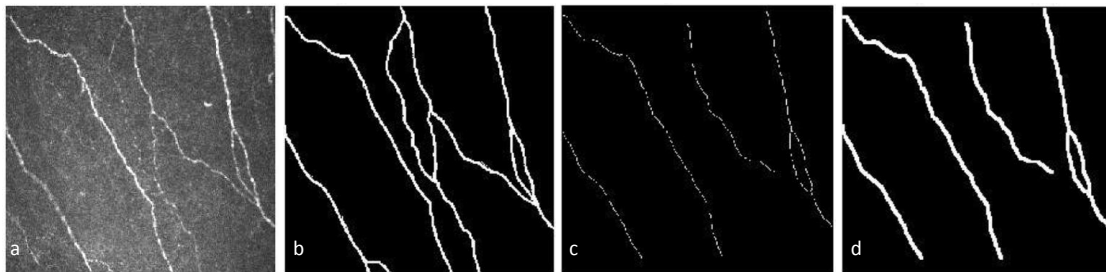


**Figure 14** – Representative sample images and obtained results after the nerve reconstruction step: **a)** original CCM image, **b)** reference image (manually delineated), **c)** segmented image and **d)** reconstructed nerves. [Results obtained in July, 2012], [138]

## **6.9 – Statistical methods**

SPSS Statistics (version 17.0) was used to compute the results of each morphometric parameter. Data are presented as means  $\pm$  standard deviation. ANOVA with Tukey' post hoc tests were used to establish differences among the four groups (control, none, mild, and moderate DPN) if the data followed a normal distribution. Otherwise the Kruskal-Wallis test with nonparametric between group comparisons using the Nemenyi test was used. A significance level of 0.05 was taken in all cases. Pearson correlation tests were used to analyze the existing correlations between the morphometric parameters and other variables. Additionally, box-plots, scatter-plots and drop-line charts were used to represent graphically specific results.

## **SECTION IV**

### **RESULTS**

**CHAPTER 7 – RESULTS ANALYSIS**

As mentioned before, all participants involved in our study were divided in four main groups, according to their DPN severity: control, absent, mild and moderate DPN (summarized in Table 7).

**Table 7** – Summary of the four participants groups (baseline evaluation).

DPN Group (severity degree)	Number of Subjects	Mean Age ± St. dev. (years)	Bilateral CCM Images	MNSI Questionnaire (0-15)	MNSI Scoring (0-10)	EMG diagnosis
Control	8	54 ± 7	80	0	0	Normal
Absent	4	53 ± 11	40	0-3	0-1	Normal
Mild	5	58 ± 9	50	4-6	2-3,5	DPN or Normal
Moderate	3	60 ± 9	30	6-8	2-3	DPN

The automatic algorithm (*Cornea3*) was evaluated comparing the results obtained with manually traced nerves, by an experienced examiner using a commercial program. The percentage of nerve length (expressed in pixels) correctly and falsely detected was calculated. Results are shown in Table 8, where the sensitivity represents the proportion of actual positives which are correctly identified:  $\frac{\text{number of true positives}}{\text{number of true positives} + \text{number of false negatives}}$ .

**Table 8** – Descriptive statistics: evaluation of the segmentation algorithm performance.

Variable	Minimum	Maximum	Average	Standard Deviation
Nerve length correctly detected (true positives) (%)	19,9	91,0	56,7	20,3
Nerve length falsely detected (false positives) (%)	0	2,1	0,5	0,8
Sensitivity (%)	19,3	91,0	57,1	20,4

**7.1 – Nerve fiber density (NFD)**

NFD represents the total number of count nerves per square millimeter of corneal tissue, expressed in number of nerve fibers / mm<sup>2</sup>. The results are summarized in Table 9, and graphically shown in Figure 15. Boxplots show the median, interquartile range, outliers, and extreme cases of individual variables.

**Table 9 – NFD for automatically segmented and manually delineated images.**

NFD: mean value ± st. dev. (count nerves / mm <sup>2</sup> )		
Groups	Automatic algorithm	Manually traced nerves
Control	44,5 ± 31,8	122,3 ± 49,3
Absent	33,6 ± 22,6	87,5 ± 54,7
Mild	20,0 ± 12,0	50,6 ± 9,7
Moderate	19,8 ± 7,9	41,7 ± 23,7

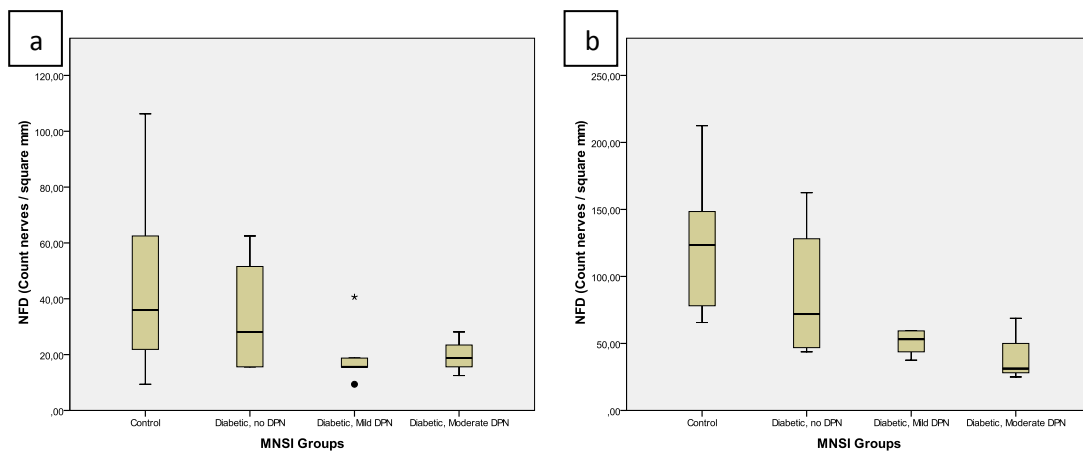


**Figure 15 – Representative boxplots (with median, interquartile range, outliers, and extreme cases of individual variables) of NFD parameter in a) segmented images by the algorithm, and b) manually traced nerves. [Results obtained in August, 2012]**

ANOVA with Tukey’ post hoc tests have shown differences only for manually traced nerves, among the following groups: Control and Mild; Control and Moderate, with mean



difference significant at 0.05 level. No significant differences were found for automatically segmented nerves.

**7.2 – Nerve fiber width (NFW)**

NFW represents the computed average axe value (in pixels) for each of corneal nerves and/or segments, expressed in  $\mu\text{m}/\text{mm}^2$ . The results were obtained only for automatic images, given that manually traced nerves have all the same width (3 pixels). The values are shown in Table 10 and Figure 16.

**Table 10 – NFW for automatically segmented nerves.**

NFW: mean value $\pm$ st. dev. ( $\mu\text{m}/\text{mm}^2$ )	
Groups	Automatic algorithm
Control	7,9 $\pm$ 1,3
Absent	8,4 $\pm$ 2,5
Mild	9,6 $\pm$ 1,1
Moderate	9,5 $\pm$ 1,0

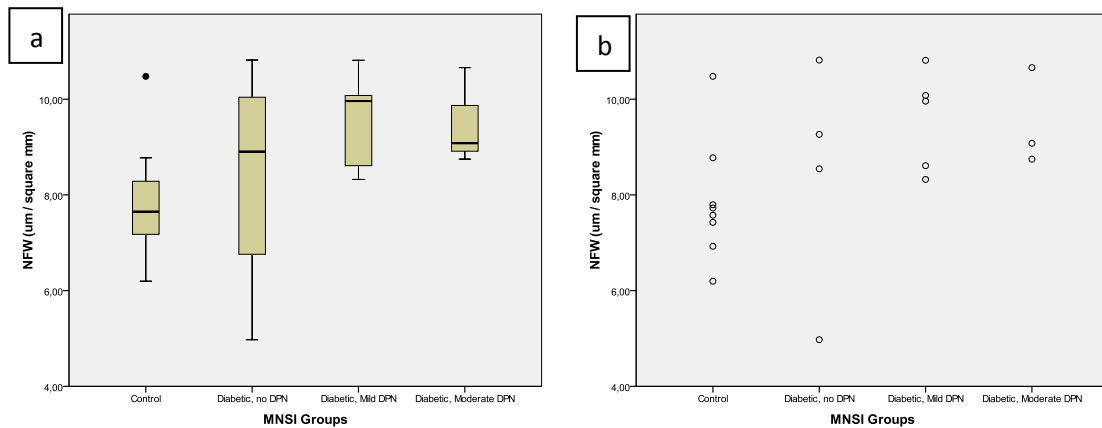


**Figure 16 – a)** Representative boxplot (with median, interquartile range, outliers, and extreme cases of individual variables) and **b)** scatterplot of NFW parameter in segmented images by the algorithm. [Results obtained in August, 2012]

ANOVA with Tukey' post hoc tests have not shown any significant difference for automatic detected nerves, among the existing groups.

**7.3 - Nerve Fiber Length (NFL)**

NFL is the total length of all nerve fibers and branches of corneal tissue, expressed in mm/mm<sup>2</sup>. The results are summarized in Table 11, and schematically shown in Figure 17.

**Table 11 – NFL for automatically segmented and manually delineated images.**

NFL: mean value ± st. dev. (mm/mm <sup>2</sup> )		
Groups	Automatic algorithm	Manually traced nerves
Control	8,9 ± 5,3	14,6 ± 3,9
Absent	7,2 ± 5,1	10,7 ± 4,1
Mild	4,8 ± 2,7	8,8 ± 1,0
Moderate	4,6 ± 2,6	6,9 ± 3,2

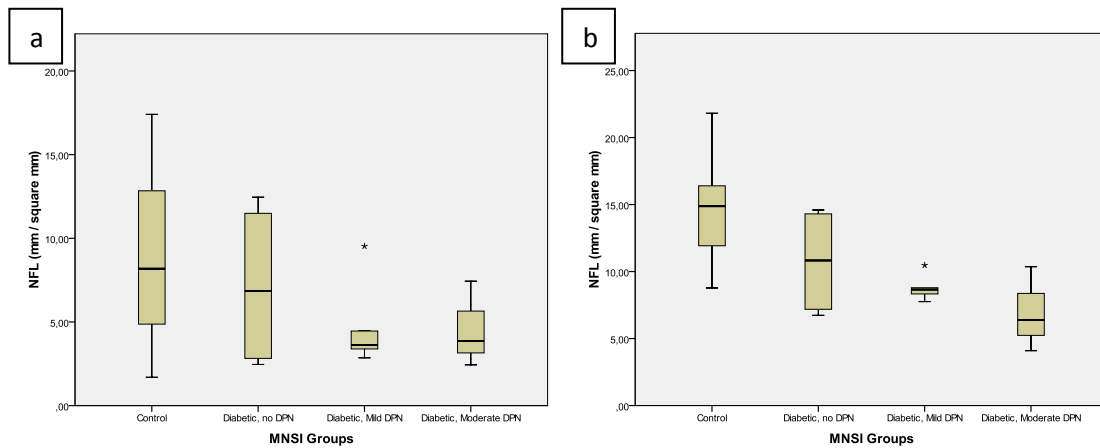


**Figure 17 – Representative boxplots (with median, interquartile range, outliers, and extreme cases of individual variables) of NFL parameter in a) segmented images by the algorithm, and b) manually traced nerves. [Results obtained in August, 2012]**

ANOVA with Tukey’ post hoc tests have shown differences only for manually traced nerves, among the following groups: Control and Mild DPN; Control and Moderate DPN, with mean differences significant at 0.05 level. No significant differences were found between diabetic groups.

### 7.4 – Tortuosity Coefficient (TC)

TC provides information on the frequency and magnitude of nerve curvature changes. To calculate this parameter is necessary to “consider each nerve as a mathematical function on the image space and compute the function first and second derivatives” [93, 135].

$$TC = \sqrt{\sum_{i=1}^{N-1} ((f'(x_i, y_i))^2 + (f''(x_i, y_i))^2)}$$

$N$  represents the number of pixels of the nerve skeleton, while  $f'(x_i, y_i)$  and  $f''(x_i, y_i)$  are the first and second derivatives at the point  $(x_i, y_i)$ , respectively. The results are summarized in Table 12, and schematically shown in Figure 18.

**Table 12** – TC for automatically segmented and manually delineated images.

TC: mean value ± st. dev.		
Groups	Automatic algorithm	Manually traced nerves
Control	52,6 ± 72,8	14,2 ± 2,4
Absent	179,7 ± 227,4	34,1 ± 39,3
Mild	36,4 ± 34,1	23,6 ± 18,7
Moderate	53,7 ± 40,9	25,2 ± 13,6

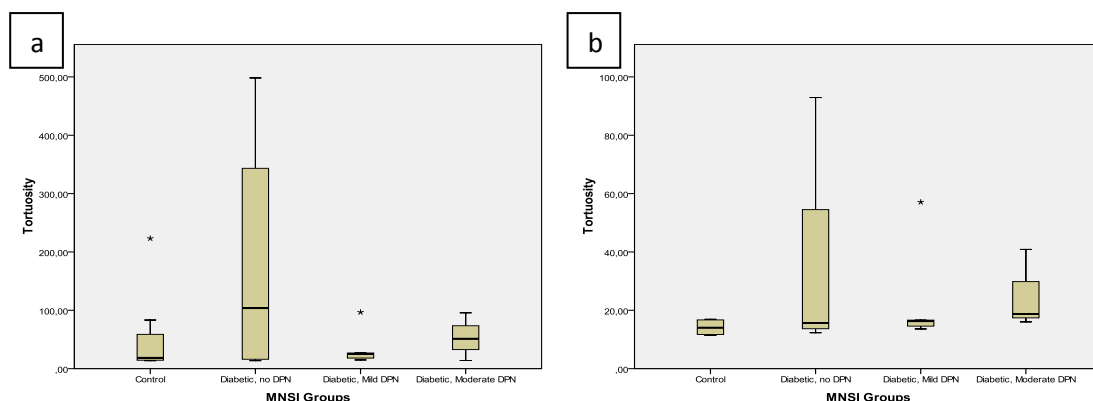


**Figure 18** – Representative boxplots (with median, interquartile range, outliers, and extreme cases of individual variables) of TC parameter in **a)** segmented images by the algorithm, and **b)** manually traced nerves. [Results obtained in August, 2012]

In both cases, automatic and manually traced nerves, ANOVA with Tukey' post hoc tests have not shown any significant difference among the existing groups.

**7.5 – Nerve Branch Density (NBD)**

NBD represents the number of branches emanating from main nerve trunks per square millimeter of corneal tissue, expressed in number of nerve branches/mm<sup>2</sup>. The results are summarized in Table 13, and schematically shown in Figure 19.

**Table 13** – NBD for automatically segmented and manually delineated images.

NBD: mean value ± st. dev. (branches/mm <sup>2</sup> )		
Groups	Automatic algorithm	Manually traced nerves
Control	23,0 ± 26,2	88,3 ± 53,6
Absent	18,0 ± 24,0	63,3 ± 61,2
Mild	3,1 ± 7,0	28,1 ± 7,3
Moderate	4,2 ± 4,8	22,9 ± 26,2

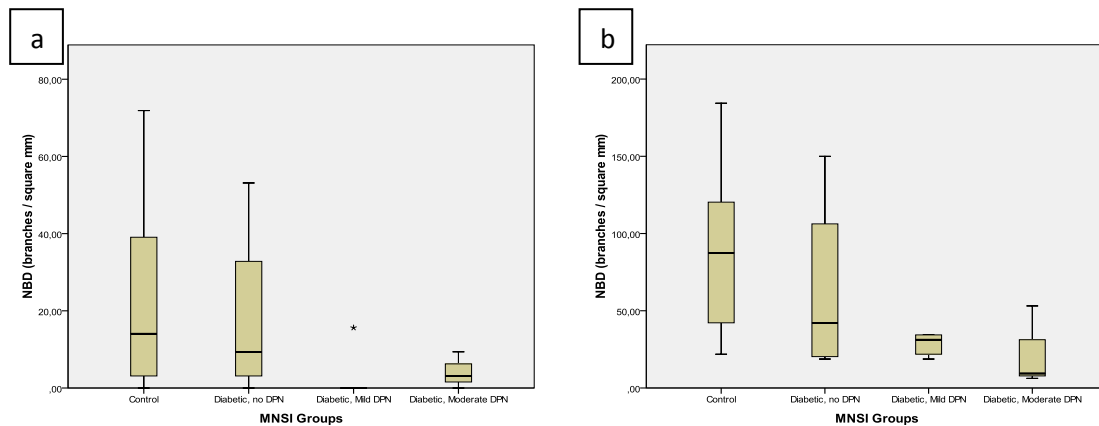


**Figure 19** – Representative boxplots (with median, interquartile range, outliers, and extreme cases of individual variables) of NBD parameter in **a)** segmented images by the algorithm, and **b)** manually traced nerves. [Results obtained in August, 2012]

As for the previous parameter (TC), in both automatic and manually traced nerves, ANOVA with Tukey' post hoc tests have not shown significant differences between the existing groups.

**7.6 – Nerve Branching Pattern (NBP)**

NBP represents the ratio between nerve branches density and nerve fibers density, expressed as the percentage of branches per total number of nerve fibers within a single frame. The results are summarized in Table 14, and schematically shown in Figure 20.

**Table 14** – NBP for automatically segmented and manually delineated images.

NBP: mean value ± st. dev. (%)		
Groups	Automatic algorithm	Manually traced nerves
Control	35,3 ± 27,3	66,3 ± 19,6
Absent	32,6 ± 26,9	60,9 ± 22,7
Mild	7,9 ± 17,6	49,5 ± 11,6
Moderate	15,6 ± 15,0	40,8 ± 23,8

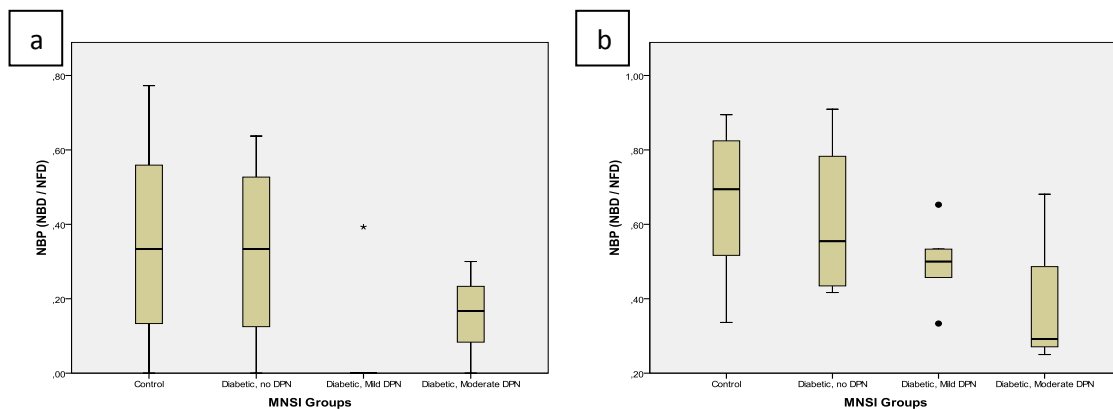


**Figure 20** – Representative boxplots (with median, interquartile range, outliers, and extreme cases of individual variables) of NBP parameter in **a)** segmented images by the algorithm, and **b)** manually traced nerves. [Results obtained in August, 2012]

ANOVA with Tukey’ post hoc tests have not shown any significant difference among the existing groups for automatic detected nerves, as well for manually traced nerves.

**7.7 – Nerve Branching Angle (NBA)**

NBA represents the mean value of the angle formed by the branches with respect to the main nerve trunk (where they start from). General orientations of a branch can be horizontal (if the angle measured between 0° and 30°), oblique (between 31° and 60°) or vertical (between 61° and 90°). The obtained results are shown in Table 15, and schematically illustrated in Figure 21.

**Table 15 – NBA for automatically segmented and manually delineated images.**

NBA: mean value ± st. dev. (degrees)		
Groups	Automatic algorithm	Manually traced nerves
Control	41,1 ± 24,2	34,0 ± 25,0
Absent	84,5 ± 39,3	25,5 ± 6,2
Mild	12,34 ± 0*	26,9 ± 28,1
Moderate	20,8 ± 9,0	16,8 ± 1,8

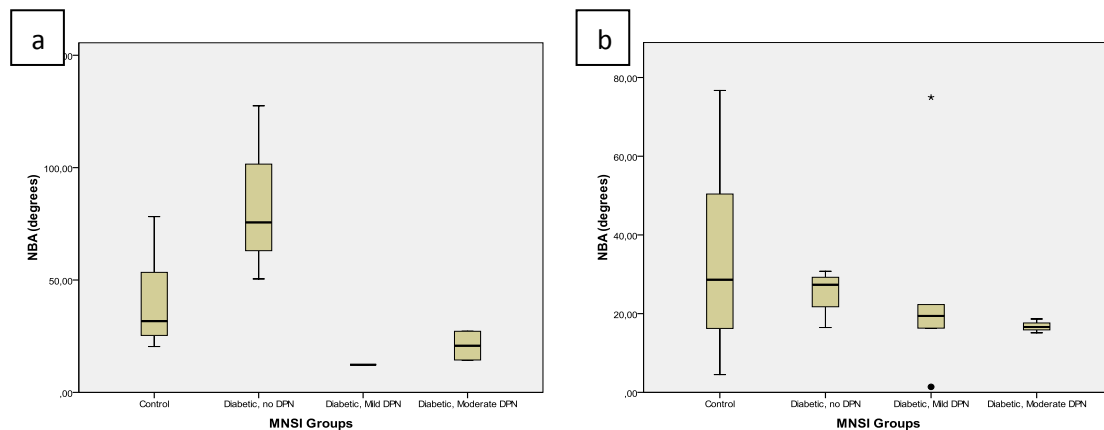


**Figure 21 – Representative boxplots (with median, interquartile range, outliers, and extreme cases of individual variables) of NBA parameter in a) segmented images by the algorithm, and b) manually traced nerves. [Results obtained in August, 2012] (\*NBA value was considered valid only for one individual with Mild DPN)**

Once more, in both automatic and manually traced nerves, ANOVA with Tukey’ post hoc tests have not shown any significant difference among the existing groups.

### 7.8 – Electrophysiological findings

EMG measurements involved nerve conduction evaluation, including motor and sensory nerves conduction velocities (NCV) and amplitudes, as well as cutaneous sympathetic response assessment. As mentioned in Chapter 3, NCS represent valuable measures, especially for the assessment of damage degree in larger nerve fibers in a trustworthy and objective way. These tests are typically demanded by a neurophysiologist for evaluating the muscle or nerve damage (when necessary), representing an important part of a medical workup. The obtained results are shown in Table 16, and schematically illustrated in Figures 22-23.

**Table 16** – Electrophysiological measurements.

NCS Results: mean ± st. dev.					
	Motor nerve		Sensory nerve		Cutaneous
Groups	NCV (m/s)	Amplitude (µV)	NCV (m/s)	Amplitude (µV)	Sympathetic response (s)
Control	46,8 ± 2,2	5,1 ± 2,0	47,9 ± 3,5	18,0 ± 6,7	1,98 ± 0,12
Absent	43,9 ± 2,4	3,5 ± 1,2	43,9 ± 4,4	12,3 ± 5,5	1,86 ± 0,35
Mild	44,1 ± 4,4	4,4 ± 3,0	46,5 ± 5,6	12,9 ± 2,2	2,16 ± 0,35
Moderate	38,3 ± 5,3	2,4 ± 1,0	43,0 ± 6,4	5,2 ± 2,9	1,89 ± 0,01

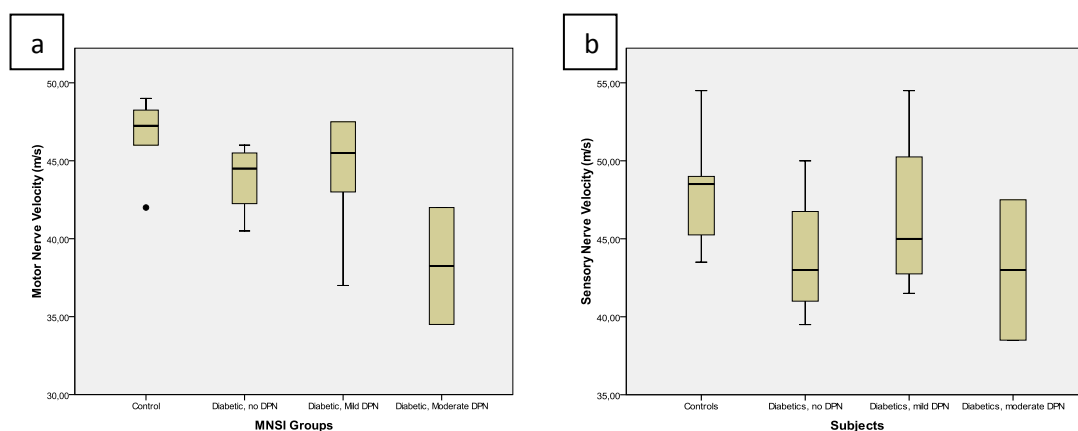


**Figure 22** – Representative boxplots (with median, interquartile range, outliers, and extreme cases of individual variables) with nerve conduction velocities for **a)** motor nerve, and **b)** sensory nerve. [Results obtained in August, 2012]

**Evaluation of Corneal Nerve Morphology for Detection and Follow-up of Diabetic Peripheral Neuropathy**

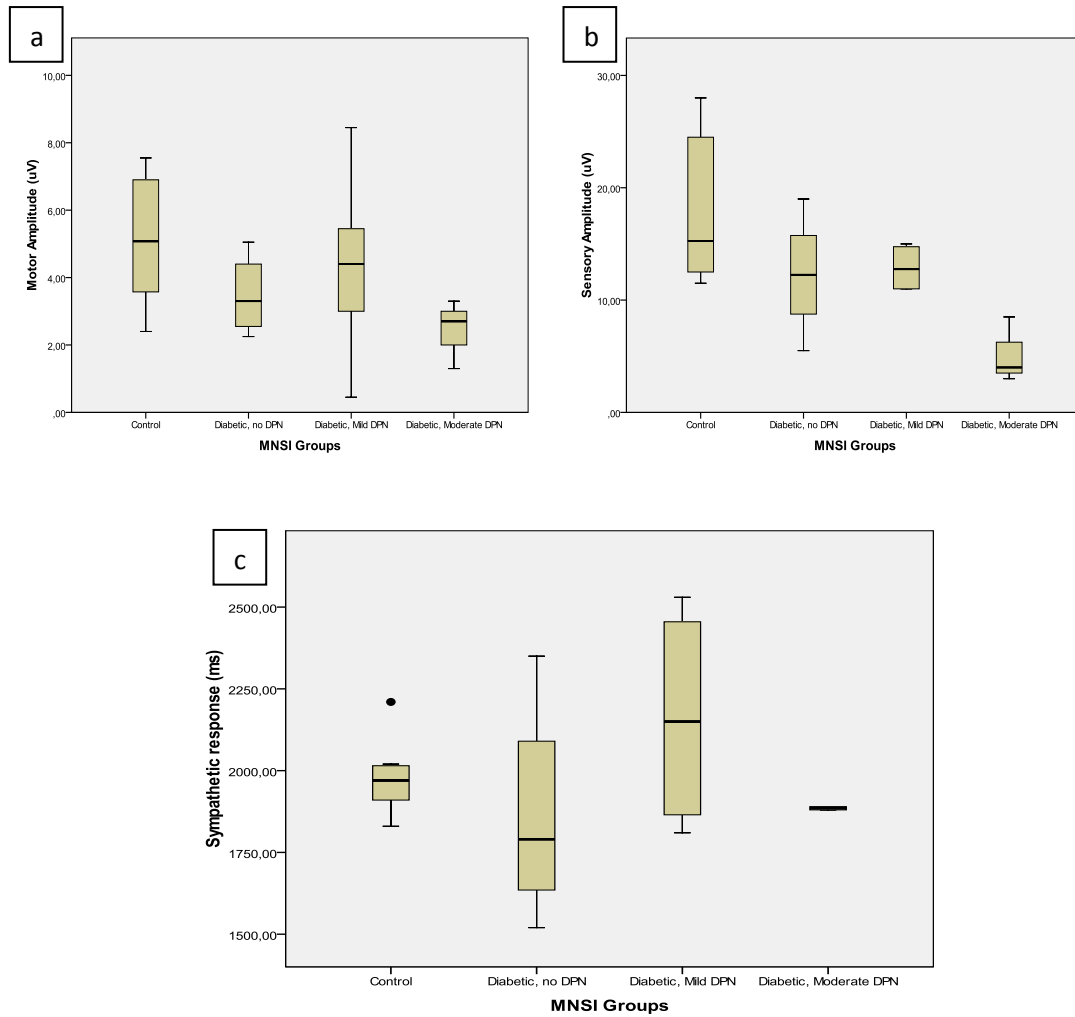


**Figure 23** – Representative boxplots (with median, interquartile range, outliers, and extreme cases of individual variables) with nerve conduction amplitudes (expressed in µV) for **a)** motor nerve, **b)** sensory nerve, and **c)** sympathetic nerve response (latency time [ms]). [Results obtained in August, 2012]

ANOVA with Tukey’ post hoc tests have shown significant differences (at 0.05 levels) for motor NCV and sensory nerve conduction amplitude, among the following DPN groups: Moderate and Control.

Although controls differ substantially from diabetic groups, statistical tests have not revealed any significant difference between the existing groups for the sensory NCV, as well as for the sympathetic response. However, sensory NCV and amplitudes were established by the neurophysiologist as abnormal (below the limit) in patients with moderate degree of DPN, because these patients have shown the lowest values of motor



and sensory NCV, showing also the lowest motor and sensory amplitude values, in comparison to mean values of the remaining groups.

NCS have also shown that patients with moderate DPN have a significant axonal loss, demonstrated by decreased motor amplitudes (CMAP) and reduced sensory amplitudes (SNAP). The low values of both motor and sensory NCV indicate that moderate DPN cases occur with severe nerve demyelination (as explained in Section I, Chapter 3).

### **7.9 – Correlations tests and distribution charts for manually segmented nerves**

This section contains representative scatter-plots and results of the correlation tests only for manually delineated nerves, since all parameter values are more accurate, when compared to automatic segmented nerves.

Pearson correlation tests, with a factor ranging between 0 and 1 (minimum and maximum, respectively) have revealed a strong correlation, significant at the 0.01 level (sig. 2-tailed) between the following morphometric parameters: NFD, NFL, NFW, NBD and NBP. Additionally, Pearson correlation tests have shown correlations, statistically significant, between NFD, NFL and motor NCV (summarized in Table 17).

**Table 17** – Summary of correlation tests between morphometric parameters.

Parameters ↩	Pearson correlation factor at p<0.01 level					
	NFD	NFL	NFW	NBD	NBP	motor NCV
<b>NFD</b>	-	0,916	-0,752	0,983	0,862	*0,487
<b>NFL</b>	0,916	-	-0,732	0,896	0,859	0,578
<b>NFW</b>	-0,752	-0,732	-	-0,767	-0,763	-

**(\*) - p<0.05 level**

No significant correlations were found between TC and other parameters, as well as NBA, sensory NCV and sympathetic response. These parameters do not depend on the variation of other parameters, mentioned above.

NFD represents an important parameter, which is strongly correlated with several other parameters. NFD is inversely correlated with NFW, and directly correlated with NFL, NBD, NBP, and motor NCV, indicating that a higher density of the nerve fibers is directly

**Evaluation of Corneal Nerve Morphology for Detection and Follow-up of Diabetic Peripheral Neuropathy**

proportional with increased nerve length and richer branching pattern, resulting in a faster conduction velocity (as shown in Figure 24).

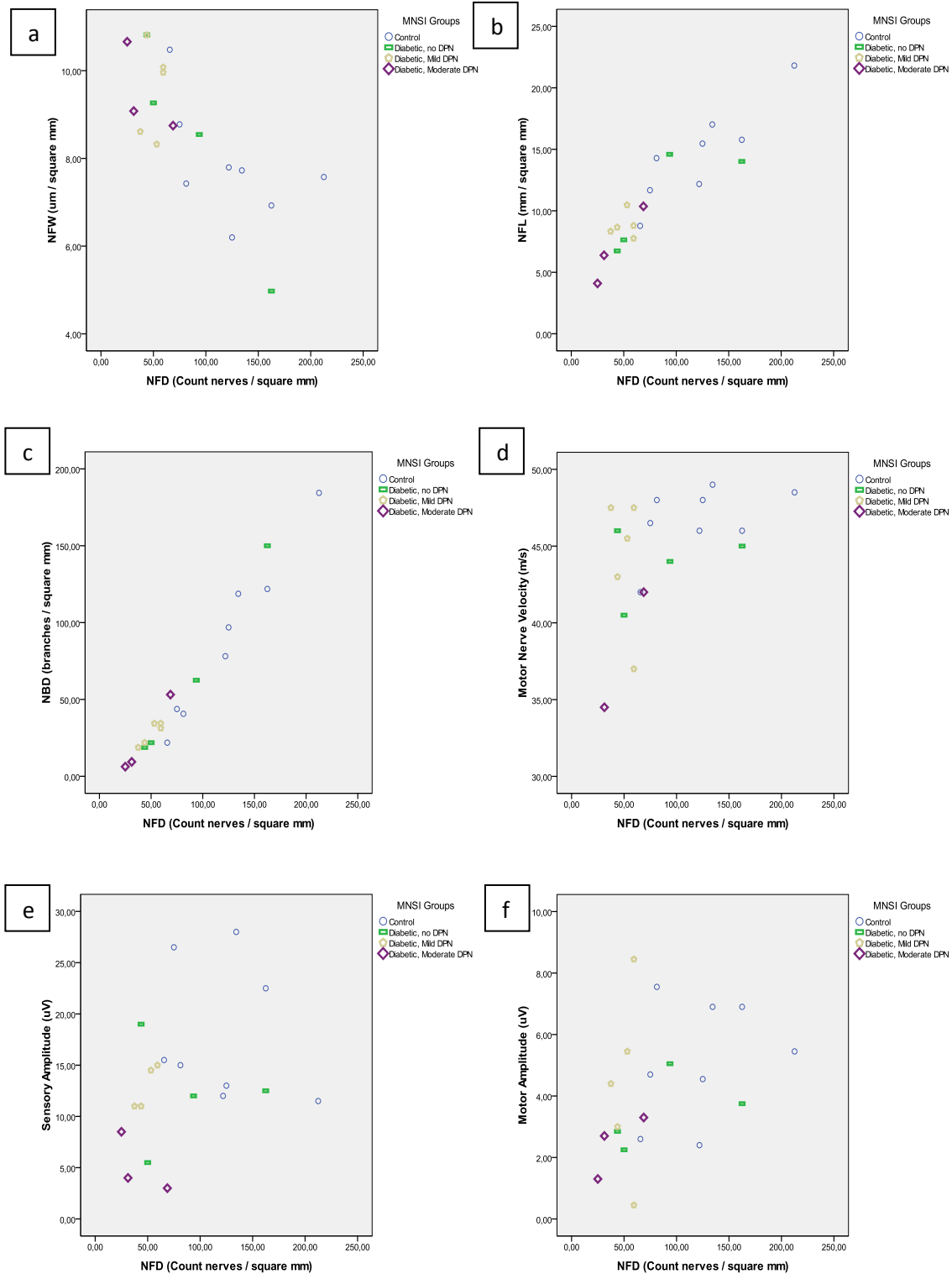


**Figure 24** – Representative scatterplots showing the distribution of individuals according to NFD and **a)** NFW; **b)** NFL; **c)** NBD; **d)** motor NCV; **e)** sensory amplitude; and **f)** motor amplitude [Results obtained in August, 2012]

**Evaluation of Corneal Nerve Morphology for Detection and Follow-up of Diabetic Peripheral Neuropathy**

Other important parameter is NFL, also significantly correlated with several parameters. NFL is inversely correlated with NFW, while directly correlated with NFD, NBD, NBP and motor NCV, suggesting that longer nerve fibers are faster conducting and directly proportional with higher nerve density and richer branching pattern (Figures 24(a) and 25).

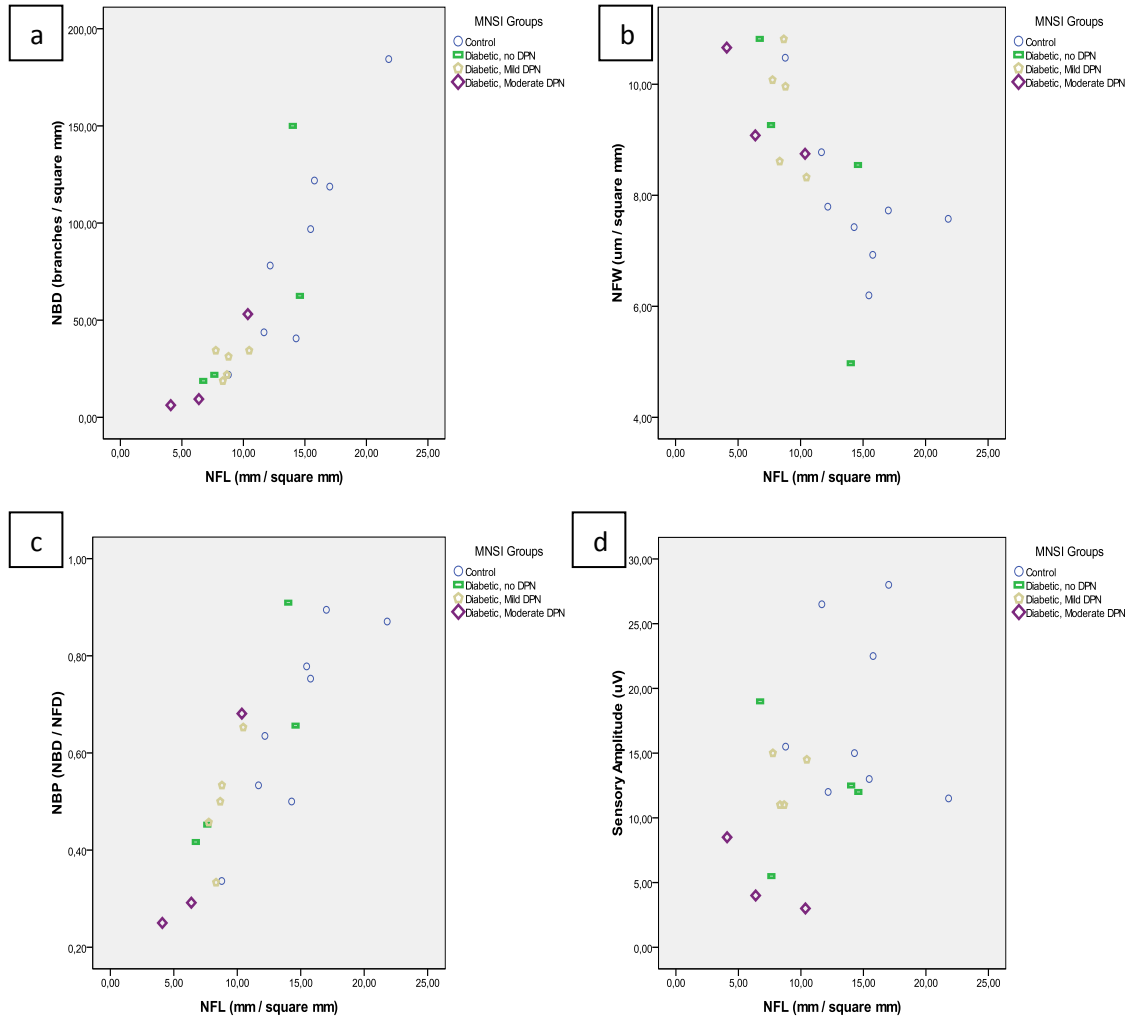


**Figure 25** – Representative scatterplots showing the distribution of individuals according to NFL and **a)** NBD; **b)** NFW; **c)** NBP; and **d)** sensory amplitude. [Results obtained in August, 2012]

NFW is also an essential parameter, which appears to correlate inversely with numerous other parameters, such as NFD, NFL, NBD and NBP. This fact demonstrates that reduced length and number of nerve fibers, as well as decreased branch density induce an increase of nerve width (Figure 26).

**Evaluation of Corneal Nerve Morphology for Detection and Follow-up of Diabetic Peripheral Neuropathy**

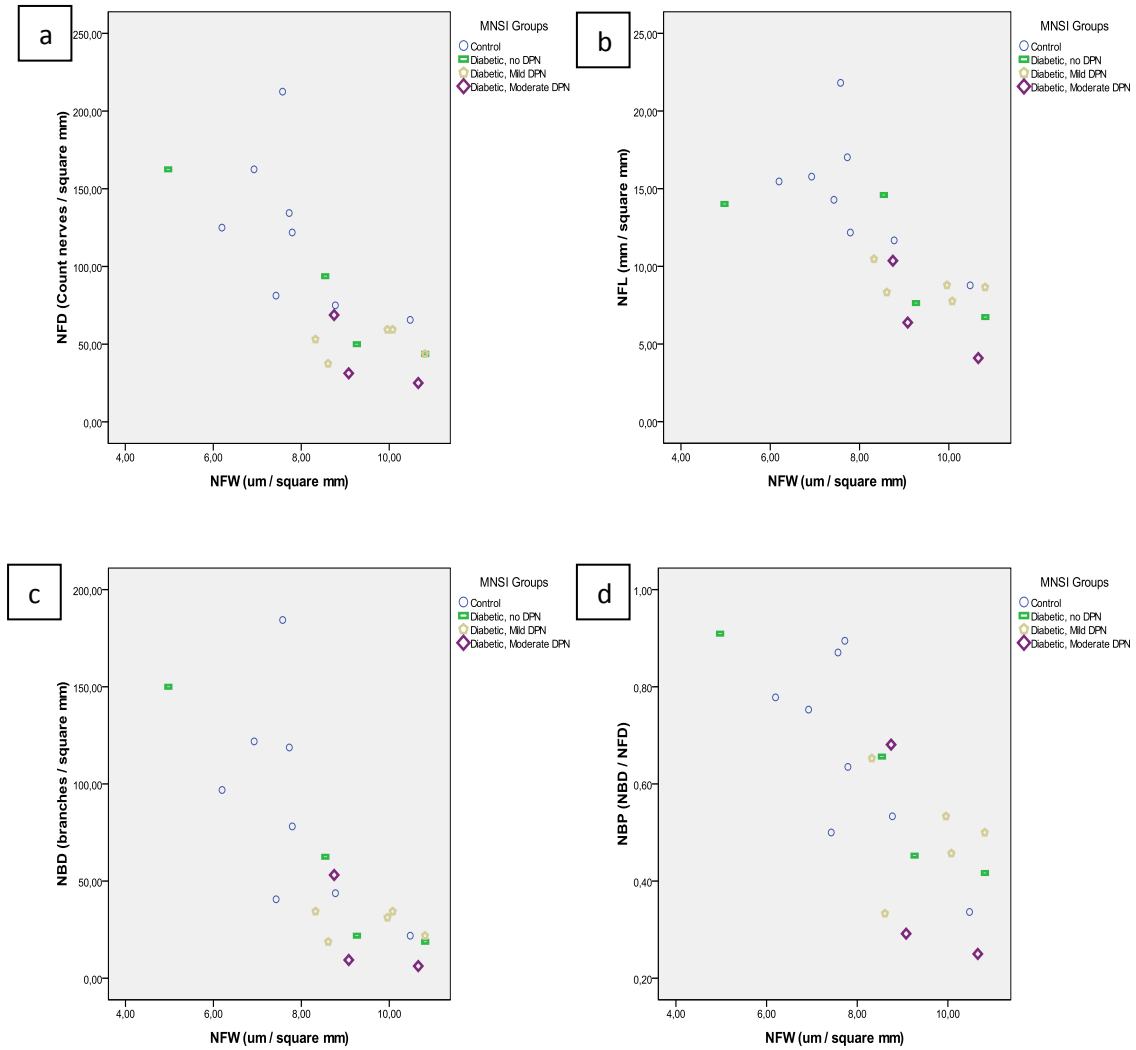


**Figure 26** – Representative scatterplots showing the distribution of individuals according to NFW and **a)** NFD; **b)** NFL; **c)** NBD; and **d)** NBP. [Results obtained in August, 2012]

Other morphometric parameters, such as TC and NBA, have not exhibited any correlation. Next scatter charts show the distribution of the subjects according to these last three parameters, where is obvious that the obtained values are widely distributed, in a “chaotic” and inconsistent manner, showing that these parameters do not follow same distribution rule, between and within groups, as NFD and NFL parameters. TC and NBA provide inconclusive information on the presence and/or severity degree of DPN (Figure 27).

**Evaluation of Corneal Nerve Morphology for Detection and Follow-up of Diabetic Peripheral Neuropathy**

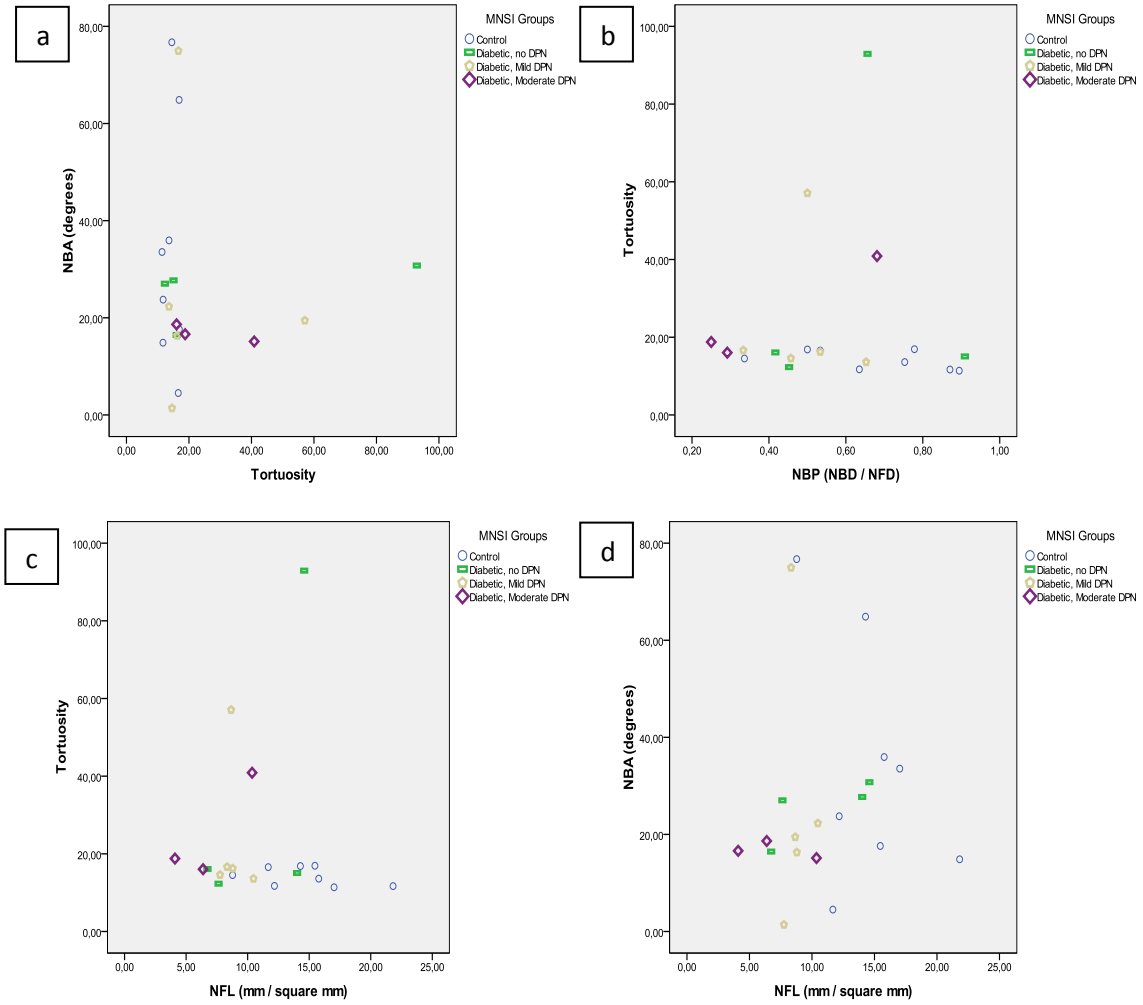


**Figure 27 – Representative scatterplots showing the distribution of individuals according to; a) TC and NBA; b) NBP and TC; c) NFL and TC; and d) NFL and NBA [Results obtained in August, 2012]**

## **SECTION V**

### **OVERVIEW**

#### **RELEVANCE OF THE STUDY**

## CHAPTER 8 – DISCUSSION AND CONCLUSIONS

Our study aimed principally to evaluate the ability of detecting and quantifying DPN using the morphology of corneal nerves measured in CCM images. In particular, we intended to assess the ability to differentiate between several groups of individuals, including healthy volunteers and diabetics type 2 (insulin-treated), divided according the presence/absence and severity degree of DPN, using numerical parameters related to corneal nerves morphology.

In this work I have presented two different sets of results. First set was obtained using a fully automatic segmentation algorithm for identifying corneal nerves in CCM images. Second set was obtained from manually traced images by an experienced examiner, using a commercial program. I evaluated the algorithm performance in a set of 40 bilateral images of the sub-basal nerve plexus of 8 healthy (non-diabetic) and 12 diabetic individuals. This set was extracted during visual inspection by the examiner on post examination analysis, from a larger set of 200 images (10 bilateral images per individual). The selection was mainly based on choosing best quality images (analyzing several quantitative and qualitative criteria, such as higher NFD, NFL, NBD and automatic detection performance) in order to have a set representative of the images obtained by an ophthalmologist with experience on CCM.

The study consisted in a detailed evaluation of a small cohort of healthy controls and type 2 diabetic patients with different degrees of neuropathy severity according to MNSI classification (absent, mild and moderate; no patients with severe neuropathy were identified). We found that CCM can be successfully used as a complementing technique for the clinical and electrophysiological diagnosis of DPN, as defined by consensus criteria using nerve conduction studies (NCS).

We have started by grading DPN in diabetic patients, according to the presence of distal symmetrical symptoms assessed by neurological examination (MNSI scoring and questionnaire), abnormal NCV assessed by electrophysiological measurements, clinical outcomes of small fiber abnormalities (with emphasis on presence of corneal nerve length and density dependent symptoms) quantified by CCM.

As would be expected, our study has shown that DSPN is one of the most frequent diabetic neuropathies (patients with moderate neuropathy were diagnosed with DSPN), affecting both sensory and motor nerves. NCS examinations have validated that DSPN is mainly axonal with a predominantly large diameter nerve fiber involvement. NCS quantified large-fiber abnormalities in all patients with moderate degree of neuropathy, and in one patient with mild degree, establishing DSPN diagnosis. Electrophysiological measurements have shown progressive axonal losses (according to the DPN severity), by exhibiting decreased amplitudes of the compound muscle action potential (CMAP), decreased sensory nerve action potential (SNAP), reduced motor and sensory nerve conduction velocities (NCV), whilst CCM have quantified small fiber disorders (gradual reduction in corneal NFD, NBD and NFL), showing that DSPN also occur with mixed large - and small diameter nerve fiber involvement.

On the other hand, NCS have shown normal NCV values (considered by the neurophysiologist) for all patients without DPN and for the majority of the patients with mild degree of severity. Nevertheless, the NCV and amplitude values for both motor and sensory nerves were lower for the patients with mild DPN, while CCM quantified accurately small fiber pathology (decreased NFD and NFL) in mild DPN patients, which did not seem to have larger nerve fiber injuries.

Although CCM is still in early phase of development and employment as a potential marker of diabetic neuropathy, the application of this non-invasive technique allowed us to obtain promising results. Once more, CCM has shown to be valuable (at least as a complementing diagnostic tool), providing useful information in order to stratify patients' neuropathic severity, confirming also the MNSI classification. We were able to distinguish the controls from diabetics, to differentiate individuals without DPN from those with DPN, and most important, to stratify the patients according to the MNSI classification for the severity of neuropathy. The outcomes from our observational study have clarified the true efficacy CCM, confirming and showing similar results to prior studies.

The parameters that have shown a good quantification and diagnostic potential performance were NFL, NFD, NFW and NBD, and consequently NBP. NFL and NFD are the



parameters that revealed significant mean value differences between and within the control and diabetic groups, with high degrees of specificity and sensitivity. As described in several prior publications [70, 91, 92, 95-98, 103], NFD and NFL are significantly lower in diabetics compared to controls ( $p < 0.05$ ), establishing inverse correlations with severity degree of DPN. It is important to mention that both parameters revealed differences statistically significant ( $p < 0.05$ ) between controls and diabetics, between no DPN cases and DPN patients, and most important, within diabetics (MNSI mild and moderate groups) and healthy controls.

NBD, NBP and NFW have not shown significant mean value differences between the MNSI groups, revealing instead differences that were statistically significant ( $p < 0.05$ ) between controls and diabetics, confirming the results published by Mocan *et al.* [96]. Moreover, diabetic patients have shown a gradual increase in nerve thickness (NFW) and a progressive reduction in nerve branching (NBD), according to their severity degree, as shown by Quattrini *et al.* [97] and Edwards *et al.* [103], respectively.

TC and NBA parameters were the only parameters that have not revealed significant differences from statistical point of view, a result also reported by Ahmed *et al.* [101]. Nonetheless, we found in diabetics a general increase in tortuosity, as mentioned by Dabbah *et al.* [8] and Mocan *et al.* [96]. As for the NBA parameter, the results have shown inconsistent fluctuations between and within diabetic and control groups, being considered as inconclusive discrimination results. We conclude that the orientation angles of nerve branches do not depend on the presence or absence of DPN. NBA parameter have not shown any correlation with other parameters, a fact that demonstrates that the angle of nerve branching varies with non-correlated patterns between different individuals, independently of their diabetic and neuropathic status, or their nerve characteristics and parameters.

Resuming, we were able to demonstrate that corneal small nerve fiber abnormalities are directly related to the severity of peripheral neuropathy. The accurate quantification of nerve fiber length and thickness (NFL and NFW, respectively), as well as nerve fiber and branch densities (NFD and NBD, respectively), allows us to conclude that an increasing

corneal nerve degeneration is directly related with increasing severity of diabetic neuropathy.

NFL, NFW, NFD and NBD parameters allowed us to identify patients at initial phase of DPN (mild degree) that are at subsequent risk of developing clinically significant DPN (moderate and severe degree DPN). The mean difference values between diabetics with mild and moderate degree of DPN were minimal, proving that all four parameters are reliable predictors for neuropathic complications.

A final conclusion can be made regarding the automatic detection and segmenting of corneal nerves, including two extremely important components: CCM images and computed algorithm (*Cornea3*). The results of automatically segmented nerves highlighted a number of technical insufficiencies and difficulties, including image quality (affected by artifacts), and algorithm performance (especially in nerve reconstruction and post-processing steps).

The algorithm performance was mainly affected by image artifacts, such as nerve discontinuities, motion or blurring effects of the nerve fibers, nerves located at different depths, focusing in or out of the sub-basal plexus plane, illumination artifacts (brightness and contrast) or the presence of small confounding bright structures (usually basal epithelial cells or keratocytes and nerve deformities). Although keratocytes should be rejected by phase symmetry, in some images they were not discriminated. Instead, they were mistakenly treated as secondary nerve branches.

Consequently, the automated algorithm still requires a substantial and sophisticated improvement, especially in post-processing steps, in order to ensure the higher accuracy, reliability and consistency required for continuing this study. This improvement is particularly needed to upgrade the ability in handling nerve deformities and discontinuities, as well as discriminating confounding keratocytes. However, an encouraging aspect would be that, despite the insufficient sensitivity values of the automatic segmentation algorithm, we were able to obtain acceptable results for NFD, NFW, NBD and NFL parameters. These results allowed us to quantify noticeable differences between controls and diabetics.

## CHAPTER 9 – FUTURE WORK

The work done during this entire academic year has been truly interesting and challenging, revealing sometimes certain limitations, mainly regarding the participants' selection and recruitment (principally due to DPN severity and age-matching factors), and technical difficulties, regarding the automatic analysis (nerve detection and segmentation). All these difficulties required for adequate solutions and gradual improvements, leading us to a better-structured and more efficient study. However, there are still few aspects related to our observational study that could be enhanced and, I have some suggestions for an eventual continuation of the project in the near future.

My suggestions regard mainly the study duration and population recruitment. The duration of a larger trial for demonstrating efficiently a significant difference in outcomes between healthy volunteers (control population) and diabetic groups (according to DPN severity grading) is directly dependent on the desired statistical power of the study and relative success rates observed in both groups. This success rate depends directly on diabetic patients and controls recruitment.

A future trial should recruit a minimum of 10 patients (ideal number would be 20) for each group, based on the severity of DPN symptoms (absent, mild, moderate and severe), summing a minimum of 40 diabetic individuals (better if 80), requiring for the same number of healthy individuals, selected carefully for an age and sex-matched study. The number of 10 patients per group provides the following least significant differences (LSD, based on the variance values obtained in our study): LSD = 33.4 fibers / mm<sup>2</sup> for NFD parameter; LSD = 2.72 mm / mm<sup>2</sup> for NFL parameter; and LSD = 36.5 branch / mm<sup>2</sup> for NBD parameter. The recruitment of 20 patients per group is justified by lower LSD values, which in this case are significantly reduced (almost half of the initial values). Nonetheless, it is important to mention that LSD depends directly on variance, and lower the variance, lower the number of participants required for the study.

Regarding the diabetics, the selection process should also consider the duration of DPN, as well the evolution of peripheral nerve complications. In healthy controls and patients with

absent, mild, moderate and severe neuropathy, neurological tests and additional assessment measures, such as nerve conduction studies (NCS) and QST, are sufficient to demonstrate a clinically meaningful and statistically significant difference, in less than one year.

Another suggestion would be to perform an observational study, simultaneously in two different diabetic populations, with Diabetes Mellitus type 1 and type 2, respectively. In this case, with three different populations (type 1, type 2 and controls) with minimal numbers of 40 people for each population (summing a total of 120), could require more time (approximately 1 year) to demonstrate a clinically important and statistically significant mean difference between the stratified groups, according to the severity degree of DPN.

A final suggestion would be to initiate a cross-sectional study for the evaluation of a population of type 2 diabetics, in order to assess and associate diabetic micro-vascular complications, namely diabetic retinopathy (both proliferative and non-proliferative, depending on the case), diabetic nephropathy and diabetic peripheral neuropathy (DPN). It would be extremely useful and interesting to associate and correlate nephropathy symptoms with retinopathy symptoms (such as presence micro aneurysms and neovascularization) and peripheral nerve abnormalities (decreased nerve fiber length and density and increased nerve fiber width), according to diabetic status and severity degree of all mentioned diabetic micro-vascular complications.

## REFERENCES

1. Lang G., "Ophthalmology: A pocket textbook atlas", 2<sup>nd</sup> edition, Thieme, 2007
2. Vander et al., "Human Physiology: The mechanism of body function", 8<sup>th</sup> edition, The McGraw-Hill Companies, 2001
3. Pocock G., Cristopher D., "Human physiology", s. 1., Oxford Core Texts, 2006
4. Patel D. V., "In vivo confocal microscopy of the cornea in health and disease", Department of Ophthalmology, University of Auckland, 2005
5. Muller L. J., et al., "Corneal nerves: structure, contents and function", Experimental Eye Research, Vol. 76, 2003
6. Washington University Physicians (Online), Cited on 05.01.2012, <http://wuphysicians.wustl.edu/dept.aspx?pageID=17&ID=6>
7. Mouhamed A Al-Aqaba, et al., "Architecture and Distribution of Human Corneal Nerves", *Br J Ophthalmol*; **94**:784-789, 2010
8. Dabbah M. A., Graham J., Tavakoli M., Petropoulos I. and Malik R. A., "Automatic analysis of diabetic peripheral neuropathy using multi-scale quantitative morphology of nerve fibers in corneal confocal microscopy imaging", Medical image analysis, Elsevier, 2011
9. Whiting D. R., Guariguata L., Weil C., Shaw J., "IDF Diabetes Atlas: Global estimates of the prevalence of diabetes for 2011 and 2030", Diabetes Research and Clinical Practice, 94: 311-321, Elsevier, 2011
10. Gooch C. and Podwall D., "The Diabetic Neuropathies", *The Neurologist*, Vol. 10, 2004
11. Soley Thrainsdottir, "Peripheral polyneuropathy in type 2 diabetes mellitus and impaired glucose tolerance: correlations between morphology, neurophysiology, and clinical findings", Department of Clinical Sciences, Malmo, Neurology, Lund University, 2009
12. <http://emedicine.medscape.com/article/117853-overview>, Type 2 Diabetes Mellitus, Authors: Romesh Khardori, MD, PhD, FACP; Chief Editor: George T Griffing, MD, 2011
13. "Diagnosis and Classification of Diabetes Mellitus and its Complications", Report of a World Health Organization Consultation, 1999

14. A. I. Vinik, T. S. Park, K. B. Stansberry, and G. L. Pittenger, "Diabetic neuropathies", *Diabetologia* 43, 957-973 (2000).
15. Ayda Moaven-Shahidi, "Assessment of retinal structure and visual function in association with diabetic peripheral neuropathy", 2011
16. FAZAN, S. V. P.; DE VASCONCELOS, C. C. A.; VALENÇA, M. M.; NESSLER, R. & MOORE, K. C. "Diabetic peripheral neuropathies: a morphometric overview", *Int. J. Morphol.*, 28(1):51-64, 2010
17. James L. Edwards, Andrea M. Vincent, Hsinlin T. Cheng, Eva L. Feldman "Diabetic neuropathy: Mechanisms to management", (2008)
18. Boulton, A.J., 2005. Management of diabetic peripheral neuropathy. *Clinical Diabetes* 23 (1)
19. Llewelyn J.G., "The diabetic neuropathies: types, diagnosis and management", *J Neurol Neurosurg Psychiatry* 2003; 74(Suppl II):ii15–ii19.
20. Peter J. Dyck et al., "Diabetic polyneuropathies: update on research definition, diagnostic criteria and estimation of severity", 2011
21. Loseth Sissel, "Studies of peripheral large and small nerve fiber disease with emphasis on diabetic polineuropathy", University of Tromso, Faculty of Medicine, Institute of Clinical Medicine, Department of Neurology, 2008
22. Vinik et al., "Diabetic autonomic neuropathy", *DIABETES CARE*, VOLUME 26, NUMBER 5, MAY 2003
23. Boulton A.J. et al., "Diabetic somatic neuropathies", *DIABETES CARE*, VOLUME 27, NUMBER 6, JUNE 2004
24. Wilbourn A. J., "Diabetic entrapment and compression neuropathies", In *Diabetic neuropathy*, Dyck P. J. et al., 481-508, 1999
25. Goldberg B. J., Light T. R., Blair S. J., "Ulnar neuropathy at the elbow: results of medial epicondylectomy", *J Hand Surg* 1419: 182-188, 1989
26. Brown W. F., Watson B. F., "AAEM case report 27: acute retro humeral radial neuropathies", *Muscle Nerve* 16:706-711, 1993
27. Goldstein J. E., Cogan D. G., "Diabetic ophthalmoplegia with special reference to the pupil", *Arch Ophthalmol* 64:592-598, 1960
28. Cornblath David R., MD, "Diabetic Neuropathy: Diagnostic Methods", 2004
29. England J.D., Gronseth G. S., Franklin G., Miller R. G., Asbury A. K., Carter G. T., Cohen J. A., Fisher M. A., Howard J. F., Kinsella L. J., Latov N., Lewis R. A., Low P. A.,

- Sumner A.J., "Distal symmetric polyneuropathy: a definition for clinical research: report of the American Academy of Neurology, the American Association of Electrodiagnostic Medicine, and the American Academy of Physical Medicine and Rehabilitation", *Neurology* 64:199-207, 2005.
30. Dyck P. J. et al., "Diabetic polyneuropathies: update on research definition, diagnostic criteria and estimation of severity", *Diabetes Metab Res Rev* 2011; 27: 620–628, 2011
31. Boulton A. J., "Guidelines for Diagnosis and Outpatient management of Diabetic Peripheral Neuropathy", *European Association for the Study of Diabetes, Neurodiab. Diabetes Metab.*; 24 (Suppl 3): 55-65, 1998
32. Skljarevski V., Malik A.R, "Clinical Diagnosis of Diabetic Neuropathy", *Contemporary Diabetes: Diabetic Neuropathy: Clinical Management, Second Edition*, Edited by: A. Veves and R. Malik, Humana Press Inc., Totowa, New Jersey, 2007
33. Smieja M., Hunt D. L., Edelman D., Etchells E., Cornuz J., Simel D. L., "Clinical examination for the detection of protective sensation in the feet of diabetic patients.", *International Cooperative Group for Clinical Examination Research, J Gen Intern Med*, 14 (7), 1999
34. Maser R. E., Nielsen V.K., Bass E. B., "Measuring diabetic neuropathy. Assessment and comparison of clinical examination and quantitative sensory testing", *Diabetes Care*, 12(4), 1989
35. Dyck P. J., Karnes J., O'Brien P. C., Swanson C. J., "Neuropathy symptom profile in health, motor neuron disease, diabetic neuropathy, and amyloidosis", *Neurology*; 36:1300–1308, 1986
36. Dyck P.J. , Kratz K. M., Lehman K. A., et al., "The Rochester diabetic neuropathy study: Design, criteria for types of neuropathy, selection bias, and reproducibility of neuropathic tests", *Neurology*; 41:799–807, 1991
37. Abbott CA, Carrington AL, Ashe H, Bath S, Every LC, Griffiths J, Hann AW, Hussein A, Jackson N, Johnson KE, Ryder CH, Torkington R, Van Ross ER, Whalley AM, Widdows P, Williamson S, Boulton AJ: The North-West Diabetes Foot Care Study: incidence of, and risk factors for, new diabetic foot ulceration in a community based patient cohort. *Diabet Med* 19:377-384, 2002

38. Young R. J., Zhou Y. Q., Rodriguez E., Prescott R. J., Ewing D. J., Clarke B.F., "Variable relationship between peripheral somatic and autonomic neuropathy in patients with different syndromes of diabetic polyneuropathy", *Diabetes* 35:192–197, 1986
39. Burns T. M., Taly A., O'Brien P. C., Dyck P. J., "Clinical versus quantitative vibration assessment: improving clinical performance", *J Peripher Nerv Syst*; 7(2):112-117, 2002
40. Dyck P.J., "Detection, characterization, and staging of polyneuropathy: assessed in diabetics", *Muscle Nerve* 11:21-32, 1988
41. Perkins B. A., Olaleye D., Zinman B., Bril V., "Simple screening tests for peripheral neuropathy in the diabetes clinic", *Diabetes Care* 24:250–256, 2001
42. Bril V., Perkins B. A., "Validation of the Toronto Clinical Scoring System for diabetic polyneuropathy", *Diabetes Care* 25:2048–2052, 2002
43. Meijer J. W., Bosma E., Lefrandt J. D., et al., "Clinical diagnosis of diabetic neuropathy with the diabetic neuropathy symptom and diabetic neuropathy examination scores", *Diabetes Care*, 26(3):697-701, 2003
44. Meijer J.W., Smit A.J., Sonderen E., Groothoff J.W., Eisma W.H., Links T.P., "Symptom scoring systems to diagnose distal polyneuropathy in diabetes: the Diabetic Neuropathy Symptom score", 2002
45. Horowitz S. H., "The diagnostic workup of patients with neuropathic pain", Elsevier Saunders, *Anesthesiology Clinic*, 25 699–708, 2007
46. Valk G. D., Nauta J. P., Strijem R. M., Bertelsmann F. W., "Clinical examination versus neurophysiological examination in the diagnosis of diabetic polyneuropathy", *Diabet Med*, 9:716–721, 1992
47. Dillingham T. R., Pezzin L. E., "Under-recognition of polyneuropathy in persons with diabetes by non-physician electrodiagnostic services providers", *Am J Phys Med Rehabil*, 84:399–406, 2005
48. Guidelines in electrodiagnostic medicine. *Muscle Nerve Suppl* 8:S3-300, 1999
49. Valk G. D., Grootenhuys P. A., van Eijk J. T., Bouter L. M., Bertelsmann F. W., "Methods for assessing diabetic polyneuropathy: validity and reproducibility of the measurement of sensory symptom severity and nerve function tests", *Diabetes Res Clin Pract*, 47:87–95, 2000



50. Shy E. M., Frohman E. M., So Y. T. et al., "Quantitative sensory testing: report of Therapeutics and Technology Assessment Subcommittee of American Academy of Neurology", *Neurology*, 60(6): 898-904, 2003
51. Yarnitsky D., Pud D. and Binnie C.D. et al. (editors), "Quantitative sensory testing", EMG, Nerve Conduction and Evoked Potentials, Clinical Neurophysiology, Volume 1 (Revised and Enlarged Edition), 2.9: 305-326, 2004
52. Thomas P. K., "Nerve biopsy", *Diabetic Med*, 16:351–352, 1997
53. Dahlin L. B., Eriksson K. F., Sundkvist G., "Persistent postoperative complaints after whole sural nerve biopsies in diabetic and non-diabetic subjects", *Diabet Med*,14:353-356, 1997
54. Malik R. A., Tesfaye S., Thompson S., Veves A., Sharma A. K., Boulton A. J., Ward J.D., "Endoneurial localisation of microvascular damage in human diabetic neuropathy", *Diabetologia*, 36:454-459, 1993
55. Holland N. R., Crawford T. O., Hauer P., Cornblath D. R., Griffin J. W., McArthur J.C., "Small-fiber sensory neuropathies: clinical course and neuropathology of idiopathic cases", *Ann Neurol*,44:47–59, 1998
56. Polydefkis M., Griffin W., McArthur J., "New insights into diabetic polyneuropathy", *JAMA*, 371–1376, 2003
57. Holland NR, Stocks A, Hauer P, Cornblath DR, Griffin JW, McArthur JC: Intraepidermal nerve fiber density in patients with painful sensory neuropathy, *Neurology* 48:708-711, 1997
58. Pittenger GL, Ray M, Burcus NI, McNulty P, Basta B, Vinik AI: Intraepidermal nerve fibers are indicators of small-fiber neuropathy in both diabetic and nondiabetic patients. *Diabetes Care* 27:1974-1979, 2004
59. Lauria G., Cornblath D.R., Johansson O, McArthur JC, Mellgren SI, Nolano M, Rosenberg N., Sommer C.: EFNS guidelines on the use of skin biopsy in the diagnosis of peripheral neuropathy. *Eur J Neurol* 12:747-758, 2005
60. Pittenger G. L., Ray M., Burcus N. I., McNulty P., Basta B., Vinik A.I., "Intraepidermal nerve fibers are indicators of small-fiber neuropathy in both diabetic and nondiabetic patients", *Diabetes Care*, 27:1974-1979, 2004
61. Sorensen L., Molyneaux L., Yue D. K., "The relationship among pain, sensory loss, and small nerve fibers in diabetes", *Diabetes Care* 29:883-887, 2006

62. Loseth S., Stalberg E., Jorde R., Mellgren S. I., "Early diabetic neuropathy: thermal thresholds and intraepidermal nerve fibre density in patients with normal nerve conduction studies", *J Neurol* 255:1197-1202, 2008
63. Magerl W, Treede RD. Heat-evoked vasodilatation in human hairy skin: axon reflexes due to low-level activity of nociceptive afferents. *J Physiol*; 15:837–848, 1996
64. Hamdy O, Abou-Elenin K, LoGerfo FW, Horton ES, Veves A. Contribution of nerve-axon reflex-related vasodilation to the total skin vasodilation in diabetic patients with and without neuropathy, *Diabetes Care*; 24:344–349, 2001
65. Caselli A, Spallone V, Marfia GA, et al. Validation of the nerve axon reflex for the assessment of small nerve fibre dysfunction. *J Neurol Neurosurg Psychiatry*; **77**(8): 927–932, 2006
66. Eaton SE, Harris ND, Rajbhandari SM, et al. Spinal-cord involvement in diabetic peripheral neuropathy, *Lancet*; 358:35–36, 2001
67. Ewing DJ, Clarke BF: Diabetic autonomic neuropathy: a clinical viewpoint. In *Diabetic Neuropathy*. Dyck PJ, Thomas PK, Asbury AK, Weingrad AI, Porte D, Eds. Philadelphia, WB Saunders, p. 66–88, 1987
68. Olaleye D., Perkins B. A., Bril V., "Evaluation of three screening tests and a risk assessment model for diagnosing peripheral neuropathy in the diabetes clinic", *Diabetes Res Clin Practice*, 54(2):115-128, 2001
69. Tavakoli M. et al., "Corneal confocal microscopy: a novel noninvasive test to diagnose and stratify the severity of human diabetic neuropathy", *DIABETES CARE*, VOLUME 33, NUMBER 8, AUGUST 2010
70. Hossain Parwez, Sachdev A., Malik R. A. "Early detection of diabetic peripheral neuropathy with corneal confocal microscopy", *The Lancet*, Vol 366:1340-1342, October 15 2005
71. Jalbert I., Stapleton F., Papas E., Sweeney D. F., Coroneo M., "In vivo confocal microscopy of the human cornea", *Br J Ophthalmol*, 87: 225–36, 2003
72. Iqbal I., Kallinikos P., Boulton A. J., Efron N., Malik R. A., "Corneal nerve morphology: a surrogate marker for human diabetic neuropathy improves with improved glycaemic control", *Diabetes*, 54 (suppl 1):871, 2005
73. Patel D. V., Ku J.Y., Kent-Smith B., McGhee C. N., "In vivo microstructural analysis of the cornea in Maroteaux-Lamy syndrome", *Cornea*; 24(5):623-5, 2005

74. Böhnke, Matthias and Barry, Masters R., "Confocal Microscopy of the Cornea", *Progress in Retinal and Eye Research.*, Vols. 18, No. 5, pp. 553 to 628, 1999
75. Masters B. R., Bohnke M., "Confocal microscopy of the human cornea in vivo", *International Ophthalmology*; 23(4-6):199-206, 2001
76. Cavanagh H. D., Petroll W.M., Alizadeh H., et al., "Clinical and diagnostic use of in vivo confocal microscopy in patients with corneal disease", *Ophthalmology*; 100(10):1444-54, 1993
77. Pawley, James B. *Handbook of Biological Confocal Microscopy*. Madison, USA : Springer, 2006
78. Claxton, Nathan S., Feleers, Thomas J. and Davidson, Michael W. "Laser Scanning Confocal Microscopy"
79. Tavakoli M., Hossain P., Malik A. R., "Clinical applications of corneal confocal microscopy", *Clinical Ophthalmology*, 2(2): 435-445, 2008
80. Kobayashi A., Sugiyama K., "In vivo laser confocal microscopy findings for Bowman's layer dystrophies (Thiel-Behnke and Reis-Bucklers corneal dystrophies)", *Ophthalmology*, 114:69-75, 2007
81. Werner L. P., Werner L., Dighiero P. et al., "Confocal microscopy in Bowman and stromal corneal dystrophies", *Ophthalmology*, 106:697-704, 1999
82. Kaufman S. C., Musch D. C., Belin M. W. ,et al., "Confocal microscopy: a report by the American Academy of Ophthalmology", *Ophthalmology*, 111:396-406, 2004
83. Moilanen J. A., Vesaluoma M. H., Muller L. J., et al., "Long-term corneal morphology after PRK by in vivo confocal microscopy", *Investigative Ophthalmology and Visual Science*, 44:1064-9, 2003
84. Kallinikos P., Morgan P., Efron N., "On the etiology of keratocyte loss during contact lens wear", *Invest Ophthalmol Vis Sci*, 45:3011-20, 2004
85. Efron N., Perez-Gomez I., Morgan P. B., "Confocal microscopic observations of stromal keratocytes during extended contact lens wear", *Clinical and Experimental Optometry*, 85:156-60, 2002
86. O'Donnell C., Efron N., "Corneal endothelial cell morphometry and corneal thickness in diabetic contact lens wearers", *Optom Vis Sci*, 81:858-62, 2004
87. Font R. L., Fine B. S., "Ocular pathology in Fabry's disease. Histochemical and electron microscope observations", *Am J Pathol*, 97:671, 1972

88. Pe'er J., Vidaurri J. Halfon S. T., "Association between corneal arcus and some of the risk factors for coronary artery disease", *Br J Ophthalmol*, 67:795-8, 1983
89. Bohnke M., Masters B. R., "Long-term contact lens wear induces a corneal degeneration with microdot deposits in the corneal stroma", *Ophthalmology*, 104:1887-96, 1997
90. Bohnke M., Thaer A., Schipper I., "Confocal microscopy reveals persisting stromal changes after myopic photorefractive keratectomy in zero haze corneas", *British Journal of Ophthalmology*, 82:1393-400, 1998
91. Rosenberg M. E., Tervo T. M., Immonen I. J., et al., "Corneal structure and sensitivity in type 1 diabetes mellitus", *Investigative Ophthalmology & Visual Science*, 41(10):2915-21, 2000
92. Malik R. A., Kallinikos P., Abbott C. A., et al., "Corneal confocal microscopy: a non-invasive surrogate of nerve fiber damage and repair in diabetic patients", *Diabetologia*, 46(5):683-8, 2003
93. Kallinikos P., Berhanu M., O'Donnell C., Boulton A. J., Efron N. and Malik R. A., "Corneal nerve tortuosity in diabetic patients with neuropathy ", *Investigative Ophthalmology & Visual Science*, Vol. 45: 418-22, Nr. 2, February, 2004
94. Stachs O., Knappe S., Zhivov A., Kraak R., Stave J., Guthoff R. F., "Three-dimensional confocal laser scanning microscopy of the corneal nerve structure", *Klin Monats Augenhkd*, 223(7):583-8, July 2006
95. Grupcheva C. N., Wong T., Riley A. F. and McGhee C., "Assessing the sub-basal nerve plexus of the living healthy human cornea by in vivo confocal microscopy", *Lens and Cornea for Clinical and Experimental Ophthalmology*, 30:187-190, 2002
96. Mocan C. M., Durukan I., Irkec M., Orhan M., "Morphologic alterations of both stromal and sub-basal nerves in the corneas of patients with diabetes", *Clinical science, Cornea*, 25:769-773, 2006
97. Quattrini C., Tavakoli M., Jeziorska M., Kallinikos P., Tesfaye S., Finnigan J., Marshall A., Boulton A., Efron N., and Malik R. A., "Surrogate Markers of Small Fiber Damage in Human Diabetic Neuropathy", *Diabetes* 56:2148-2154, 2007
98. Tavakoli M., Marshall A., Thompson L., Kenny M., Waldek S., Efron N., Malik R. A., "Corneal confocal microscopy: a novel non-invasive means to diagnose neuropathy in patients with Fabry disease", *Muscle & Nerve*, 40(6): 976-84, December 2009

99. Lalive P. H., Truffert A., Magistris M. R., Landis T., Dosso A., "Peripheral autoimmune neuropathy assessed using corneal in vivo confocal microscopy", *Arch, Neurology*; 66(3):403-405, 2009
100. Visser N., McGhee C. N., Patel D. V., "Laser-scanning in vivo confocal microscopy reveals two morphologically distinct populations of stromal nerves in normal human corneas", *Br J Ophthalmology*; 93(4):506-509, 2009
101. Ahmed A., Bril V., Orszag A., Paulson J., Yeung E., Ngo M., Orlov S., Perkins B., "Detection of diabetic sensorimotor polyneuropathy by corneal confocal microscopy in type 1 diabetes", *Pathophysiology/Complications, Diabetes Care*, February 2012
102. Labbé A., Alalwani H., Van Went C., Brasnu E., Denoyer A., Baudouin C., "The relationship between sub basal nerve morphology and corneal sensation in patients treated for glaucoma", *10<sup>th</sup> EGS Congress, Copenhagen*, 2012
103. Edwards K., Pritchard N., Vagenas D., Russell A., Malik R. A., Efron N., "Utility of corneal confocal microscopy for assessing mild diabetic neuropathy: baseline findings of the landmark study", *Clin Exp Optom.*, 95(3):348-54, May 2012
104. Nitoda E., Kallinikos P., Pallikaris A., Moschandrea J., Amoiridis G., Ganotakis E. S., Tsilimbaris M., "Correlation of Diabetic Retinopathy and Corneal Neuropathy Using Confocal Microscopy", *Current Eye Research*, May 2012
105. Popper M., Quadrado M. J., Morgado A. M., Murta J. N., Van Best J. A., and Muller L. J., "Subbasal nerves and highly reflective cells in corneas of diabetic patients: in vivo evaluation by confocal microscopy," *Invest Ophthalmol Vis. Sci.*, vol. 46, no. Suppl S, p. 2194, 2005
106. Michigan Neuropathy Screening Instrument, University of Michigan, 2000, [http://www.med.umich.edu/mdrtc/profs/documents/svi/MNSI\\_patient.pdf](http://www.med.umich.edu/mdrtc/profs/documents/svi/MNSI_patient.pdf), cited on 03.03.2012
107. Russell L., "Neuropathy and the Gastrointestinal System" , <http://www.neuropathy.org/site/DocServer/nutritionGIRussellCMD.pdf?docID=1601>, cited on 07.06.2012
108. Shields R. W., Brown W. F., Bolton C. F., Aminoff M. J., "Alcoholic and nutritional polyneuropathies", *Neuromuscular function and disease*, Vol 2. Philadelphia, WB Saunders, 1109-1125, 2002

109. Chaudhry V., Umapathi T., Ravich W. J., "Neuromuscular disease and disorders of the alimentary system", *Muscle Nerve*, 25:768-784, 2002
110. Types of peripheral neuropathy: Systemic/Metabolic, Center for Peripheral Neuropathy, [http://peripheralneuropathycenter.uchicago.edu/learnaboutpn/types\\_ofpn/systemic/nutrition.shtml](http://peripheralneuropathycenter.uchicago.edu/learnaboutpn/types_ofpn/systemic/nutrition.shtml), cited on 09.07.2012
111. Futterleib A., Cherubini K., "Importance of vitamin B12 screening in clinical evaluation of elderly patient", *Acta Haematol*, 81: 186-91, 1989.
112. Harrison's Principles of Internal Medicine (Volume 1), 14<sup>th</sup> edition. Edited by Harrison T. R. and Fauci A. S. Authors: Braunwald E., Isselbacher K. J., Wilson J. D., Martin J. B., Kasper D., Hauser S. L., Longo D. L.
113. Cecil Textbook of Medicine, 19<sup>th</sup> edition. Edited by James B. Wyngaarden, Lloyd H. Smith, Jr., and J. Claude Bennett. 2380 pp., illustrated. Philadelphia, W.B. Saunders, 1992
114. Azhary H., et al., "Peripheral neuropathy: Differential diagnosis and management", *American Family Physician*, 81:887, 2010
115. Bolton C. F., Young G. B., "Neurological Complications of Renal Disease", *Stoneham, Mass: Butterworth-Heinemann*; 1-256, 1990
116. Fraser C. L., Arieff A. I., "Nervous system complications in uremia", *Ann Intern Med*, 109(2):143-53, July 1988
117. Bolton C. F., "Peripheral neuropathies associated with chronic renal failure", *Can J Neurol Sci*, 7(2):89-96, May 1980
118. Yeasmin S., Begum N., Begum S., "Motor neuropathy in Hypothyroidism: Clinical and Electrophysiological Findings", *BSMMU Journal*, 1(1): 15-18, 2008
119. Lowrance Jim, "Thyroid Disease and Peripheral Neuropathy", <http://suite101.com/article/thyroid-disease-and-neuropathy-symptoms-a140669>, cited on 10.07.2012
120. Nemni R., Bottacchi E., Fazio R., et al., "Polyneuropathy in hypothyroidism: Clinical, Electrophysiological and morphological findings in 4 cases", *J Neurol Neurosurg Psychiatry*, 50: 1454-1460, 1987.
121. Coyle N., Silver J., Meuche G., Messner C., "Understanding peripheral neuropathy", *Cancer Care, Help and Hope*, 2008, [www.cancer.org](http://www.cancer.org), cited on 11.07.2012

122. Dropcho Edward J., "Cancer-related neuropathies", December 2002, [http://www.neuropathy.org/site/DocServer/Cancer-Related Neuropathies.pdf](http://www.neuropathy.org/site/DocServer/Cancer-Related_Neuropathies.pdf), cited on 11.07.2012
123. Russel L. Chin, MD, "Neuropathy and the Gastrointestinal System"
124. King P. H., Petersen N. E., Rakhra R., Schreiber W. E., "Porphyria presenting with bilateral radial motor neuropathy: evidence of a novel gene mutation", *Neurology*, 58:1118-1121, 2002
125. Barohn R. J., Sanchez J. A., Anderson K. E., "Acute peripheral neuropathy due to hereditary coproporphyrin", *Muscle Nerve*, 17:793-799, 1994
126. Kochar D. K., Poonia A., Kumawat B. L., Shubhakaran, Gupta B. K., "Study of motor and sensory nerve conduction velocities, late responses (F-wave and H-reflex) and somatosensory evoked potential in latent phase of intermittent acute porphyria", *Electromyography and Clinical Neurophysiology*, 40:73-79, 2000
127. Whitesell Jackie, "Inflammatory neuropathies", *Peripheral Neuropathy*, (Guest Editor Bromberg M.), *Thieme, Medical Publishers Inc., Semin Neurol*, 30:356-364, 2010
128. Hadden R. and Hughes R., "Management of Inflammatory Neuropathies", *J Neurol Neurosurg Psychiatry*, 74(2):ii9-ii14, 2003
129. Macalester, (online), cited on 14.07.2012  
<http://www.macalester.edu/psychology/whathap/UBNRP/neuropathy/Homepage.html>
130. Jain K. K., "Drug-induced peripheral neuropathies", Jain K. K., ed. *Drug-induced neurological disorders*, 2<sup>nd</sup> ed. Seattle: Hogrefe & Huber, 263-294, 2001
131. Weimer L. H., "Medication-induced peripheral neuropathy", *Curr Neurol Neurosci Rep*, Jan 2003
132. Quasthoff S., Hartung H. P., "Chemotherapy induced peripheral neuropathy", *J Neurol*, 249:9-17, 2002
133. Results and notes taken during the EMG measurement sessions, performed in Coimbra University Hospitals, Department of Neurology, EMG and Evoked Potentials Lab; measurement performed in May, 2012
134. Gerdle B., Karlsson S., Day S., Djupsjöbacka M. "Acquisition, Processing and Analysis of the Surface Electromyogram", Eds: Windhorst U. and Johansson H. Springer Verlag, Berlin, *Modern Techniques in Neuroscience*, 26: 705-755, 1999

135. Results and notes taken during the CCM image acquisition sessions, performed in Coimbra University Hospitals, Department of Ophthalmology; measurements performed in February, 2012
136. Ferreira A., Morgado A. M., and Silva J. S., "Corneal nerves segmentation and morphometric parameters quantification for early detection of diabetic neuropathy", *12<sup>th</sup> Mediterranean Conference on Medical and Biological Engineering and Computing (MEDICON 2010)*, pp.264–267, Chalkidiki–Grécia, 2010
137. Silva J.S., Silva A., Santos B.S., "Image denoising methods for tumor discrimination in high resolution computed tomography", *Journal of Digital Imaging* (24)464–469, 2011
138. Samples of image segmentation results with *Cornea3*, obtained in July, 2012